MISSOURI S&T

CENTER FOR INFRASTRUCTURE ENGINEERING STUDIES

Development and Field Testing of an FRP Composite Bridge Deck Comprising of Guard Rail System for Bridge 1480230, Greene County, MO

Authors:

Lawrence C. Bank
Nestore Galati
Spencer N. Jones
Fabio Matta
Antonio Nanni,
Michael G. Oliva
Brian M. Orr
Thomas E. Ringelstetter
Jeffrey S. Russell

Compiled by:

John J. Myers

A University Transportation Center Program at Missouri University of Science and Technology

Disclaimer

The contents of this report reflect the views of the author(s), who are responsible for the facts and the accuracy of information presented herein. This document is disseminated under the sponsorship of the Department of Transportation, University Transportation Centers Program and the Center for Infrastructure Engineering Studies UTC program at the Missouri University of Science and Technology, in the interest of information exchange. The U.S. Government and Center for Infrastructure Engineering Studies assumes no liability for the contents or use thereof.

Technical Report Documentation Page

1. Report No.	2. Government Accession No.	3. Recipient's Catalog No.
UTC R143		

4. Title and Subtitle	5. Report Date
Development and Field Testing of an FRP Composite Bridge Deck Comprising of Guard Rail System for Bridge 1480230, Greene County, MO	January 2010
	6. Performing Organization Code

7. Author/s	8. Performing Organization Report No.
Lawrence C. Bank, Nestore Galati, Spencer N. Jones, Fabio Matta, Antonio Nanni, Michael G. Oliva, Brian M. Orr, Thomas E. Ringelstetter, Jeffrey S. Russell and Compiled by: John J. Myers	R0001758

9. Performing Organization Name and Address	10. Work Unit No. (TRAIS)
Center for Infrastructure Engineering Studies/UTC program Missouri University of Science and Technology 220 Engineering Research Lab Rolla, MO 65409	11. Contract or Grant No. DTRS98-G-0021

12. Sponsoring Organization Name and Address	13. Type of Report and Period Covered
U.S. Department of Transportation Research and Innovative Technology Administration 1200 New Jersey Avenue, SE Washington, DC 20590	Final
	14. Sponsoring Agency Code

15. Supplementary Notes

16. Abstract

The objective of the rehabilitation program of Bridge 1480230 in Springfield, MO in Greene County is to remove the 15 Ton load posting that has been imposed on it. An inspection of the bridge revealed a severely damaged deck in need to be replaced. The structural analysis has demonstrated deficiency in the steel girders as well as possible deficiencies in bents and piers. The rehabilitation plan will consist in the following steps: 1) Replacing the concrete deck using a low weight, high perforce Glass FRP composite deck; 2) Retrofitting or replacement of existing steel girders. Different solutions will be considered to determine the optimal design in terms of structural performances, durability and cost of the structure. Also the possibility of using Carbon FRP composite girders is under investigation allowing to reduce the weight of the superstructure and therefore to avoid the strengthening of bents and piers; 3) Design of the strengthening of bents and piers if needed; 4) Developing of an FRP guard rail system ensuring the durability of the entire superstructure and therefore reducing the maintenance costs.The project will include a field and laboratory investigations necessary to validate the assumptions to be made for design of the rehabilitation. In addition, sensors will be embedded in the FRP members in order to monitor the structural performances of the bridge over time. The different sensors will be remotely read allowing in such way detecting any possible structural flaw. Missouri S&T (formerly UMR) will perform a load test after construction to ensure the in-situ structural performances of the bridge and it will perform a five years inspection (one load test per year). It is envisioned that this rehabilitation technique will lead to a design/maintenance protocol for consideration by Counties for future applications

17. Key Words	18. Distribution Statement
FRP decks, Fiber reinforced polymer, fiber optics, wireless network, in-situ load testing, deck replacement, guard rail system, crush test and pendulum test	No restrictions. This document is available to the public through the National Technical Information Service, Springfield, Virginia 22161.

19. Security Classification (of this report)	20. Security Classification (of this page)	21. No. Of Pages	22. Price
unclassified	unclassified	47	

Form DOT F 1700.7 (8-72)

Table of Contents

CONNECTION OF CONCRETE RAILING POST AND BRIDGE DECK WITH INTERNAL FRP REINFORCEMENT by Fabio Matta and Antonio Nanni
Journal of Bridge Engineering – January/February 2009

COST-EFFECTIVE, STRUCTURAL STAY-IN-PLACE FORMWORK SYSTEM OF FIBER-REINFORCED POLYMER FOR ACCELERATED AND DURABLE BRIDGE DECK CONSTRUCTION by Thomas E. Ringelstetter, Lawrence C. Bank, Michael G. Oliva, Jeffrey S. Russell, Fabio Matta and Antonio Nanni
Transportation Research Record: Journal of the Transportation Research Board – 2006

DESIGN OF CONCRETE RAILING REINFORCED WITH GLASS FIBER REINFORCED POLYMER BARS by Fabio Matta and Antonio Nanni
2006 ASCE/SEI Structures Congress – May 18-20, 2006

RAPID CONSTRUCTION OF CONCRETE BRIDGE DECK USING PREFABRICATED FRP REINFORCEMENT by Fabio Matta, Antonio Nanni, Thomas E. Ringelstetter, Lawrence C. Bank
Third International Conference on FRP Composites in Civil Engineering – December 13-15 2006

PULTRUDED GRID AND STAY-IN-PLACE FORM PANELS FOR THE RAPID CONSTRUCTION OF BRIDGE DECKS by Fabio Matta, Nestore Galati, Antonio Nanni, Thomas E. Ringelstetter, Lawrence C. Bank, Michael G. Oliva
COMPOSITES 2005 Convention and Trade Show American Composites Manufacturers Association – September 28-30, 2005

PREFABRICATED MODULAR GFRP REINFORCEMENT FOR ACCELERATED CONSTRUCTION OF BRIDGE DECK AND RAIL SYSTEM by Fabio Matta, Antonio Nanni, Nestore Galati, Thomas E. Ringelstetter, Lawrence C. Bank, Michael G. Oliva, Jeffrey S. Russell, Brian M. Orr, and Spencer N. Jones
Proc. FHWA Accelerated Bridge Construction Conference – Path to Future – December 14-16, 2005

Connection of Concrete Railing Post and Bridge Deck with Internal FRP Reinforcement

Fabio Matta, A.M.ASCE[1]; and Antonio Nanni, P.E., F.ASCE[2]

Abstract: The use of fiber-reinforced polymer (FRP) reinforcement is a practical alternative to conventional steel bars in concrete bridge decks, safety appurtenances, and connections thereof, as it eliminates corrosion of the steel reinforcement. Due to their tailorability and light weight, FRP materials also lend themselves to the development of prefabricated systems that improve constructability and speed of installation. These advantages have been demonstrated in the construction of an off-system bridge, where prefabricated cages of glass FRP bars were used for the open-post railings. This paper presents the results of full-scale static tests on two candidate post–deck connections to assess compliance with strength criteria at the component (connection) level, as mandated by the *AASHTO Standard Specifications*, which were used to design the bridge. Strength and stiffness until failure are shown to be accurately predictable. Structural adequacy was then studied at the system (post-and-beam) level by numerically modeling the nonlinear response of the railing under equivalent static transverse load, pursuant to well-established structural analysis principles of FRP RC, and consistent with the *AASHTO LRFD Bridge Design Specifications*. As moment redistribution cannot be accounted for in the analysis and design of indeterminate FRP RC structures, a methodology that imposes equilibrium and compatibility conditions was implemented in lieu of yield line analysis. Transverse strength and failure modes are determined and discussed on the basis of specification mandated requirements.

DOI: 10.1061/(ASCE)1084-0702(2009)14:1(66)

CE Database subject headings: Bridge decks; Concrete structures; Design; Fiber reinforced polymers; Reinforcement.

Introduction

The use of fiber-reinforced polymer (FRP) reinforcement ideally eliminates corrosion in concrete bridge decks, which accrues from exposure to deicing salts and harsh environments and affects a large portion of the bridge inventory worldwide. Glass-FRP (GFRP) bars are a practical alternative to steel reinforcement for nonprestressed bridge decks (Bradberry 2001; Nanni and Faza 2002). A number of field implementations, typically as parts of research projects conducted in North America, have demonstrated the validity of the technology (Phelan et al. 2003; Benmokrane et al. 2004, 2006). In addition, recent findings from tests performed on concrete cores containing portions of GFRP bars, which were removed from four bridges and a wharf that had operated from 5 to 8 years under aggressive environments, did not reveal any chemical or physical degradation upon frequent exposure to wet and dry and freezing and thawing cycles, chlorides from deicing salts or salt water, and concrete alkaline environment (Mufti et al. 2007). The demand is strong from the construction industry and practitioners to exploit this technology by developing material and construction specifications, as well as limit-state based design specifications written in mandatory language (Busel et al. 2008) such as those incorporated in the *Canadian Highway Bridge Design Code* (CSA 2006).

Degradation also affects RC railings, and in particular their connection to bridge decks, and may compromise crashworthiness. The development and validation of corrosion-free railings and connections of railing posts to FRP RC decks have been addressed in very few research efforts that followed the pioneering development of the hybrid steel–GFRP RC Ontario Bridge Barrier (Maheu and Bakht 2004). In that case, carbon FRP grids were used as flexural reinforcement in the deck and barrier wall, along with stainless steel double-headed tension bars to provide sufficient anchorage. The performance of connections between a steel RC barrier and a deck overhang reinforced with GFRP bars in the top mat was investigated through pendulum impact tests on full-scale subassemblies (Trejo et al. 2001). The hybrid steel–GFRP specimens attained a maximum load between 3 and 16% smaller than the steel RC counterparts, with larger deformations. Based on the fact that in either configuration the barrier remained attached to the deck without showing any sign of further movement or instability during inspection, it was concluded that the hybrid configuration granted adequate performance for implementation. In another experimental research (Deitz et al. 2004), GFRP, steel and hybrid (that is, having GFRP and steel bars in the top and bottom mat, respectively) RC overhang subassemblies cast with steel RC New Jersey barrier walls were subjected to transverse static loading. All connections met the American Association of *State Highway and Transportation Officials (AASHTO) Standard Specifications* criteria (AASHTO 2002),

[1]Research Assistant Professor, and Associate Director, NSF Industry/University Cooperative Research Center "Repair of Buildings and Bridges with Composites," Dept. of Civil, Architectural and Environmental Engineering, Univ. of Miami, MEB-317 McArthur Engineering Bldg., 1251 Memorial Dr., Coral Gables, FL 33176 (corresponding author). E-mail: fmatta@miami.edu

[2]Fisher Endowed Scholar, Professor and Chair, Dept. of Civil, Architectural, and Environmental Engineering, Univ. of Miami, Coral Gables, FL 33146.

Note. Discussion open until June 1, 2009. Separate discussions must be submitted for individual papers. The manuscript for this paper was submitted for review and possible publication on January 7, 2008; approved on July 15, 2008. This paper is part of the ***Journal of Bridge Engineering***, Vol. 14, No. 1, January 1, 2009. ©ASCE, ISSN 1084-0702/2009/1-66–76/$25.00.

which require the connection to resist a load of 44.5 kN applied at the top of the continuous barrier.

A comprehensive investigation was undertaken to study the behavior of concrete bridge barriers internally reinforced with GFRP bars under static and pendulum impact loads (El-Salakawy et al. 2003). The results of full-scale testing, where the GFRP RC subassemblies were designed on a strength equivalence basis with their steel RC counterparts, showed similar behavior at failure. The former solution was approved by the Ministry of Transportation of Québec, Canada, for use in construction. The crashworthiness of an open-post railing internally reinforced with GFRP bars, which was developed for use in highway bridges, was assessed through two crash tests (Buth et al. 2003) as per the NCHRP Report 350 Test Level 3 (TL-3) criteria (Ross et al. 1993). The test demanded a 2.040 kg pickup truck to impact the railing at a speed of 100 km/h and at an angle of 25° with respect to the roadway direction, as typically required on the National Highway System (Mak and Bligh 2002). The first test failed due to vehicle rollover, which was attributed to the insufficient height of the railing. The second, successful test was performed on a railing having a steel tube bolted on top to increase the height from 686 to 762 mm. In both cases, the structural performance was acceptable as the railing withstood the impact load and negligible deflections were reported (Buth et al. 2003).

The use of prefabricated GFRP reinforcement was implemented in the reconstruction of the deck and open-post railings of a severely degraded off-system bridge (No. 14802301) in Greene County, Mo (Matta et al. 2007). Prefabricated, light-weight GFRP bar cages were designed for the railings following the *ACI 440.1R-03 Guidelines* (ACI 2003) and the *AASHTO Standard Specifications* (AASHTO 2002), which were used to design the bridge. The bar cages were used in combination with a deck reinforcement grating made of smooth pultruded GFRP profiles, where load transfer is attained by mechanically constraining the core concrete rather than through bond, and is not explicitly covered in the current ACI guidelines (ACI 2006). This research had two objectives. First, to select a GFRP RC post–deck connection design for Bridge No. 14802301 by proof testing two full-scale overhang subassemblies, and assess compliance with specification mandated strength requirements at the component (rail beam and post–deck connection) level (AASHTO 2002). Second, to analytically model the connection response under static loading, and incorporate it into the nonlinear analysis of the railing to verify the strength and stiffness response at the system (post-and-beam) level under equivalent static load, pursuant to the requirements of Section 13 (Railings) of the AASHTO LRFD design specifications (AASHTO 2004).

Research Significance

Design principles for FRP RC are well established and reflect the different philosophy with respect to traditional steel RC design, which stems from the peculiar physical and mechanical properties of FRP materials (Nanni 1993, 2003). The most relevant are the brittle behavior in tension in the fiber (axial) direction, which make overreinforced sections more desirable; the smaller axial stiffness than steel, which results in greater deflections and crack widths, and in shear design that accounts for reduced aggregate interlock and concrete strength contribution; and the reduced transverse strength and stiffness of the bars, where the properties are resin dominated. Understanding the structural implications of designing FRP RC deck and railing systems is instrumental to rationally develop safety appurtenances or crash test specimens, and, in perspective, to economically screen candidate systems for the assessment of structural and functional crashworthiness by means of advanced numerical tools (Bligh et al. 2004). The overarching objective is to develop a knowledge base for the efficient validation of more durable and sustainable solutions for field implementation.

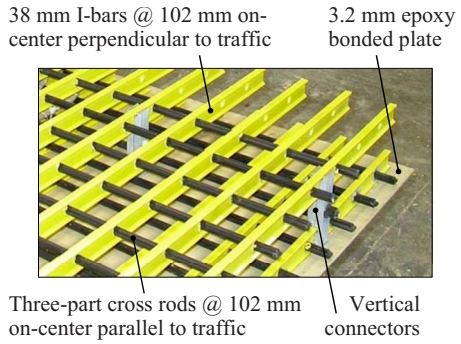

Fig. 1. Prefabricated GFRP stay-in-place deck reinforcement

Experimental Investigation

Two full-scale post-overhang subassemblies were tested under quasi-static loading as part of a research program aimed at developing and implementing a steel-free concrete deck and railing system for the accelerated construction of an off-system bridge (Matta et al. 2007). Large size stay-in-place (SIP) panels with an integrated double-layer grating fabricated from GFRP pultruded I-bars and cross rods were used as the deck reinforcement (Fig. 1). GFRP bar cages were used for the open-post railings, producing a GFRP RC version of the required Modified Kansas Corral Rail (MKCR). Open-post railings are constructed with a cast-in-place continuous rail beam on top of suitably spaced posts, and are often preferred due to aesthetics and efficient drainage, along with the stiffness, inertial properties, and relatively low-cost maintenance typical of concrete railings.

Figs. 2(a and b) show the new reinforcement prior to casting and the finished railing, respectively. The original MKCR profile, which performed adequately under crash testing by preventing vehicle rollover and snagging, was improved by increasing the height of the rail beam from 356 to 432 mm, for a total height of 762 mm, to further reduce the risk of rollover (Matta and Nanni 2006). In addition, the original width of intermediate posts and openings, L_P and L_O, of 914 and 2,134 mm, respectively, was changed into 1.22 m for both [Fig. 2(b)] to be geometrically compatible with the 2.44 m long SIP panels.

Specimens Design

The geometry and reinforcement layout of the post–deck connection in Specimens M1 and M2 are detailed in Figs. 3(a and b), respectively. The latter was implemented in Bridge No. 14802301. Both configurations use two layers of bent No. 5 (16 mm) GFRP bars to connect the post to the 2.44 m by 2.44 m, 178 mm thick concrete slab, whose 914 mm overhang shown in Fig. 4 replicates that of the bridge. The slab dimensions and boundary conditions were selected as representative of the continuous deck structure. The posts were cast 3 days after the slab.

(a)

(b)

Fig. 2. Reconstruction of Bridge No. 14802301: (a) GFRP reinforcement cages prior to casting of railing; (b) open-post railing in service

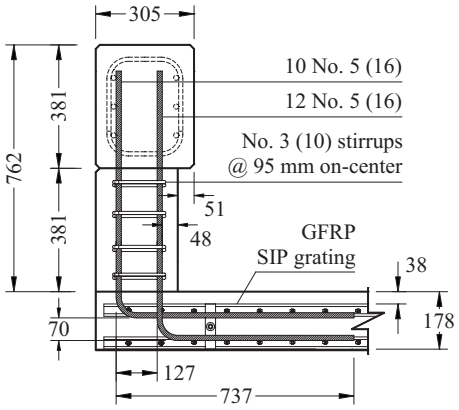

(a)

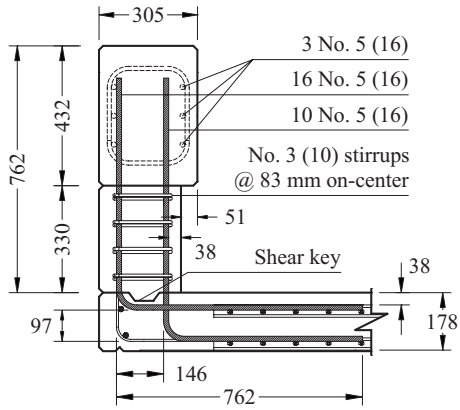

(b)

Fig. 3. Reinforcement layout of post–deck connection subassemblies: (a) Specimen M1; (b) Specimen M2 (dimensions are in millimeters)

Specimen M1 was designed with three main objectives. First, to provide a nominal moment capacity of the 1.22 m by 254 mm post section not smaller than that of the steel RC MKCR, which is about 203.4 kN m. Second, to provide a nominal moment capacity of the deck section at the connection similar to that away from the connection, where the SIP reinforcement satisfies the AASHTO (2002) strength requirements. It should be noted that the two exterior longitudinal cross rods on the top grating layer underneath the post were removed to allow insertion of the post bar cages: as the forces are transferred into the smooth I-bars by mechanically constraining the core concrete between the cross rods, the contribution thereof was neglected in the design. The third objective was to provide a reinforcement layout geometrically compatible with the deck grating. Table 1 summarizes the flexural capacity of the 1.22 m wide post and deck section at the connection (GFRP bars only) and away from the connection (I-bars only). The design goals were met by using concrete with a nominal compressive strength f'_c of 41.4 MPa. An environmental reduction factor C_E of 0.7 was applied to the guaranteed tensile strength f^*_{fu} of the GFRP bars to determine their design strength. The construction joint was prepared by providing a dry and roughened surface prior to casting the post.

Design of safety barriers and their connections based on empirical or analogy considerations as for Specimen M1 is common and often effective. In fact, until the late 1980s when crash testing for highway safety appurtenances was not mandatory, systems successfully crash tested could be used even without meeting geometry and static strength criteria. A rigorous procedure was followed for the structural design of Specimen M2 to resist the required 44.5 kN transverse load applied at the midheight of the 432 mm high rail beam face (AASHTO 2002). Concrete with compressive strength of 27.6 MPa was assumed, as typically used in steel RC MKCRs. Failure may be governed by concrete crushing or FRP reinforcement rupture in flexure at the weakest connected section, insufficient anchorage of the post or development length of the deck reinforcement, or diagonal tension cracking at the corner. In the last three cases, the design fails to fully utilize the reinforcement, and may yet be preferred due to constructability and cost considerations, provided that the strength requirements are met.

The design in Fig. 3(b) requires a check against diagonal tension failure at the corner. The transverse load F_p applied to the post produces a compression force C_p in the post, which is transferred to the deck via formation of a diagonal compression strut of length l_{dc}. In addition, the shear force F_p is transferred to the deck as an axial force $-F_p$ and a bending moment $0.5F_pt_d$, which adds to F_pH_e to produce the resultant moment in the deck M_d that generates the force couple C_d and $F_{f,d}$, as detailed in Figs. 5(a and b). Diagonal cracking may occur prior to flexural failure in the deck as the concrete modulus of rupture f_r is reached along the diagonal strut.

The accuracy of analytical results based on the theory of elasticity, where a parabolic distribution of the tensile stress along l_{dc}

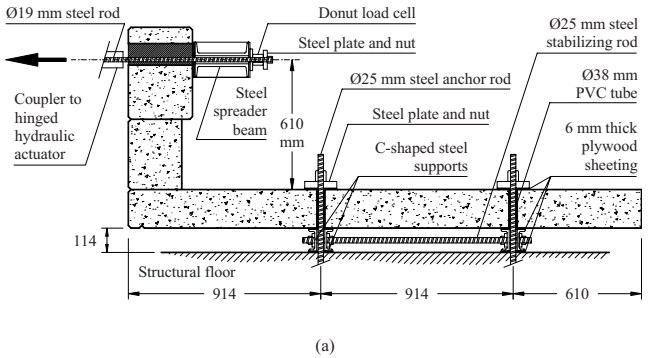

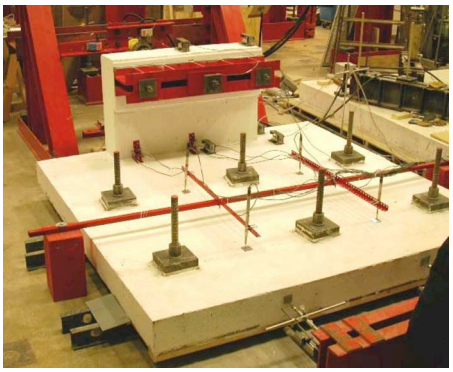

Fig. 4. Test setup: (a) schematic; (b) photograph (dimensions are in millimeters)

is assumed, has been demonstrated with respect to experimental results (Nilsson and Losberg 1976). The original closed-form procedure was herein modified and rendered in an iterative fashion to explicitly account for the effect of the shear force F_p in addition to the bending moment M_d, and is summarized in the flowchart in Fig. 6. The tensile force T acting perpendicular to the diagonal strut is computed neglecting any strength contribution of the slab portions adjacent to the connection, and assuming $f_r = 0.623\sqrt{f'_c}$ (MPa) (ACI 2005). Fig. 5(c) shows the free-body diagram of the corner in Specimen M2 with the resultant internal forces. Convergence is achieved for a nominal strength $F_{n,p}$ of 52.8 kN at 30% of the nominal flexural capacity of the deck section in Table 1. The design strength is computed as $\phi_{dt}F_{n,p} = 44.9$ kN by assuming a reduction factor for diagonal tension $\phi_{dt} = 0.85$, thus exceeding the required 44.5 kN. A shear key was included at the construction joint, and pockets were cut from the deck grating to simplify installation of the bar cages.

Table 1. Reinforcement and Flexural Capacity of Post and Deck Sections at Connection

Specimen	Connection section	Reinforcement	Nominal moment capacity M_n (kN m)	Design moment capacity $\phi_f M_n$ (kN m)
M1 (f'_c=41.4 MPa)	Post	12 No. 5 (16 mm) ρ_f=1.1%	218.7	109.4
	Deck (bars only)	10 No. 5 (16 mm), ρ_f=1.7%	78.3	54.8
	Deck (I-bars only)	12 grating I-bars ρ_f=1.7%	92.8	58.9
M2 (f'_c=27.6 MPa)	Post	10 No. 5 (16 mm) ρ_f=0.9%	172.9	87.7
	Deck	16 No. 5 (16 mm), ρ_f=2.2%	112.3	79.0

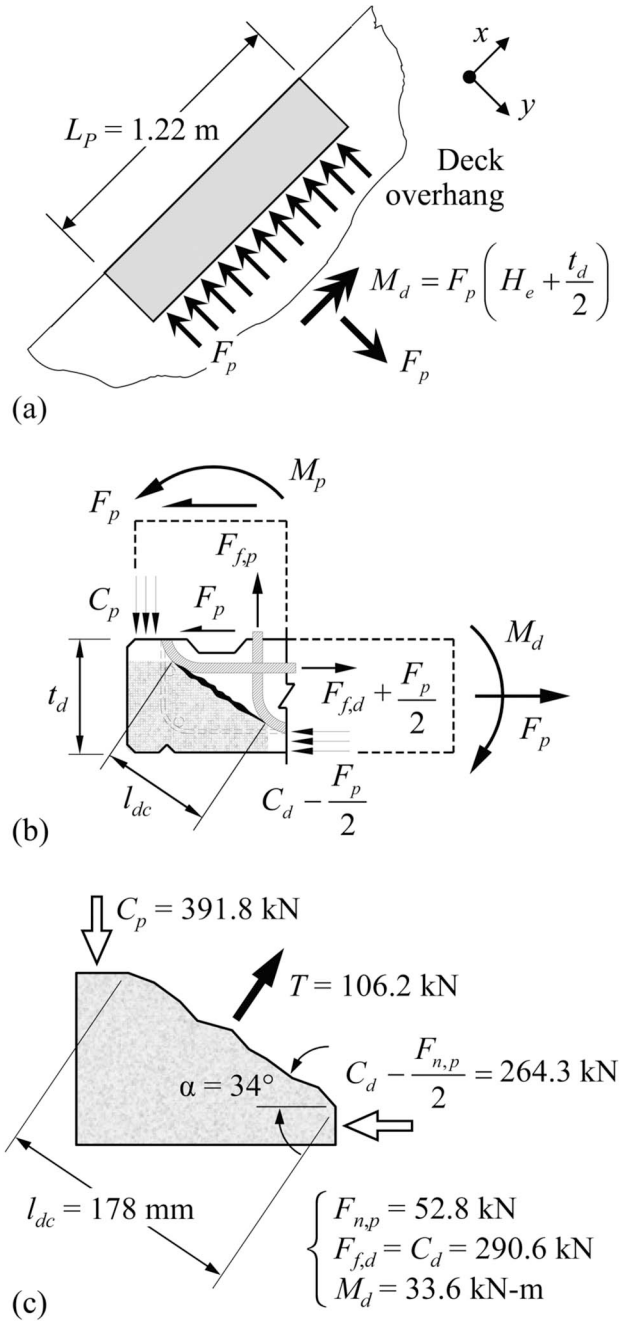

Fig. 5. Design of Specimen M2: (a) applied force and reactions in deck; (b) internal forces at connection; and (c) free-body diagram of corner joint

AASHTO (2002) also requires that the rail beam be designed for a bending moment due to concentrated load of 44.5 kN at the midsection of the opening of 44.5 kN$[L_O(m)/6]$=9.0 kN m using a 1.22 m opening length L_O. The beam design includes three No. 5 (16 mm) tension bars per side [Fig. 3(b)] with effective depth d of 259 mm, thus providing a nominal and design moment capacity $M_{n,b}$ and $\phi_f M_{n,b}$ of 70.5 and 35.2 kN m, respectively. The shear reinforcement consists of No. 4 (13 mm) double-C GFRP

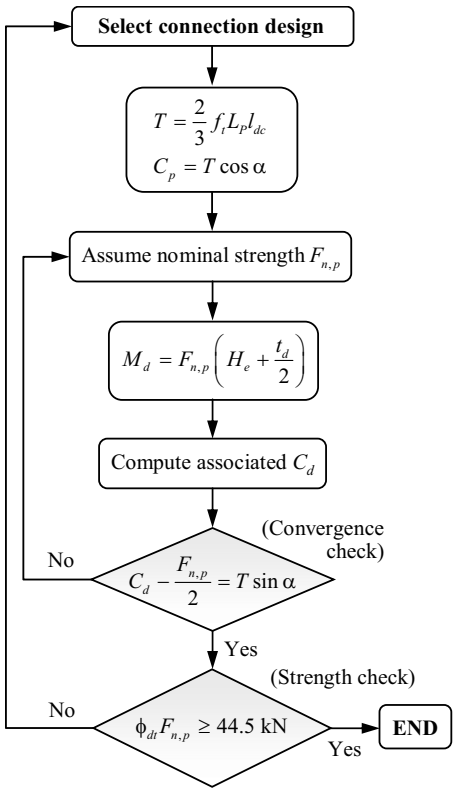

Fig. 6. Flowchart for post–deck connection design controlled by diagonal tension failure at corner

stirrups spaced at 102 mm on-center, which provide a design shear strength of 111.6 kN. The design allows for withstanding the maximum moment and shear produced by the design load, and to transfer it to the adjacent posts.

Materials

The reinforcement cages were constructed with pultruded E-glass/vinyl ester GFRP bars. The bars are deformed by means of helicoidal fiberglass wraps, and the surface is sand-coated to enhance compatibility with the surrounding concrete. Relevant properties are reported in Table 2, along with those of the I-bars in the deck reinforcement. Normal weight concrete was used, with maximum aggregate size of 9.5 mm. Six 152 mm (diameter) by 305 mm (height) cylinders were tested for each casting in accordance with ASTM C 39. The average compressive strength f_c for Specimen M1 was 53.7 MPa in the slab, and 40.3 MPa in the post. The values for Specimen M2 were 34.3 MPa in the slab, and 58.1 MPa in the post.

Table 2. Properties of GFRP Reinforcement

Reinforcement type	Cross-sectional area A_f (mm^2)	Modulus of elasticity E_f (GPa)	Tensile strength f^*_{fu} (MPa)	Ultimate strain ε^*_{fu} (%)
No. 5 (16 mm) bar	217.5	40.8	654.6	1.60
SIP grating I-bar	206.4[a]	31.0	551.2	1.78

[a]Net of predrilled holes for longitudinal cross rods.

Test Setup and Instrumentation

The test setup is detailed in Fig. 4. The slab was supported on 3.0 m long steel beams and tightened to the laboratory strong floor using two rows of three 25 mm steel threaded rods each spaced at 0.91 m on-center. The load was applied at a height of 610 mm from the slab surface using a steel double-C spreader beam, which was engaged by a steel plate and threaded rod assembly that connected to the hinged fitted end of a manually operated hydraulic jack.

The load was measured with a 111.2 kN capacity load cell. Direct current voltage transformer and draw-wire sensors were used to measure: transverse displacements at the top of the post, and at the base to check for slip at the post–deck interface; vertical displacements at the slab edge at the connection and at the tie-downs; and in-plane slab displacements. Inclinometers were mounted at the connection area and on top of the post to measure absolute and differential rotations. Linear potentiometers were used to check vertical and transverse crack openings at the post–deck interface. Several electrical-resistance strain gauges were used to measure strains in the FRP reinforcement in the connection and in the concrete at the base of the post.

Results and Discussion

Structural Behavior

The transverse displacement measured at the midsection on top of the post in Specimens M1 and M2 is plotted with respect to the applied load in Figs. 7(a and b), respectively. The dark dashed lines mark the strength requirement for the connections scaled from 44.5 to 39.8 kN to account for the height of the applied load line H_e increased from 546 to 610 mm. The gray continuous and dashed lines mark the nominal and design load, respectively, as per analysis according to the procedure in Fig. 6.

Linear response was recorded for Specimen M1 until cracking of the deck underneath the post and at the cold joint interface developed between 33.8 and 45.4 kN, with a marked decrease in stiffness [Fig. 7(a)] accompanied by increasing crack widths. Following, hairline cracks were observed in the slab between the post and the first tie-down line, which did not affect the overall stiffness. At a load of 59.4 kN and transverse displacement of 22 mm, a net stiffness loss was observed that was likely triggered by the loss of bond of the smooth I-bars in the top layer of the deck grating, with strain readings in the deck and the post well below that associated with flexural failure. An internal load transfer mechanism developed that allowed the connection to carry additional load up to 66.7 kN under very large deformations. Diagonal failure at the corner joint was accompanied by a drop in strain in the concrete at the base of the post and in the GFRP tension bars in the deck after attaining a maximum of $-939\ \mu\varepsilon$ and $756\ \mu\varepsilon$, respectively, again well below the analytical levels compatible with flexural failure controlled by concrete crushing. The interlaminar shear failure observed in the I-bars underneath the post indicated that the deck reinforcement contributed to the resisting mechanism either via bond or constraining action of the surrounding concrete. No slip was measured at the cold joint. The corner crack did not extend into the post, which remained attached to the deck, and could be inspected without showing signs of instability. The transverse strength exceeded that required as well as the theoretical nominal value, which may be partially attributed to the contribution of the deck I-bars in the load-resisting mechanism.

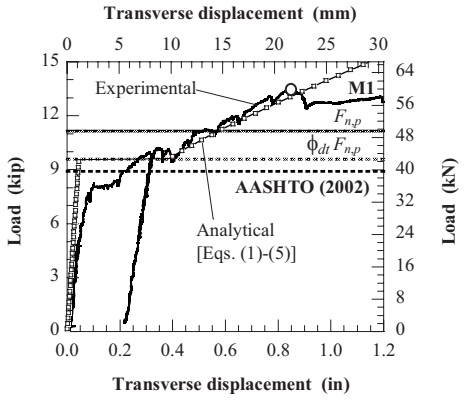

(a)

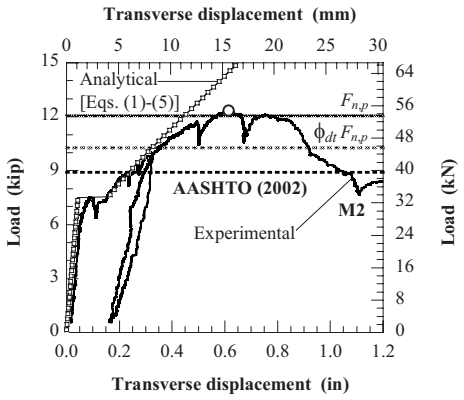

(b)

Fig. 7. Load–displacement response: (a) Specimen M1; (b) Specimen M2. Open circles indicate experimental strength of connections.

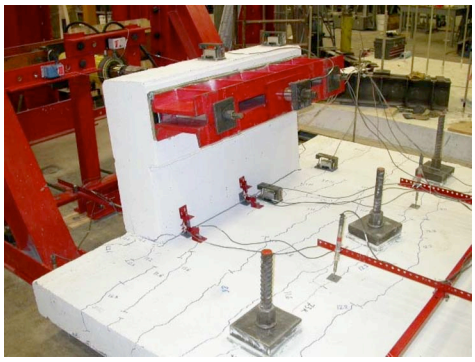

(a)

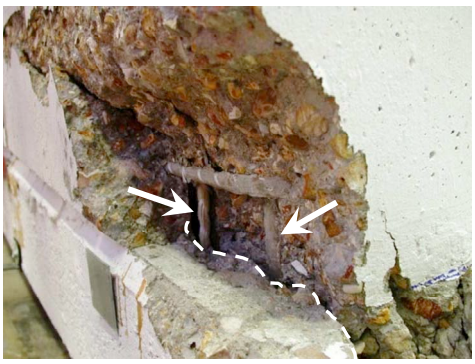

(b)

Fig. 8. Failure of Specimen M2: (a) photograph; (b) close-up of diagonal fracture surface at corner joint. Open arrows and dashed line indicate back of bent bars within post and fracture surface, respectively.

In Specimen M2, deck and post–deck interface cracking developed between 27.5 and 33.4 kN and was accompanied by a marked reduction in stiffness similar to Specimen M1, as seen in Fig. 7(b), and increasing crack widths. Following, hairline cracks developed in the slab as shown in Fig. 8(a) without affecting the overall stiffness, until failure occurred at a load of 54.7 kN. The value is in good agreement with the analytical prediction of 54.1 kN, and meets the AASHTO (2002) requirements. Fig. 8(b) shows a close-up of the diagonal fracture surface at the connection extending into the post behind the bent bars, likely driven by the shear key. No slip was measured at the construction joint. The maximum transverse displacement and rotation at the top of the post were 15.8 mm and 1.1°, respectively. Fig. 9(a) shows the location of the strain gauges in a typical section of Specimen M2. The diagonal crack occurred at a concrete strain at the base of the post of -119 $\mu\varepsilon$ as shown in Fig. 9(b), again far below that attributable to flexural failure of the overreinforced section. The tensile strain $t1$ measured in two bars at a section close to the diagonal strut is also plotted with respect to the load in Fig. 9(b). It can be seen that the theoretical limit of 2,265 $\mu\varepsilon$ associated with a net tensile force $F_{f,d}+0.5F_p=317.1$ kN from Fig. 5(c), thus significantly smaller than the ultimate value of 1.6%, was not exceeded. The post remained attached to the slab and could still carry load up to 28.1 kN when undergoing large deformations, in excess of the 152 mm stroke of the actuator.

Both designs did not allow one to fully exploit the flexural strength of the FRP RC deck section. The design of Specimen M2 was used for the bridge, as: (1) the reinforcement layout was believed to offer constructability advantages; (2) the code requirements could be met when using nominal 27.6 MPa concrete typically used for bridge decks and railings; (3) transverse strength could be accurately predicted; and (4) after failure, the connection did not separate and could still withstand load.

Analytical Modeling of Connection Response

The maximum transverse displacement at the top of the post with respect to the applied load, $u(F_p)$, can be approximated as the sum of two contributions, namely: that from the rigid body motion due to the rotation θ_d of the overhang subjected to a moment M_d/L_P per unit width; and that from the post cantilever subjected to a transverse load F_p/L_P per unit width applied at a height H_e from the slab surface. The two contributions are illustrated in Figs. 10(a and b), respectively, where a slab strip of width L_P is used for convenience. Therefore, the displacement function can be expressed in the form

$$u(F_p) = H \sin \theta_d + u_p \cos \theta_d \tag{1}$$

where the overhang rotation is

$$\theta_d(F_p) = F_p\left(H_e + \frac{t_d}{2}\right)\frac{l_{\text{overhang}}}{E_c I_d} \tag{2}$$

and the transverse displacement u_p from cantilever response is

$$u_p(F_p) = \frac{F_p H_e^3}{3E_c I_p}\left[1 + \frac{3}{2}\left(\frac{H}{H_e} - 1\right)\right] \tag{3}$$

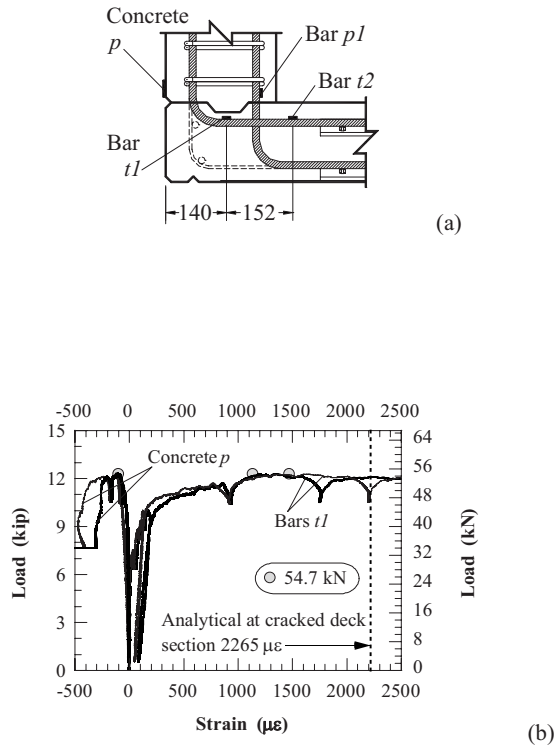

Fig. 9. Load–strain response of Specimen M2: (a) location of sensors at typical section (dimensions in mm); (b) concrete p and bar $t1$ strains at two sections. Gray circles indicate strain at failure.

The nonlinear behavior of the overhang is rendered by replacing the gross moment of inertia with the effective moment of inertia of the connected section as the bending moment M_d exceeds the cracking level M_{cr}. The format of the modified Branson's equation in the current ACI 440 guidelines (ACI 2006)

$$I_d(M_d) = \left(\frac{M_{cr}}{M_d}\right)^3 \beta_d I_g + \left[1 - \left(\frac{M_{cr}}{M_d}\right)^3\right] I_{cr} \leq I_g \tag{4}$$

is adopted, and simultaneously incorporates the reduction coefficient

$$\beta_d = \left(3.3\frac{I_{cr}}{I_g}\right) \tag{5}$$

to account for the reduced tension stiffening in FRP RC (Bischoff 2007). Cracking in the slab at the connection is assumed to occur concurrently with that at the cold joint between post and slab, as confirmed by the experiments. The gross moment of inertia of the post section is then replaced in Eq. (3) with the cracked moment of inertia. A concrete elastic modulus $E_c = 4733\sqrt{f_c}$ (MPa) is assumed in the calculations (ACI 2005).

The displacement function in Eq. (1) is plotted for Specimens M1 and M2 in Figs. 7(a and b), respectively. Both the strength and stiffness response of Specimen M2 selected for implementation were accurately modeled using the procedure in Fig. 6 and Eqs. (1)–(5), respectively. The connection model was integrated into the structural analysis of a post-and-beam railing system based on Specimen M2, which is addressed in the next section.

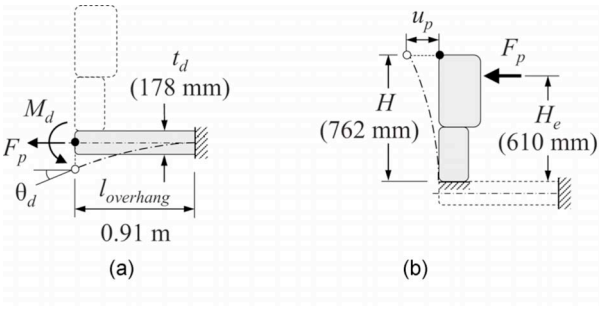

Fig. 10. Analytical modeling of transverse post displacement: (a) rotation of overhang under applied moment M_d; (b) post cantilever under applied force F_p

Implications in Structural Design

Differently from the *AASHTO Standard Specifications* (AASHTO 2002), Section 13 (Railings) of the LRFD Bridge Design Specifications (AASHTO 2004) mandates strength criteria at the system level. Whereas the former approach lends itself to analogy- and empirical-based design of post, beam, and connection sections, the latter demands more rigorous procedures to evaluate integrated post-and-beam structural systems. Based on the results of full-scale crash tests performed as part of programs conducted under the aegis of the Federal Highway Administration, the American Association of State Highway and Transportation Officials, the National Cooperative Highway Research Program, and individual states, the dynamic loads imparted by an impacting vehicle under specified crash test conditions (Ross et al. 1993) are translated into equivalent factored transverse, longitudinal, and vertical static loads (AASHTO 2004). The transverse load F_t is typically the one of concern for RC railing structures. For the case of TL-2 crash test level applicable to the railing of Bridge No. 14802301, the transverse load demand is 120.1 kN, where the load is assumed uniformly distributed along a length L_t of 1.22 m, at a vertical distance of 508 mm from the deck surface.

Yield line analysis is typically invoked to evaluate the nominal strength of steel RC railings (Hirsch 1978; AASHTO 2004). Due to the linear elastic behavior of FRP bars up to failure, moment redistribution cannot be accounted for in design. The methodology used herein to study the structural behavior of the GFRP RC railing in Fig. 2 is pursuant to the analysis and design principles set forth in the ACI 440 guidelines (ACI 2006). First, the post and beam finite elements are defined. Second, the global stiffness matrix is assembled and implemented into the nonlinear finite-element analysis (FEA) of the post-and-beam system. Design strength and failure modes are determined and discussed on the basis of code requirements.

Numerical Formulation of Post and Beam Elements

A nonlinear spring is used to idealize the post and its connection to the deck, with a single degree of freedom (DOF) of the node i associated with the transverse displacement u_i at the top of the post, as illustrated in Fig. 11(a). The load–displacement function described by Eq. (1) is accurately approximated by a trilinear function. It should be noted that the strength reduction factor for diagonal tension ϕ_{dt} is reduced from 0.85 to 0.75 to reflect use of ACI 440.1R-06 (ACI 2006) in lieu of the 2003 guidelines (ACI 2003).

Fig. 11(b) shows the idealization and the numerical formulation of the GFRP RC beam element along the railing opening. A single DOF associated with transverse displacement is assigned to each end node i and j, where rigid connections to the adjacent posts are assumed. Torsional effects are neglected, which is a

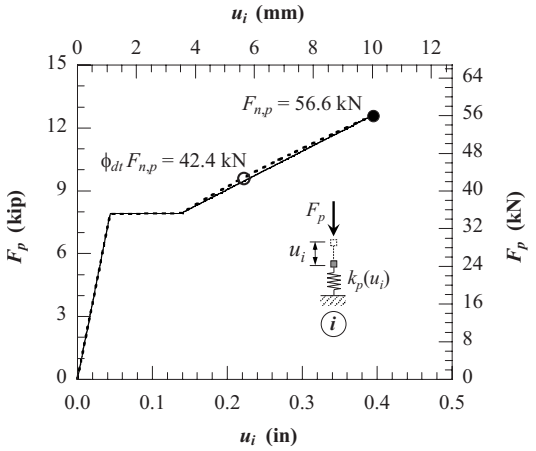

(a)

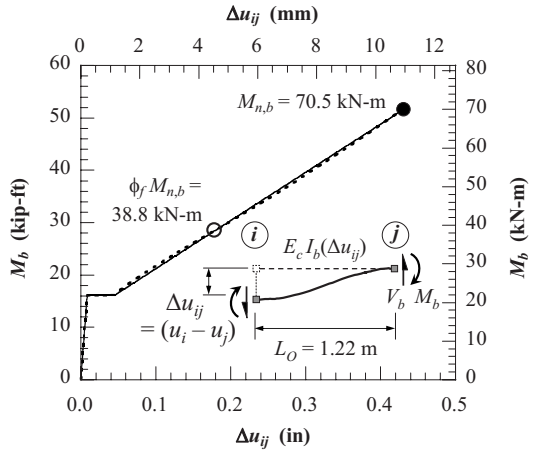

(b)

Fig. 11. Finite-element formulation: (a) spring element for post; (b) beam element along opening. Dashed and continuous lines indicate analytical solution and trilinear approximation, respectively. Closed and open circles indicate nominal and design strength, respectively.

reasonable assumption under small displacements. The nonlinear moment-net displacement function M_b-Δu_{ij} defined via Eqs. (4) and (5) is again approximated in a trilinear form. Concrete with compressive strength of 27.6 MPa is assumed for both elements. An enviromental reduction factor C_E of 0.7 is used to compute the design strength of the FRP bars.

Nonlinear Finite-Element Analysis of Railing

Two critical transverse loading scenarios are identified for the open-post railing in Fig. 2. *Case A* is sketched in Fig. 12(a) and accounts for the equivalent static load F_t applied on a rail beam at the midsection of the opening. *Case B* is sketched in Fig. 12(b) and accounts for the transverse load applied directly on an intermediate post.

The symmetric finite-element model (FEM) shown in Fig. 12(c) is used to study the structural response of the railing system, where the stiffness k_1 of the post closest to the impact section (that is, at the node $i=1$) is reduced from k_p in the first load case to $0.5k_p$ in the second load case. The vector of the transverse displacement of the posts

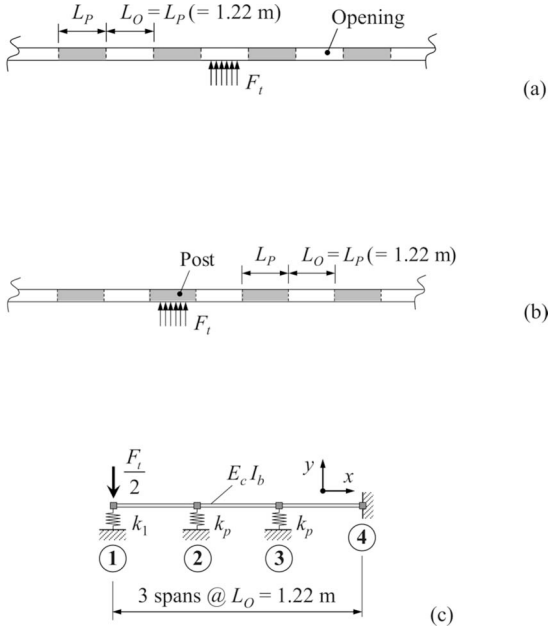

Fig. 12. Structural analysis of railing: (a) load applied to rail beam at opening (*Case A*); (b) load applied to post (*Case B*); and (c) three-DOF FEM of symmetric post-and-beam system

$$\mathbf{u} = \begin{bmatrix} u_1 \\ u_2 \\ u_3 \end{bmatrix} \tag{6}$$

is computed for a given transverse force vector

$$\mathbf{F}_t = \begin{bmatrix} \frac{F_t}{2} \\ 0 \\ 0 \end{bmatrix} \tag{7}$$

by solving the nonlinear system

$$\mathbf{u} = \mathbf{K}(\mathbf{u})^{-1}\mathbf{F}_t \tag{8}$$

where the global stiffness matrix of the post-and-beam system in Fig. 12(c) is assembled as

$$\mathbf{K}(\mathbf{u}) = \begin{bmatrix} K_{11}(\mathbf{u}) & K_{12}(\mathbf{u}) & 0 \\ K_{21}(\mathbf{u}) & K_{22}(\mathbf{u}) & K_{23}(\mathbf{u}) \\ 0 & K_{32}(\mathbf{u}) & K_{33}(\mathbf{u}) \end{bmatrix} \tag{9}$$

with

$$K_{11}(\mathbf{u}) = \frac{2}{L_O}\frac{|M_b(\Delta u_{12})|}{\Delta u_{12}} + k_1(u_1)$$

$$k_1(u_1) = \begin{cases} k_p(u_1) & \text{for impact on rail beam (\textit{Case A})} \\ \frac{1}{2}k_p(u_1) & \text{for impact on post (\textit{Case B})} \end{cases} \tag{10a}$$

$$K_{12}(\mathbf{u}) = K_{21}(\mathbf{u}) = -\frac{2}{L_O}\frac{|M_b(\Delta u_{12})|}{\Delta u_{12}} \tag{10b}$$

Table 3. Convergence Check for Railing FEA for $F_t=\phi R_t$ for Load *Case A* and *Case B*[a]

DOF number in post-and-beam FEM	$N=1$	$N=2$	$N=3$
Maximum transverse post displacement u_1 (mm)	4.8 4.7	5.4	5.4
Maximum transverse force resisted by post $k_1(u_1)$ (kN)	39.5 39.2	41.5	41.5
Maximum bending moment in railing beam $M_b(\Delta u_{12})$ (kN m)	40.6 39.5	38.8[b]	38.8[b]
Shear force transmitted by railing beam to end post $V_b(\Delta u_{N,N+1})$ (kN)	65.6 64.8	35.9	30.2

[a]Values on top for *Case A* and bottom for *Case B* when different ($N=1$).

[b]Design moment capacity of beam $\phi_f M_{n,b}=38.8$ kN m controls.

$$K_{22}(\mathbf{u}) = \frac{2}{L_O}\left[\frac{|M_b(\Delta u_{12})|}{\Delta u_{12}} + \frac{|M_b(\Delta u_{23})|}{\Delta u_{23}}\right] + k_p(u_2) \quad (10c)$$

$$K_{23}(\mathbf{u}) = K_{32}(\mathbf{u}) = -\frac{2}{L_O}\frac{|M_b(\Delta u_{23})|}{\Delta u_{23}} \quad (10d)$$

$$K_{33}(\mathbf{u}) = \frac{2}{L_O}\left[\frac{|M_b(\Delta u_{23})|}{\Delta u_{23}} + \frac{|M_b(\Delta u_{34})|}{\Delta u_{34}}\right] + k_p(u_3) \quad (10e)$$

Optimal solution strategies may be selected (for example, conjugate gradient, Levenberg–Marquardt, quasi-Newton) to compute the post displacement vector **u**, from which the internal forces can be retrieved.

The structural adequacy is evaluated on the basis of three criteria: first, the maximum reaction force at a connection cannot exceed the design strength $[k_1(u_1) \leq \phi_{dt} F_{n,p}]$; second, the maximum bending moment at the beam ends cannot exceed the design strength $[M_b(\Delta u_{12}) \leq \phi_f M_{n,b}]$, provided that shear does not control design; and third, the outermost post $[i=3$ in Fig. 12(c)$]$ must be able to resist the shear transmitted by the beam $[V_b(\Delta u_{34}) = 2M_b(\Delta u_{34})/L_O \leq \phi_{dt} F_{n,p}]$.

Table 3 summarizes the maximum post displacement u_1 and the resulting internal forces for load *Case A* and *Case B* at the railing design strength level ϕR_t of 210.2 and 168.7 kN, respectively, which are controlled by the beam flexural strength. The FEA results are given for a DOF number N of 1, 2, and 3 to check convergence of the selected discretization. For $N=1$ and $N=2$, the stiffness matrix was derived by simply eliminating the last two and one rows and columns, respectively, from $\mathbf{K}(\mathbf{u})$ in Eq. (9). It can be seen that assuming three unknown post displacements as in Fig. 12(c) allows one to achieve a good convergence in the maximum connection displacement (and thus reaction force) and beam moment, whereas the shear transmitted at the end post rapidly drops well within the design limit. The nonlinear load–maximum displacement (F_t–u_1) response is plotted in Fig. 13 for load *Case A* and *Case B*. The design strength ϕR_t always exceeds the 120.1 kN TL-2 transverse load demand (AASHTO 2004), whose level is associated with very small displacements, as desirable for RC railings for which negligible values are typically measured during crash tests.

The FEA was repeated considering a beam opening length L_O increase from 1.22 to 1.83 m, thus similar to the geometry of the steel RC MKCR, and up to 3.66 m, where the component strength requirements in the AASHTO Standard Specifications (2002) are still satisfied. At increased opening lengths, design is controlled by the connection strength instead of the beam moment capacity. The design strengths for load *Case A* and *Case B* are plotted in Fig. 14 with respect to the opening length L_O. It is noted that the modifications may result in insufficient design strength when applying the 120.1 kN TL-2 load demand. In such instances, the design may require modification of either or both the post–deck connection, for example by increasing the post width, and the rail beam, for example by adding longitudinal bars.

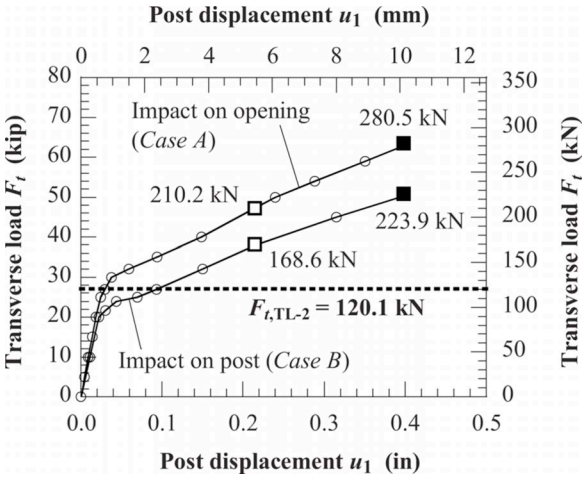

Fig. 13. Numerical load–displacement response of Bridge No. 1482301 railing. Closed and open squares indicate nominal and design strength, respectively.

Impact on Design Guidelines

The current ACI guidelines (ACI 2006) do not include specific recommendations for the design of discontinuity regions in FRP RC frames, despite such details are well known as being affected by a variety of design errors in practice. In light of the increasing use of FRP bars in a number of structural applications where connections may be present, it is believed that a section should be added that addresses design for common reinforcement layouts and load conditions.

Approaches that combine basic structural analysis principles with FRP RC theory should be selected on a case-by-case basis. The case study presented herein has demonstrated the use of a simple method to determine the nominal and design strength of a FRP RC corner joint subjected to combined shear force and open-

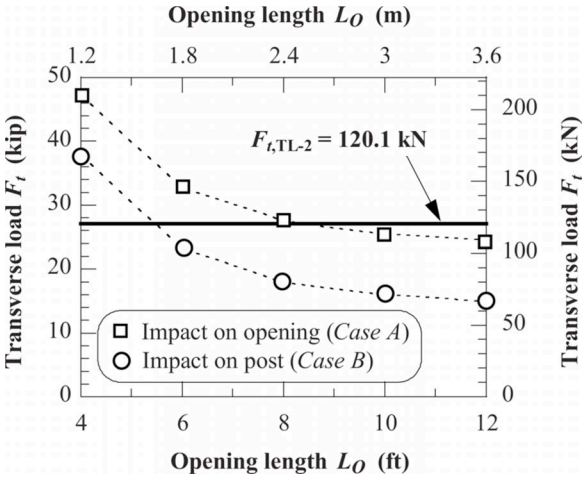

Fig. 14. Design strength of railing at varying opening length L_O

ing bending moment. The internal forces were computed by imposing equilibrium conditions at the corner, and the associated bending moment was back-calculated consistently with well-established flexural analysis principles for FRP RC. The adoption of similar design algorithms for different details and load cases may enable one to design and retain structurally sound solutions where the full flexural strength of the connected sections may not be attained, thereby providing the rational basis to underpin legitimate practical and economical decision making.

The theoretical results on the lateral strength of rigidly connected post-and-beam systems at increasing beam opening length indicate that a component-based design approach, although accepted for steel RC, may not be as adequate in the current terms (AASHTO 2002). The implementation of analytical or numerical methods that impose equilibrium and compatibility at the system level becomes necessary to ensure strength and to preliminarily evaluate functionality performances that relate to deflection, such as in the case of bridge railings.

Conclusions

In the first part of this paper, moving from the results of quasi-static testing of two GFRP RC post–deck subassemblies where deformed bars were used in combination with a smooth deck grating, a rational design for the connection to meet specification mandated criteria at the component level (AASHTO 2002) has been validated, and selected for implementation in the open-post railing of an off-system bridge in Missouri. The structural response of the connection until failure was accurately modeled on the basis of simple structural analysis pursuant to well-established design principles of FRP RC.

The second part of the paper has demonstrated the application of a methodology for the structural analysis and design of FRP RC open-post railing systems where internal forces, deformations, and failure modes are rationally determined. The analytical model of the post–deck connection was incorporated into a finite-element model defined to study the structural behavior of the post-and-beam system subjected to the equivalent static load up to failure, as prescribed in the current LRFD specifications (AASHTO 2004). The railing design implemented was shown to meet the global strength requirement when undergoing very small deformations, which is typical of crashworthy RC railings.

In terms of potential impact on the ACI 440 (2006) design guidelines, the research presented herein has introduced the need to rationally address the design of common discontinuity regions in FRP RC frames. The common case of a corner joint subjected to combined shear and opening bending moment has been illustrated. Specific to the analysis and design of open-post concrete railings, the case studies analyzed numerically show that a simplified nonlinear analysis methodology that satisfies basic equilibrium and compatibility assumptions may be applied to devise more rational design solutions for either implementation or, when required, for crash testing.

Acknowledgments

The financial support of the Missouri University of Science and Technology (Missouri S&T; formerly, University of Missouri-Rolla) National University Transportation Center on Advanced Materials and NDT Technologies is acknowledged. The assistance of the industry members of the NSF I/UCRC "Repair of Buildings and Bridges with Composites" (RB^2C), Hughes Brothers, Inc. and Strongwell Corp., in supplying the FRP reinforcement for the railing and the slab, respectively, is acknowledged. Special thanks are extended to the personnel of the Missouri S&T Structures Laboratory for valuable help in the test phases, and to the Greene County Highway Department and Great River Engineering of Springfield, Inc., for the technical support provider.

Notation

The following symbols are used in this paper:

A_f = cross-sectional area of FRP tension reinforcement;
C_d, C_p = compression force at deck and post connection section;
d = distance from extreme compression fiber to centroid of tension reinforcement;
E_c = modulus of elasticity of concrete;
E_f = longitudinal modulus of elasticity of FRP;
$\mathbf{F}_t$ = transverse force vector;
$F_{f,d}$, $F_{f,p}$ = tension force in reinforcement at deck and post connection section;
F_l, F_t, F_v = longitudinal, transverse, and vertical equivalent static load;
$F_{n,p}$ = nominal strength of post–deck connection;
F_p = transverse load applied to post–deck connection;
$F_{t,\mathrm{TL\text{-}2}}$ = equivalent transverse static strength requirement for crash Test Level 2 railing;
f_c = cylinder compressive strength of concrete;
f_{fu}^* = guaranteed tensile strength of FRP bar;
f_r = modulus of rupture of concrete;
H = height of railing;
H_e = height of applied transverse and longitudinal load line with respect to deck surface;
I_b, I_d, I_p = section moment of inertia of rail beam, deck at connection, and post;
I_{cr} = moment of inertia of transformed cracked section;
I_g = gross moment of inertia;
$\mathbf{K}(\mathbf{u})$ = nonlinear stiffness matrix of railing FEM;
k_1 = stiffness of post closest to applied equivalent static load in FEM;
k_p = stiffness of intermediate post in FEM;
L_O = length of rail beam opening;
L_P = width of post;
L_t = uniform distribution length for transverse static load;
l_{dc} = length of diagonal crack;
l_{overhang} = overhang length;
M_b = moment at ends of rail beam element;
M_{cr} = cracking moment;
M_d = deck moment at connection section;
$M_{n,b}$ = nominal moment capacity of FRP RC rail beam section;
N = number of DOF in symmetric railing FEM;
R_t, ϕR_t = nominal and design strength of railing under equivalent transverse static load;
T = tensile force on diagonal crack;
t_d = thickness of bridge deck at connection with post;
$\mathbf{u}$ = transverse post displacement vector;

u = maximum displacement of post subassembly under transverse load;
u_i, u_j = transverse displacement of post element at nodes i and j of post-and-beam FEM;
u_p = cantilever displacement component of post subassembly;
u_1, u_2, u_3 = transverse displacement of post element at nodes 1, 2, and 3 of post-and-beam FEM;
V_b = shear at ends of rail beam element;
α = angle of diagonal crack with respect to deck plane;
β_d = reduction coefficient used in computing effective moment of inertia;
Δu_{ij} = net displacement of rail beam element between nodes i and j;
ε^*_{fu} = guaranteed rupture strain of FRP bar;
θ_d = maximum rotation of overhang under bending moment;
ρ_f = FRP reinforcement ratio;
ϕ_{dt} = strength reduction factor for diagonal tension; and
ϕ_f = strength reduction factor for flexure.

References

American Association of State Highway and Transportation Officials (AASHTO). (2002). *Standard specifications for highway bridges*, 17th Ed., Washington, D.C.

American Association of State Highway and Transportation Officials (AASHTO). (2004). *Load and resistance factor design (LRFD) bridge design specifications*, 3rd Ed., Washington, D.C.

American Concrete Institute (ACI). (2003). "Guide for the design and construction of concrete reinforced with FRP bars." *ACI 440.1R-03*, ACI Committee 440, Farmington Hills, Mich.

American Concrete Institute (ACI). (2005). "Building code requirements for structural concrete." *ACI 318-05*, Farmington Hills, Mich.

American Concrete Institute (ACI). (2006). "Guide for the design and construction of structural concrete reinforced with FRP bars." *ACI 440.1R-06*, ACI Committee 440, Farmington Hills, Mich.

Benmokrane, B., El-Salakawy, E., Desgagné, G., and Lackey, T. (2004). "FRP bars for bridges." *Concr. Int.*, 26(8), 84–90.

Benmokrane, B., El-Salakawy, E., El-Ragaby, A., and Lackey, T. (2006). "Designing and testing of concrete bridge decks reinforced with glass FRP bars." *J. Bridge Eng.*, 11(2), 217–229.

Bischoff, P. H. (2007). "Deflection calculation of FRP reinforced concrete beams based on modifications to the existing Branson equation." *J. Compos. Constr.*, 11(1), 4–14.

Bligh, R. P., Abu-Odeh, A. Y., Hamilton, M. E., and Seckinger, N. R. (2004). "Evaluation of roadside safety devices using finite element analysis." *Rep. No. FHWA/TX-04/0-1816-1*, Texas Transportation Institute, College Station, Tex.

Bradberry, T. E. (2001). "Fiber-reinforced-plastic bar reinforced concrete bridge decks." *Proc., 80th Annual Transportation Research Board Meeting* (CD-ROM 01-3247), Transportation Research Board, Washington, D.C.

Busel, J. P., Gremel, D., Jutte, B., Barefoot, G., Carson, J., and Matta, F. (2008). "Composites in concrete structures, state of the practice—Part 2." *Compos. Manuf. Mag.*, 24(3), 38–41 and 56–57.

Buth, C. E., Williams, W. F., Bligh, R. P., Menges, W. L., and Haug, R. R. (2003). "Performance of the TxDOT T202 (MOD) bridge rail reinforced with fiber reinforced polymer bars." *Rep. No. FHWA/TX-03/0-4138-3*, Texas Transportation Institute, College Station, Tex.

Canadian Standards Association (CSA). (2006). "Canadian highway bridge design code." *CAN/CSA-S6-06*, Mississauga, Ont., Canada.

Deitz, D. H., Harik, I. E., Gesund, H., and Zatar, W. A. (2004). "Barrier wall impact simulation of reinforced concrete decks with steel and glass fiber reinforced polymer bars." *J. Compos. Constr.*, 8(4), 369–373.

El-Salakawy, E., Benmokrane, B., Masmoudi, R., Brière, F., and Breaumier, E. (2003). "Concrete bridge barriers reinforced with glass fiber-reinforced polymer composite bars." *ACI Struct. J.*, 100(6), 815–824.

Hirsch, T. J. (1978). "Analytical evaluation of Texas bridge rails to contain buses and trucks." *Rep. No. FHWATX-78-230-2*, Texas Transportation Institute, College Station, Tex.

Maheu, J., and Bakht, B. (2004). "A new connection between concrete barrier walls and bridge decks." *Proc., Annual Conf. of the Canadian Society of Civil Engineering*, Canadian Society of Civil Engineering (CSCE), Montreal, QC, Canada, 224–229.

Mak, K. K., and Bligh, R. P. (2002). "Assessment of NCHRP Report 350 test conditions." *Transportation Research Record. 1797*, Transportation Research Board, Washington, D.C., 38–43.

Matta, F., and Nanni, A. (2006). "Design of concrete railing reinforced with glass fiber reinforced polymer bars." *Proc., 2006 ASCE/SEI Structures Congress* (CD-ROM), ASCE, Reston, Va.

Matta, F., Nanni, A., and Bank, L. C. (2007). "Prefabricated FRP reinforcement for concrete bridge deck and railing: Design, laboratory validation, and field implementation." *Proc., Inaugural IIFC Asia-Pacific Conf. on FRP in Structures (APFIS 2007)*, Vol. 1, Department of Civil Engineering, University of Hong Kong, Hong Kong, 319–324.

Mufti, A., Banthia, N., Benmokrane, B., Boulfiza, M., and Newhook, J. (2007). "Durability of GFRP composite rods." *Concr. Int.*, 29(2), 37–42.

Nanni, A. (1993). "Flexural behavior and design of RC members using FRP reinforcement." *J. Struct. Eng.*, 119(11), 3344–3359.

Nanni, A. (2003). "North American design guidelines for concrete reinforcement and strengthening using FRP: Principles, applications and unresolved issues." *Constr. Build. Mater.*, 17(6–7), 439–446.

Nanni, A., and Faza, S. (2002). "Designing and constructing with FRP bars: An emerging technology." *Concr. Int.*, 24(11), 53–58.

Nilsson, I. H. E., and Losberg, A. (1976). "Reinforced concrete corners and joints subjected to bending moment." *J. Struct. Div.*, 102(6), 1229–1254.

Phelan, R. S., Vann, W. P., and Bice, J. (2003). "FRP reinforcing bars in bridge decks—Field instrumentation and short-term monitoring." *Rep. No. FHWA/TX-06/9-1520-4*, Texas Tech Univ., Lubbock, Tex.

Ross, H. E., Sicking, D. L., Zimmer, R. A., and Michie, J. D. (1993). "Recommended procedures for the safety performance evaluation of highway features." *NCHRP Report No. 350*, National Academy Press, Washington, D.C.

Trejo, D., Aguiniga, F., Buth, E. C., James, R. W., and Keating, P. B. (2001). "Pendulum impact tests on bridge deck sections." *Rep. No. FHWA-01/1520-1*, Texas Transportation Institute, College Station, Tex.

Cost-Effective, Structural Stay-in-Place Formwork System of Fiber-Reinforced Polymer for Accelerated and Durable Bridge Deck Construction

Thomas E. Ringelstetter, Lawrence C. Bank, Michael G. Oliva, Jeffrey S. Russell, Fabio Matta, and Antonio Nanni

This paper describes research on the evolution of a cost-effective, structural stay-in-place (SIP) formwork bridge deck system with an integrated modular three-dimensional fiber-reinforced polymer (FRP) reinforcement cage. Recent research conducted at the University of Wisconsin is reviewed to show the evolution of the reinforcing system to include an integral FRP SIP form. The evolution occurred through laboratory testing, which was followed by the design and construction of two bridge structures owned by the State of Wisconsin. Each structure used different FRP reinforcement and formwork. These projects pointed out the need for a competitive SIP formwork to be used in conjunction with FRP reinforcement. Two specimens with different FRP reinforcement and SIP formwork arrangements were tested. Full-scale deck slab specimens were tested by applying a simulated wheel design load to investigate the static response, ultimate capacity, and failure mechanism. The most economical FRP reinforcing system has been implemented in a superstructure replacement project in Greene County, Missouri.

Many highway bridges in the United States are located in climates where deicing salts are used on the highway systems. Deicing agents can cause corrosion of the metallic elements of the bridge structure, thereby shortening its useful life and requiring either repair or replacement. The economic impact of construction operations for bridge rehabilitation or replacement drives the need for cost-effective and durable structural deck systems. Implementation of a pultruded fiber-reinforced polymer (FRP) reinforcement system promises to eliminate the effects of corrosion on the reinforcing system.

The use of permanent stay-in-place (SIP) formwork systems in highway bridge construction is standard practice for many departments of transportation throughout the United States, especially in regions where deicing agents are not typically used. Conventional bridge deck forming typically requires labor to install and remove plywood formwork, which translates into additional time on the project and potentially increased project cost. Because the SIP forms are not removed after the concrete has hardened, labor costs and possibly project duration are decreased. Essentially, two SIP formwork systems have been implemented in the United States: preformed steel deck panels and partial depth precast–prestressed concrete panels. In states with aggressive environments, metallic forms can corrode, but the use of either SIP form system does not allow for the inspection of the underside of the deck. The use of an FRP reinforcing system reduces the need for visual inspection of the underside of the deck, because corrosion of the reinforcement is not an issue. Use of a nonmetallic FRP SIP form that is not susceptible to electrochemical corrosion would provide a more acceptable system for use in highway bridge decks, even in aggressive environments.

SIP formwork is classified as either structural or nonstructural. Structural SIP forms are part of the structural system that acts compositely with the framing system to resist the in-service live load, as well as the wet concrete load during deck placement. Conversely, nonstructural SIP forms are designed to resist only the loads from the wet concrete and construction live load until the concrete has hardened. Structural SIP forms are more economical than nonstructural SIP forms because of integration of the formwork with the reinforcing system, which also reduces the amount of material that needs to be installed.

RESEARCH AND DEVELOPMENT OF FRP STRUCTURAL SIP

Experimental Use of FRP Reinforcement

Through FHWA's Innovative Bridge Research and Construction (IBRC) program, the Wisconsin Department of Transportation (WisDOT) supported an experimental and analytical investigation into the use of an FRP reinforcement system for highway bridge decks as a method of increasing their long-term durability (*1*). The investigation culminated in the construction of a twin, two-lane bridge structure with two continuous spans near the city of Fond du Lac, Wisconsin, that used a reinforcement system composed of two layers of FRP reinforcing.

The top layer was a bidirectional FRP grid panel that provided both transverse and longitudinal reinforcement (with respect to the centerline of girders). The transverse reinforcing was provided by

T. E. Ringelstetter, Room 2225; L. C. Bank, Room 1218; M. G. Oliva, Room 2212; and J. S. Russell, Room 2258, Department of Civil and Environmental Engineering, University of Wisconsin–Madison, Engineering Hall, 1415 Engineering Drive, Madison, WI 53706. F. Matta, 220 Engineering Research Laboratory, and A. Nanni, 223 Engineering Research Laboratory, Center for Infrastructure Engineering Studies, University of Missouri–Rolla, 1870 Miner Circle Drive, Rolla, MO 65409.

Transportation Research Record: Journal of the Transportation Research Board, No. 1976, Transportation Research Board of the National Academies, Washington, D.C., 2006, pp. 183–189.

pultruded FRP I-bars 2 in. (50.8 mm) deep. Temperature and shrinkage reinforcement, as well as distribution reinforcement, was provided by a three-piece cross rod that penetrated through the web of the transverse I-bars. The cross rods mechanically locked into the I-bar webs. Both the I-bars and cross rods were spaced at 4 in. (101.6 mm) on center (*1*).

Bottom layer reinforcing was provided by a pultruded FRP SIP deck form. Composite Deck Solutions, Inc. (CDS), of Dayton, Ohio, produced the SIP form used. The deck form panels were 18 in. (457.2 mm) wide, with a shiplap joint to allow the forms to overlap and prevent concrete leakage during placement. The form panels were stiffened by hollow corrugations 3 in. (76.2 mm) square. The form panel was made composite with the concrete deck through the use of ¼-in. (6.35-mm) aggregate that was epoxy bonded to a large portion of the horizontal surfaces of the panel.

The installation of the CDS deck panels is shown in Figure 1. Installation of this system is described elsewhere (*2, 3*).

Jacobson et al. (*4, 5*) investigated the use of a full-width double-layer FRP grating system that employed conventional bridge deck forming (Figure 2). The double-layer FRP grating was successfully implemented in a bridge deck for a structure on US-151 over De Neveu Creek in Wisconsin. To provide clearance between the bottom of the reinforcing and the bottom surface of the concrete deck, the connectors were extended 1 in. (25.4 mm) to act as chairs. This was an important step in the evolution of the system from the one-layer FRP grid with SIP form to the current system, a modular double-layer FRP grating with integral SIP formwork.

SIP Formwork Optimization Research

Two configurations of reinforcing and SIP formwork systems have been investigated to optimize strength and economic characteristics. The FRP shapes used in the reinforcing were off-the-shelf components of existing products.

One system incorporated an existing pultruded FRP decking product, SafPlank, produced by Strongwell of Bristol, Virginia, as shown in Figure 3. This product consisted of two layers of reinforcing—a bottom panel and a top grid—and had a deck thickness of 8 in. (203.2 mm). This system is referred to as the SafPlank system.

FIGURE 1 Installation of CDS deck panels.

FIGURE 2 Installation of full-width double-layer grid.

The bottom layer was composed of modular 2-ft (0.609-m) panels that had a nominal 1/8-in. (3.175-mm) bottom plate with integral 2-in. (50.8-mm) T-rib sections placed at nominal 4-in. (101.6-mm) spacing. The decking panel provided the positive-moment reinforcing for the deck structure as well as for the SIP form. Perpendicular to the T-ribs, three-piece cross rods spaced at 4 in. (101.6 mm) on center were placed in holes that were drilled through the web of the T-rib. These cross rods mechanically locked to the ribs and provided the distribution, temperature, and shrinkage reinforcing, as well as the anchorage of the main reinforcement, for the bridge deck.

A bidirectional FRP grid panel provided the top layer reinforcement. Transverse reinforcement for the top layer consisted of pultruded FRP I-bars 1½ in. (38.1 mm) deep. Temperature and shrinkage reinforcing for the top layer was provided by three-part cross rods in a similar manner to the bottom layer of reinforcing. Both the cross rods and the I-bars were spaced at 4 in. (101.6 mm) on center.

The two reinforcing layers were connected together with two-part epoxy-bonded pultruded FRP connectors machined to fit the profile of the adjoining parts within tight tolerances. Temporary clamping of the two halves was accomplished through the use of a FRP bolt and nut.

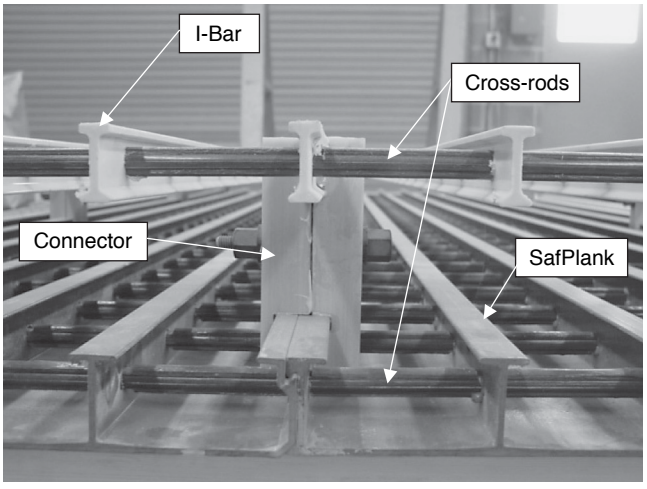

FIGURE 3 SafPlank panel reinforcement detail.

A second system of reinforcing and SIP formwork was investigated. Again, this system incorporated top and bottom layers of reinforcement, with SIP formwork provided by the bottom layer; this system is referred to as the Gridform system.

The bidirectional FRP grating used in the first system was incorporated into both the top and bottom layers. Deck formwork was provided by a ⅛-in. (3.175-mm) pultruded FRP plate that was epoxy bonded to the outer face of the bottom I-bar (Figure 4). Connectors similar to those already described linked the two layers. Joints between the individual panels that were perpendicular to traffic were accomplished by means of a 1-ft (0.305-m) overlap of the top and bottom layers of the grid. The failure mode of FRP-reinforced concrete panels has been shown to be caused by punching shear (*1, 4*). Punching shear capacity is dependent on the depth from the top surface to the tension reinforcing. The Gridform panel placed the bottom reinforcing at the bottom of the concrete. This allowed the overall deck thickness to be reduced from 8 in. (203 mm) to 7 in. (178 mm).

STRUCTURAL TESTING

Laboratory testing for the two systems previously described was performed at the Structures and Materials Testing Laboratory at the University of Wisconsin–Madison. Loads were applied to the FRP-reinforced specimens through use of a 200-kip (890-kN) MTS Systems Corporation closed-loop servohydraulic actuator anchored to the strong floor through a heavy steel frame and prestressing rods. Panel and beam specimens were tested by applying a single-point load at the center of the specimen span. All specimens were supported on gypsum cement plaster bearings 6 in. (152.4 mm) wide.

The first tests conducted were the panel tests for the SafPlank and Gridform specimens. One specimen was tested for each reinforcing type. Each specimen was loaded through a 10- × 25-in. (254- × 635-mm) loading patch to simulate a dual-tire contact area in the center of the panel. Before the static ultimate test, both specimens were loaded through 10 cycles of 0 to 21 kips (0 to 93.45 kN). These loading cycles provided specimens that emulated the in-service state of an actual bridge deck. The SafPlank specimen was 8 in. × 8 ft × 10 ft (203.2 mm × 2.438 m × 3.048 m). The panel was tested on an 8-ft (2.438-m) simple span (Figure 5). This specimen did not have a transverse splice included in the test specimen. The Gridform specimen was 7 in. × 7 ft × 8 ft (177.8 mm × 2.135 m × 2.438 m) and was tested on a 6.33-ft (1.932-m) simple span. Electrical strain gauge data and deflection measurements were recorded as the load was increased to the ultimate capacity of the specimen.

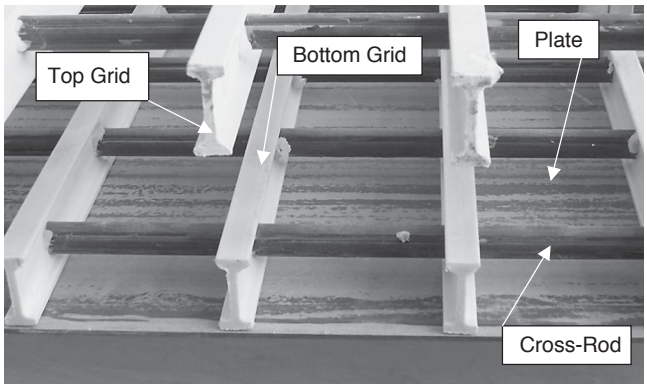

FIGURE 4 Gridform reinforcement detail.

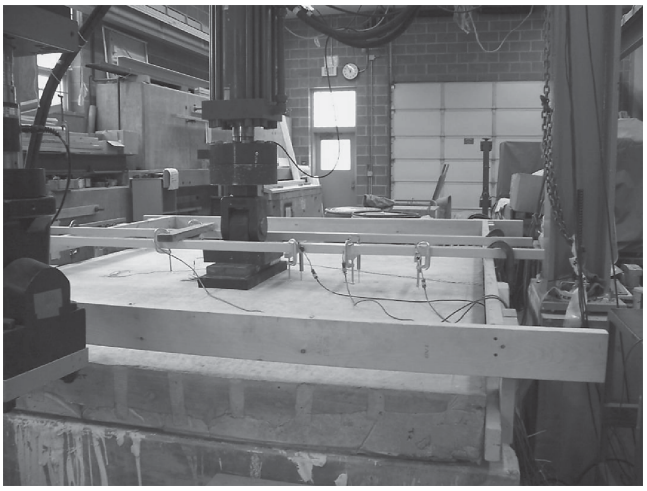

FIGURE 5 SafPlank panel specimen test setup.

Following the panel tests, simple-span, positive-moment bending-capacity tests were conducted for each of the reinforcing systems. One specimen for each reinforcing type was tested. To ensure flexural behavior, a small width-to-span ratio was selected for the beam specimens. This narrow width allowed the flexural behavior to be isolated and observed. The SafPlank and Gridform specimens had a span of 8 ft (2.438 m) and 6.33 ft (1.932 m), respectively. Loading was applied to the beam specimens from the actuator through a steel bar 3 ft (0.914 m) long and 3 in. (76.2 mm) square placed at the middle of the span. Specimens were manually loaded until the ultimate capacity was attained. Strains were measured at the top and bottom surfaces of the concrete and FRP form. Deflections were measured with respect to a reference frame that was connected to the mid-depth of the specimen at the centerline of the supports.

TEST RESULTS

The objectives of the experimental testing were to determine the ultimate capacity, to understand the failure modes of these systems, and to compare these results with previous research of double-layer FRP reinforcement of concrete bridge decks. Selected results and preliminary conclusions are presented here. Measurements of strain and deflection were recorded at various locations on the specimens, but not all data are presented.

Deck Panels

On the basis of previous research, the expected failure mode was punching shear (*1, 4*). The SafPlank specimen failed through the shear failure of the T-rib webs at the junction of the web and the bottom plate. The bottom plate delaminated from the rest of the deck panel; that action was followed by concrete crushing at the top of the slab (Figure 6). The specimen did not include a lap splice, which is recognized to be the weakest point in the decking system. Had a joint been included, the failure characteristics may have been different from what was observed. The ultimate capacity was 180.5 kips (802.8 kN).

FIGURE 6 Concrete crushing on top surface of SafPlank panel.

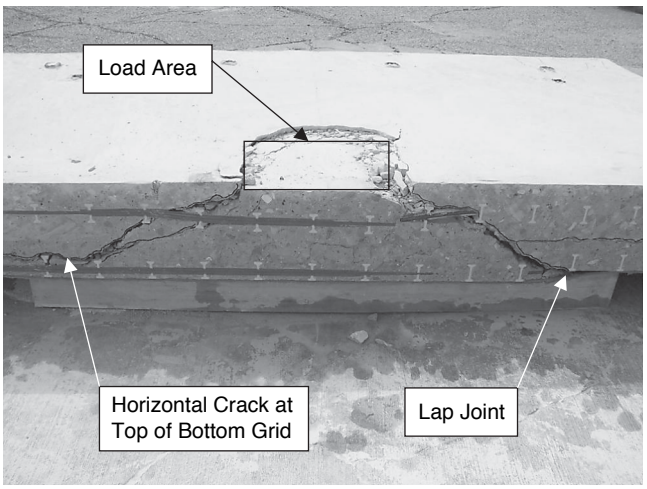

FIGURE 7 Gridform section through failure plane.

The Gridform panel failed because of punching shear. Very little cracking was observed before failure. The specimen included a lap splice, through which the shear cone failure surface propagated (Figure 7). The ultimate capacity was 124.95 kips (556 kN).

The CDS system tested on an 8-ft (2.44-m) span reached a maximum load of 91 kips. As noted earlier, the failure mode for all the CDS panels was punching shear (*1*). The nature of the CDS system provided a joint or weak point every 18 in. (457.2 mm). A comparison of load versus potentiometer deflection of the three systems is shown in Figure 8. As the graph shows, both the SafPlank and Gridform panels exhibited significantly higher strength and stiffness than the CDS system.

AASHTO specifies a HS20-44 truck service wheel load of 16 kips (71.2 kN) be used in the design of highway bridge decks (*6*). Using the maximum impact factor of 30% results in a total service live load, P_{LL+I}, of 21 kips (93.45 kN). The SafPlank specimen did not include a joint; therefore, the result may not be representative of a worst-case scenario. A factor of safety calculation is not prudent and will not be given here. Testing of the Gridform panel provided a factor of safety of 5.95 with respect to P_{LL+I}, thus confirming a significant safety margin. The maximum deflection under P_{LL+I} was 0.02 in. (0.508 mm), corresponding to a span to deflection ratio of L/3,800, which is less than one-fourth the AASHTO-recommended limit of L/800.

Positive Moment Beam Specimens

Testing of the SafPlank beam specimens showed that the failure mode was shearing of the web tees at the junction of the webs with the bottom plate, the same failure mode as for the SafPlank panel. The Gridform panel failure was caused by concrete crushing at the top of the beam specimen. As Figure 9 shows, the compressive concrete strain in the SafPlank panel was well below the ACI-recommended ultimate compressive strain for concrete of 0.003 unit (*7*), indicating that failure was not the result of concrete crushing. Concrete strain in the Gridform beam specimen was ϵ_{conc} = 0.0026 (87% of maximum

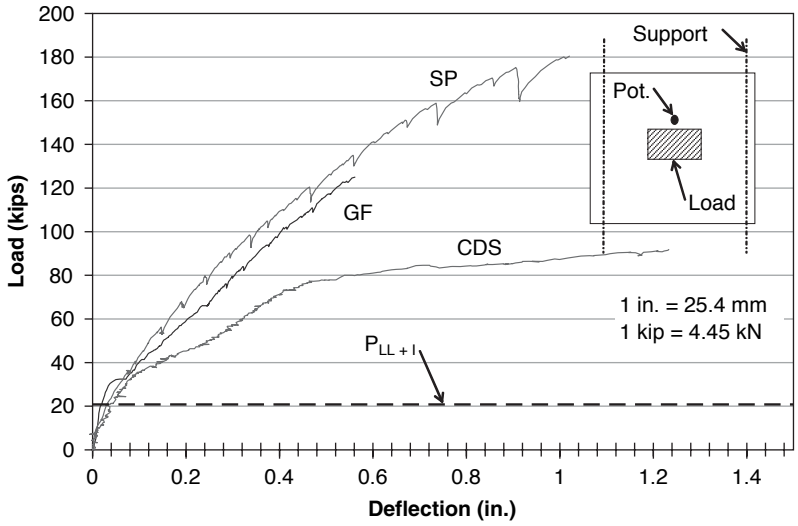

FIGURE 8 Load and deflection behavior for panel specimens (Pot. = potentiometer).

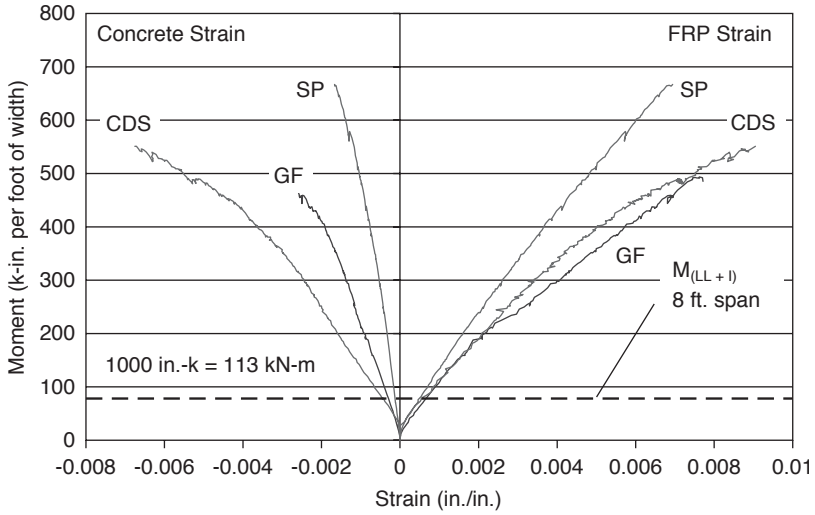

FIGURE 9 Moment versus strain for beam specimens.

concrete strain, $\epsilon_{cu} = 0.003$). This measurement was taken 4 in. (101.6 mm) from the span's centerline, which experienced 84% of the maximum moment, showing close agreement with the measured value of concrete strain. The stress level in the FRP material at failure is shown in Table 1, as is the experimentally determined modulus of elasticity, E, and mean tensile strength, $f_{u,ave}$. The data show that the stress level at the external FRP surface is significantly smaller than the ultimate tensile stress. The level of concrete strain, when coupled with the visual evidence of concrete crushing and the low level of stress at the outer FRP surface, led to the conclusion that the failure mode for the Gridform beam specimen was concrete crushing.

All three systems were tested in a simple span configuration with varying span lengths. To remove the span variable from the comparison, it is instructive to evaluate using a moment-versus-curvature plot (Figure 10). The CDS system tested by Dieter et al. (*1*) exhibits virtually the same behavior as the Gridform system. The SafPlank specimen had a significantly higher stiffness than the two FRP-reinforced counterparts.

ECONOMIC EVALUATION

The IBRC program is meant to be a way to bring about innovation in bridge design and construction. Laboratory testing and analysis can inform and advance the technological aspects of bridge design and construction. Economics should also be taken into account when a new technology is being developed.

Construction of the US-151 bridge through use of the CDS system revealed that the system was constructible, but the reinforcing materials cost 60% more than the steel reinforcing for the twin bridge (*3*). The FRP reinforcing system cost \$34.39/ft² (\$370.17/m²) for the CDS system, with the SIP deck panels costing \$25.08/ft² (\$270.00/m²) (*3*), or approximately 73% of the reinforcing system cost. Increased labor productivity, possibly shorter duration of construction, and long-term durability of the CDS system can help to offset the higher initial cost for this system. The successful implementation of an FRP-reinforced deck with an integrated SIP form system revealed the need to reduce its cost.

Jacobson et al. (*4, 5*) performed testing by using a double-layer FRP grating with conventional plywood formwork. The cost of the double-layer FRP reinforcing system was \$22.68/ft² (\$243.87/m²) (*8*), 34% less than the CDS system. The labor cost for installing and removing the plywood deck formwork is not included in the double-layer FRP grating price. Data were unavailable for the actual labor costs incurred by the contractor to place and remove the formwork, and a \$5.00/ft² (\$53.76/m²) estimate was obtained from a local bridge contractor. With the additional formwork labor cost included, the total cost of the double-layer FRP grating, \$27.68/ft² (\$297.63/m²), was 19.5% less than that of the CDS system.

The next step in the evolution of the system was the SafPlank solution. The time-consuming process of manufacturing the SafPlank system was considerably more expensive, essentially due to drilling the holes for the cross-rods in the T-rib webs. This resulted in an estimated reinforcing system cost of \$55.00/ft² (\$591.40/m²), which was considered to be cost prohibitive for practical application.

Previous experience with the double-layer FRP grid led to the current Gridform system. Provision for a SIP form was accomplished by epoxy bonding a 1/8-in. (3.175-mm) FRP plate to the bottom of the

TABLE 1 Beam Specimen FRP Stress at Failure

Beam Specimen	Modulus of Elasticity, E (ksi)	FRP Strain at Failure	Average Tensile Strength, $f_{u,ave}$ (ksi)	Material Stress at Failure, σ_{max} (ksi)
SafPlank beam	3900	0.006942	69.8	27.1
Gridform beam	2760	0.007726	39.3	21.3

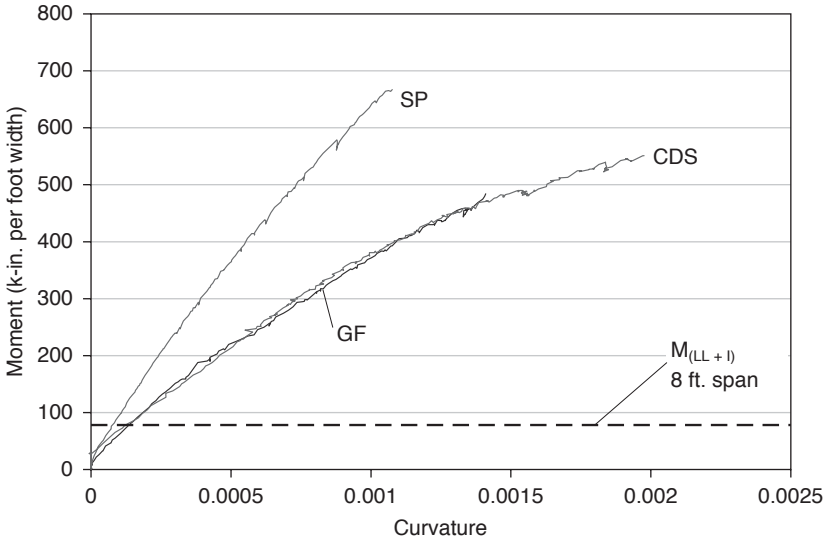

FIGURE 10 Moment versus curvature for beam specimens.

double-layer grating investigated by Jacobson et al. (*4, 5*). The manufacturing process was essentially identical to that of the double-layer grid, with the additional step of installing the FRP plate. Estimated cost for this reinforcing system is \$26.00/ft^2 (\$279.57/m^2). This represents a 24% reduction in cost compared with the CDS system. The cost of the double-layer grating including forming costs was comparable to the estimated cost for the Gridform system. The potential advantage of the Gridform system over the double-layer grating is the reduction in project labor hours required, with the subsequent reduced impact to traffic.

Comparison of in-place reinforcing costs between the CDS system (*9*) and the Gridform system is summarized as follows: CDS, \$33.21/ft^2; Gridform, \$28.22/ft^2 (1 ft^2 = 0.093 m^2). The Gridform panels had a 15% lower in-place cost than the CDS system.

A candidate bridge for implementation of the Gridform solution was located through cooperation with the Center for Infrastructure Engineering Studies, University of Missouri–Rolla. The FRP solution was implemented in the replacement of the superstructure of a slab-on-girder bridge located in Greene County, Missouri (*10*). The bridge structure consisted of four spans, with two exterior spans of 37 ft (11.3 m) and two interior spans of 35 ft (10.7 m), for a total length of 144 ft (43.9 m). The new superstructure consists of a FRP-reinforced concrete deck 7 in. (177.8 mm) thick acting noncompositely with four W24×84 steel girders spaced at 6 ft (1.8 m) on center. The out-to-out roadway width is 24 ft (7.3 m), with a clear roadway width of 22 ft (6.7 m). The girders are two-span continuous with an expansion joint at the center pier. A newly designed Modified Kansas Corral Rail reinforced with glass FRP bars complemented the Gridform system to provide a steel-free bridge deck and rail. Deck construction took place in November 2005, with installation of the deck panels, rail post reinforcement, and deck casting being completed in only 3 days. Figures 11 and 12 show the casting operation and the finished bridge deck, respectively.

FIGURE 11 Placement of deck concrete with Gridform system.

FIGURE 12 Finished bridge deck with rail dowels.

CONCLUSIONS

A cost-effective structural FRP stay-in-place formwork system that is integrated with the reinforcing for concrete highway bridge decks has been developed and tested at the University of Wisconsin–Madison.

Its evolution has progressed from a structural SIP form separated from the top layer of the reinforcing grating to a double-layer grating with no SIP form, to the current solution, a double-layer grating fully integrated with an FRP structural SIP form. All these systems have been shown to be able to provide safe support of the design loads for highway bridges. The ongoing search for more efficient use of FRP materials and more constructible solutions can lead to further optimization. The most promising option is currently the Gridform system, because of the material cost and the potential for rapid construction. Laboratory testing of full-scale panel and beam specimens has shown that the Gridform system meets the strength and deflection code requirements; the strength is over five times that required and the stiffness over four times the recommended stiffness. Benefits of the Gridform over conventional steel reinforcement are the corrosion resistance and the potential for accelerated construction because of the modular nature of the system.

The Gridform solution has been successfully implemented in the superstructure replacement of a slab-on-girder bridge in Greene County, Missouri, where the duration of deck construction was 3 days.

ACKNOWLEDGMENTS

The authors acknowledge the following persons for their contributions: Stan Woods and Gerry Anderson of the Wisconsin Department of Transportation; Bill Lang and John Dreger of the Structures and Materials Testing Laboratory, University of Wisconsin; and Eric Baker, Blair Hildahl, Randy Kolinske, and Mike Arnold of the University of Wisconsin. This project has been made possible through the financial support of the Innovative Bridge Research and Construction Program, the Wisconsin Department of Transportation; the University Transportation Center, University of Missouri–Rolla (UMR); and UMR's National Science Foundation Industry/University Cooperative Research Center on Repair of Buildings and Bridges Using Composites. The assistance of the Strongwell Corporation is gratefully acknowledged.

REFERENCES

1. Dieter, D. A., J. S. Dietsche, L. C. Bank, M. G. Oliva, and J. S. Russell. Concrete Bridge Decks Constructed with Fiber-Reinforced Polymer Stay-in-Place Forms and Grid Reinforcing. In *Transportation Research Record: Journal of the Transportation Research Board, No. 1814,* Transportation Research Board of the National Academies, Washington, D.C., 2002, pp. 219–226.
2. Berg, A. C., L. C. Bank, M. G. Oliva, and J. S. Russell. Construction of Fiber-Reinforced Polymer Bridge Deck on US 151 in Wisconsin. Presented at 83rd Annual Meeting of the Transportation Research Board, Washington, D.C., 2004.
3. Berg, A. C., L. C. Bank, M. G. Oliva, and J. S. Russell. Construction and Cost Analysis of an FRP Reinforced Concrete Bridge Deck. *Construction and Building Materials,* Vol. 20, 2006, pp. 515–526.
4. Jacobson, D. A., L. C. Bank, M. G. Oliva, and J. S. Russell. Punching Shear in Fiber-Reinforced-Polymer Bilayer Grid-Reinforced Concrete Bridge Decks. Presented at 83rd Annual Meeting of the Transportation Research Board, Washington, D.C., 2004.
5. Jacobson, D. A., L. C. Bank, M. G. Oliva, and J. S. Russell. Punching Shear Capacity of Double Layer FRP Grid Reinforced Slabs. *Proc., 7th International Conference on Fiber Reinforced Plastics for Reinforced Concrete Structures,* American Concrete Institute, New Orleans, La., Nov. 2005, pp. 857–871.
6. *Standard Specifications for Highway Bridges,* 16th ed. AASHTO, Washington, D.C., 1996.
7. *Guide for the Design and Construction of Concrete Reinforced with FRP Bars.* ACI 440.1R-01. American Concrete Institute, Farmington Hills. Mich., 2001.
8. Bank, L. C., M. G. Oliva, J. S. Russell, D. A. Jacobson, M. J. Conachen, B. Nelson, and D. McMonigal. Double Layer Prefabricated FRP Grids for Rapid Bridge Deck Construction: Case Study. *Journal of Composites for Construction,* Vol. 10, No. 3, May–June 2006, pp. 204–212.
9. Berg, A. C. *Analysis of a Bridge Deck Built on U.S. Highway 151 with FRP Stay-in-Place Forms, FRP Grids, and FRP Rebars.* Master's thesis. University of Wisconsin–Madison, 2004.
10. Matta, F., A. Nanni, N. Galati, T. E. Ringelstetter, L. C. Bank, M. G. Oliva, J. S. Russell, B. M. Orr, and S. N. Jones. Prefabricated Modular GFRP Reinforcement for Accelerated Construction of Bridge Deck and Rail System. *Proc., FHWA Accelerated Bridge Construction Conference,* San Diego, Calif., Dec. 2005, pp. 129–134.

The Structural Fiber-Reinforced Polymers Committee sponsored publication of this paper.

Matta, F., and Nanni, A., (2006), "Design of Concrete Railing Reinforced with Glass Fiber Reinforced Polymer Bars," *Proc. 2006 ASCE/SEI Structures Congress*, St. Louis, MO, May 18-20, 2006, CD-ROM, 9 pp.

Design of Concrete Railing Reinforced with Glass Fiber Reinforced Polymer Bars

Authors:

Fabio Matta, Center for Infrastructure Engineering Studies, University of Missouri-Rolla, 220 Eng. Research Lab, 1870 Miner Circle, 65409 Rolla, MO, mattaf@umr.edu
Antonio Nanni, Center for Infrastructure Engineering Studies, University of Missouri-Rolla, 223 Eng. Research Lab, 1870 Miner Circle, 65409 Rolla, MO, nanni@umr.edu

ABSTRACT

The use of Fiber Reinforced Polymer (FRP) reinforcement is a practical alternative to conventional steel rebars in concrete structures subjected to aggressive environments. The solution is attractive for bridge deck and rail applications, as it eliminates corrosion of the steel reinforcement, which is the major instrument of degradation. Due to the peculiar physical and mechanical characteristics of advanced composite materials, the design philosophy of FRP reinforced concrete (RC) structures differs from that of traditional RC. This paper introduces a systematic approach adopted for the structural and functional design of an open-post bridge railing reinforced with Glass FRP bars (GFRP) as compared to steel RC counterparts, according to the AASHTO LRFD Bridge Design Specifications. Design examples, accounting for different gap opening length and rail beam reinforcement, and based on the experimental static response of full-scale post/deck connections, are finally presented and discussed.

INTRODUCTION

Corrosion of the steel reinforcement is a major cause of degradation of concrete decks in a large portion of the bridge inventory worldwide. Effects accrue from the routine use of deicing salts on roads and exposure to harsh environments, leading to reduced strength and functionality, and to safety concerns. The use of GFRP reinforcement ideally eliminates the issue and represents a practical alternative to conventional steel for non-prestressed structures [1]. A number of field implementations, typically as parts of research projects, have demonstrated the validity of the technology. Design principles are fairly well established [2] and guideline documents have been published in North America, Europe, and Japan. In the US, the 2005 "Guide for the Design and Construction of Concrete Reinforced with FRP Bars" by the American Concrete Institute (ACI) [3] will shortly superseed the 2003 document (ACI 440.1R-03).

A new version of the open post Federal Lands Modified Kansas Corral Bridge Rail (MKCR) [4] reinforced with GFRP rebars was designed to develop a truly steel-free deck and rail system, as recently showcased in the accelerated construction of a bridge deck in Greene County, MO, using innovative prefabricated GFRP stay-in-place (SIP)

reinforcing panels [5]. Previous research demonstrated the structural adequacy of highway GFRP RC barriers under pendulum impact load, where the original steel rebars were replaced on a strength equivalence basis [6]. The crashworthiness of a GFRP RC TxDOT T203 open-post rail was also assessed via crash test as per National Cooperative Highway Research Program (NCHRP) Report 350 Test Level 3 (TL-3) criteria [7], i.e. with a 4500 lb pickup truck impacting at a speed of 60 mph and crash angle of 25° [8], as typically required on the National Highway System [9]. The objective of the design presented herein is twofold. First, ensure compliance with the Test Level 2 strength criteria (TL-2, same as TL-3 with speed reduced to 45 mph), i.e. the category of the steel RC MCKR replaced [4], while providing additional redundancy to evaluate upgrade to the TL-3 category. Second, devise a simple prefabricated reinforcement geometrically compatible with the GFRP deck panels. Rapid pre-assembling of lightweight rail post and beam rebar cages significantly improves productivity, while the ease of installation minimizes time-consuming and labor-intensive field operations, thereby conferring actual economical appeal to the solution, besides its safety and durability characteristics.

RAILING DESIGN

Bridge railings must contain and redirect errant vehicles while preventing rollover and snagging, and allowing deceleration to a stop at a relatively short distance from the impact section. Therefore, crash testing of bridge safety appurtenances aims at assessing both the structural and geometrical crashworthy, depending on the level of service sought (TL-1 to TL-6, being the latter the most demanding), along with the vehicle occupant risk. Based on the results of a number of full-scale crash tests performed as part of programs under the Federal Highway Administration (FHWA), the American Association of State Highway and Transportation Officials (AASHTO), NCHRP and individual states, the AASHTO LRFD Bridge Design Specifications, Section 13 [10], set forth strength and geometry criteria for preliminary design.

Geometry

The safety performance of an open-post concrete railing greatly depends on its geometry. Critical requirements are:

- sufficient rail height, H, and suitable profile shape to reduce the potential for vehicle rollover. A minimum value $H = 27"$ is recommended for both TL-2 and TL-3;
- continuous solid rail beam with smooth and sufficient contact width, A, with respect to H, to reduce the potential for vehicle wheel, bumper or hood impact with the post. A minimum A/H ratio of 0.25 is recommended, along with specified graphical parametric criteria;
- sufficient post setback distance, S, with respect to combination of A and H, to reduce the potential for vehicle snagging. Parametric recommendations are provided in graphical fashion to select design alternatives that proved to perform satisfactorily.

Figure 1(a) and 1(b) show the geometry of the GFRP RC MKCR designed. Compared to the profile of the original design (dashed line), A has been increased from 14" to 17", with H increased from 27" to 30". Although vertical barriers typically offer the greatest reduction in rollover potential, despite the tradeoff of increased lateral accelerations [11],

the recommended minimum height may be inadequate, especially in case of higher service levels. This has been recently observed in the (failed) TL-3 crash test of a 27" GFRP RC railing [7, Appendix A], whereas a similar configuration with increased height performed well [7, Appendix B]. The post setback was kept at the original distance $S = 2$" from the rail beam contact surface, similarly to other steel RC counterparts of same or higher category, such as the Modified Corral Rail (TL-2) and 32" Corral Rail (TL-4) in Kansas, or the Concrete Beam and Post (TL-2) and Open Concrete Bridge Rail (TL-4) in Nebraska [4]. Figure 1(c) and 1(d) show the compliance of the selected design with the LRFD recommendations to minimize the risk of impact on the rail post and vehicle snagging, also correcting the slightly low A/H ratio of 0.52 of the original profile. It is seen from the grey arrows that the addition of any wearing surface would further move the geometric parameters into the preferred safety areas.

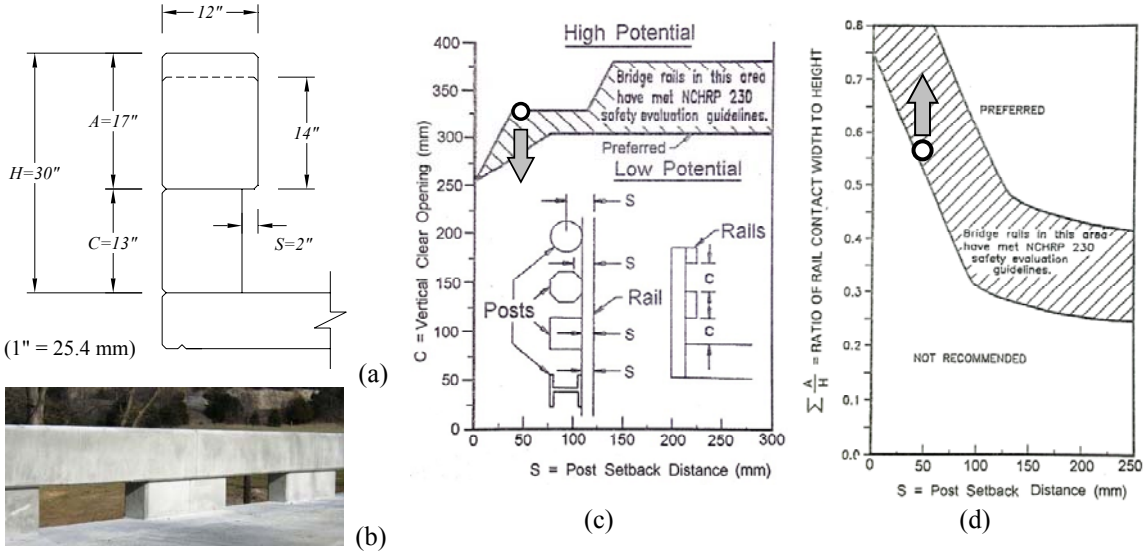

FIGURE 1
GEOMETRY OF GFRP RC FEDERAL LANDS MKCR WITH POST AND GAP LENGTH OF 4' (a, b) AND COMPLIANCE WITH AASHTO LRFD BRIDGE DESIGN SPECIFICATIONS (BLANK CIRCLE) [10] (c, d)

The post and gap opening length, P and G, have been changed from the original 3' and 7', respectively, to 4' each (Figure 1(b)), in order to provide additional redundancy needed to evaluate upgrade to TL-3, as well as geometrical compatibility with the 8' long modular GFRP SIP reinforcing panels.

Load Demand

The dynamic loads imparted by an impacting vehicle under specified crash test conditions [8] are translated by AASHTO into equivalent factored static loads (transverse, F_t, longitudinal, F_l, and vertical, F_v) to be used for structural design, as summarized in Table 1 [10]. In case of concrete railings designed to resist F_t, the effects of F_l and F_v are generally not of concern. For TL-2 and TL-3 crash Test Level, a transverse strength of 27 kip and 54 kip applied on the rail beam at a height $H_e = 20$" and 24" from the roadway, respectively, is required. F_t should be uniformly distributed along $L_t = 4$', which is the typical length of significant contact observed experimentally.

Railing Test Level	TL-2	TL-3
Transverse Force, F_t	27 kip (uniformly distributed along L_t = 4')	54 kip (uniformly distributed along L_t = 4')
Longitudinal Force, F_l	9 kip (uniformly distributed along L_l = 4')	18 kip (uniformly distributed along L_l = 4')
Vertical Force, F_v	4.5 kip (uniformly distributed along L_v = 4')	4.5 kip (uniformly distributed along L_v = 4')
Height of F_t and F_l application, H_e	20" (min)	24" (min)

TABLE 1
EQUIVALENT STATIC DESIGN FORCES FOR TL-2 AND TL-3 TRAFFIC RAILINGS [10]

Relatively older traffic railings, such as the Federal Lands MKCR, have been proof tested according to the AASHTO Standard Specifications, Section 2.7.1.3 [12], which prescribe a minimum transverse force of 10 kip, uniformly distributed along a length of 5', be applied on single posts at the center of gravity of the rail beam.

Resistance Function

The nominal resistance to transverse load of steel RC railings is typically determined via yield line analysis [10, 13]. Upon postulation of a failure mode in the form of a kinematically admissible collapse mechanism that satisfies the yield criterion at the yield lines, an upper-bound ultimate load is determined by equating the work done by the external load and the resisting forces. Hence, in case of statically indeterminate systems, redistribution of the bending moments must be assumed with plastic rotations. Possible failure modes considered in the AASHTO LRFD specifications, when a single rail beam span is strong enough to resist F_t and transfer it to the connected posts ("strong beam-strong post" system), involve either a single post and the two adjacent beam spans (1-post) or two posts and adjacent beam spans (2-post), as illustrated in Figure 2. The latter is typically applicable to open post RC railings [13].

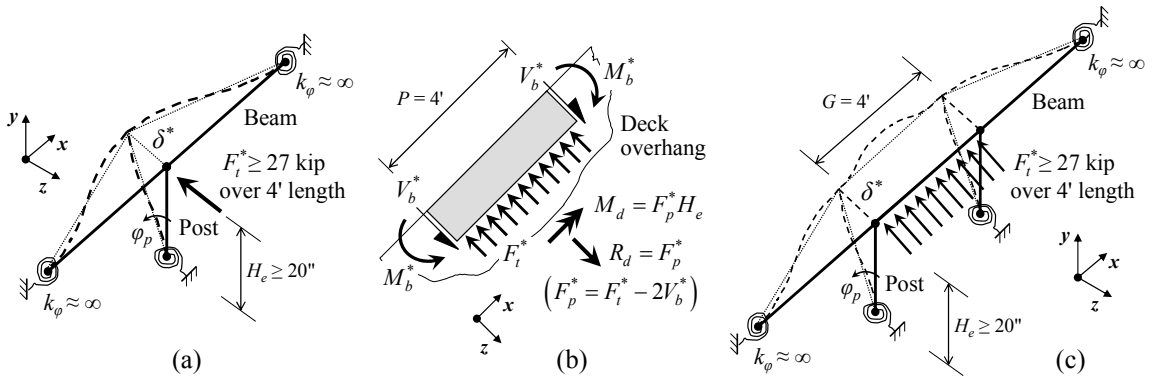

FIGURE 2
SCHEMATIC OF 1-POST FAILURE MODE (a) WITH POST FREE BODY DIAGRAM (b), AND 2-POST FAILURE MODE (c)

Due to the linear elastic behavior of FRP materials, moment redistribution cannot be accounted for in RC design, and for each failure mode assumed both equilibrium and deformation compatibility must be verified. The methodology proposed herein to assess the strength level of a GFRP RC railing is consistent with the bases of the AASHTO

LRFD approach, while the ACI 440 provisions are followed for the flexural and shear design and analysis of the FRP reinforced members and the rail structure.

Failure is assumed to occur either at the post/deck connections or at the rail beam ends, whose rotation is constrained (rotational stiffness $k_\varphi \approx \infty$ along with translational constraints along z at the connection with the exterior posts), when the post attains a compatible displacement $\delta = \delta^*$ at H_e (Figure 2(a) and 2(c)). The height H_e is assumed for simplicity, since it lies close to the center of gravity of the beam and small displacements are accounted for. In fact, relatively large deformations are not observed in successful crash tests and are incompatible with optimal functionality characteristics, and thus should be prevented. Hence, torsional effects on the beam can be neglected. The transverse force resisted by the railing, assuming a 1-post or 2-post failure mode (n = 1 and n = 2, respectively, where n is the number of posts considered), is computed either via equilibrium method or imposing conservation of energy, i.e.

$$F_t\left(\delta^*\right) = F_t^* = \frac{4M_b^*}{G} + nF_p^* = 2V_b^* + nF_p^*, \tag{1}$$

as illustrated in Figure 2(b) for n = 1, wherein the bending moments and shear forces acting at the beam ends in the gap opening are expressed as

$$M_b^* = \frac{6E_c I_{e,b}(M_b^*)}{G^2}\delta^* \text{ and } V_b^* = \frac{12E_c I_{e,b}(M_b^*)}{G^3}\delta^*, \tag{2, 3}$$

respectively, and the combined tension force and bending moment at the connection are given as

$$F_p^* \text{ and } M_p^* = F_p^* H_e, \tag{4, 5}$$

respectively.

In computing the nonlinear beam displacement as a function of the bending moment or shear from (2) or (3), when the applied moment exceeds the cracking limit, $M_{cr,b}$, and the section moment of inertia drops below its gross value, $I_{g,b}$, the flexural stiffness is determined by multiplying the concrete elastic modulus, E_c, by the effective moment of inertia

$$I_{e,b}(M_b^*) = \left(\frac{M_{cr,b}}{M_b^*}\right)^3 \beta_{d,b} I_{g,b} + \left[1 - \left(\frac{M_{cr,b}}{M_b^*}\right)^3\right] I_{cr,b} \le I_{g,b}. \tag{6}$$

(6) is the well known Branson's equation, which has been modified to account for reduced tension stiffening in FRP RC members by means of the factor

$$\beta_{d,b} = \frac{1}{5}\left(\frac{\rho_{f,b}}{\rho_{fb,b}}\right), \tag{7}$$

wherein $\rho_{f,b}$ and $\rho_{fb,b}$ are the FRP reinforcement ratio and balanced reinforcement ratio, respectively.

The ultimate transverse load in (1) is attained when the post/deck connection reaches its strength, or when the beam moment reaches its nominal value, $M_{n,b}$, assumed equal for both positive and negative bending (symmetric reinforcement). It should be noted that connections of vertical posts often exhibit only a fraction of the theoretical resistance of either the adjoined post or deck sections. Failure patterns may thus develop within the bridge deck at load levels considerably smaller than that otherwise expected. Typical factors that affect the behavior of connection details (not necessarily concurrently) are:

- effectiveness of the post/deck construction joint;
- effectiveness of the anchorage of the post tension bent bars within the deck;
- developable tensile stress in straight or bent bars in the deck top mat;
- contribution of adjacent deck portions.

The resistance function (1) can be rearranged to yield the strength demand function

$$F_{p,\min}(\delta) = \frac{F_t - 2V_b(\delta)}{n}, \tag{8}$$

wherein F_t = 27 kip and 54 kip for TL-2 and TL-3, respectively. For each compatible displacement δ and given rail beam design, (8) defines the minimum load applied at a height H_e to be resisted at the connection, without contribution of the beam elements, in order to meet the equivalent static strength of the selected crash Test Level. Therefore, the resistance function F_p-δ of a candidate connection can be determined experimentally, and evaluated using (8) for a given beam resistance function M_b-δ and rail geometry. Similar connections may be considered for railings with different service levels by modifying the beam design (geometry, reinforcement) and/or the gap opening length. A similar approach was used to modify the post and beam design at the open joints.

DESIGN EXAMPLES

Two full-scale post/deck overhang subassemblies were tested under static load to determine their force-displacement response (Figure 3), in order to assess compliance of the new design with strength requirements. A preliminary linear elastic finite element analysis was performed to select a setup representative of the actual boundary conditions. Experiments were conducted as part of a research program aimed at developing and implementing a steel-free deck and railing system for accelerated bridge construction, thereby complementing an innovative GFRP deck reinforcement made of large-size lightweight SIP grating panels [5]. The configurations shown in Figure 3(a) and 3(b), herein referred to as M1 and M2, respectively, were tested to evaluate the influence of reinforcement layout and construction details devised to improve constructibility.

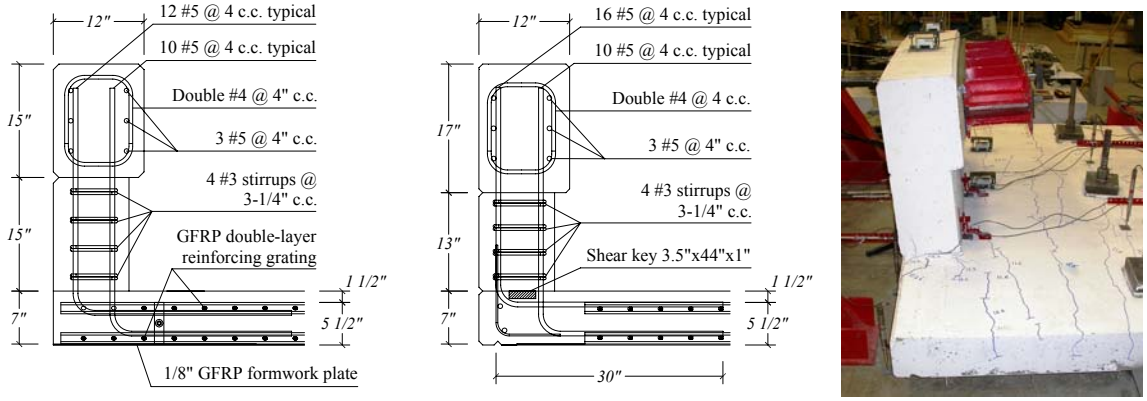

(a) (b) (c)

FIGURE 3
THRU-POST GFRP REINFORCEMENT IN SPECIMEN M1 (a) AND M2 (b), AND STATIC TEST OF POST/DECK OVERHANG SUBASSEMBLY (c)

Table 2 summarizes the nominal moment capacity of the GFRP RC structural sections (beam, post and deck), computed according to the ACI 440 provisions, and the actual ultimate capacity of the connections tested. All the sections were over-reinforced, since a concrete crushing failure mode is preferred to more brittle FRP rupture [3]. The theoretical beam M_b-δ response was used to define the strength demand function $F_{p,\min}$-δ (8) for the post/deck cantilever subassembly under different scenarios, as illustrated in Figure 4, where (8) has been scaled to account for horizontal deflection measured at H = 29-1/2" instead of the H_e value for the crash Test Level considered.

Connection specimen ID	M1	M2
Nominal moment beam, $M_{n,b}$	58.8 kip-ft (f'_c = 4 ksi, theoretical)	58.8 kip-ft (f'_c = 4 ksi, theoretical)
Nominal moment post, $M_{n,p}$	158.2 kip-ft (f'_c = 5.8 ksi, experimental)	173.8 kip-ft (f'_c = 8.4 ksi, experimental)
Nominal moment deck, $M_{n,d}$ (contribution of sections adjacent to post is neglected)	66.5 kip-ft (f'_c = 7.8 ksi, experimental)	94.4 kip-ft (f'_c = 5.1 ksi, experimental)
Ultimate moment (load) post/deck connection, $M_{u,c}$ ($F_{u,p}$) (load uniformly distributed along L_t = 4' applied at H_e = 2')	26.7 kip-ft (13.3 kip) (experimental)	24.5 kip-ft (12.2 kip) (experimental)
$M_{n,d}$ / $M_{u,c}$	0.40	0.26

TABLE 2
NOMINAL MOMENT CAPACITY OF GFRP RC POST, DECK SECTION AT CONNECTION (C_E = 1), AND ULTIMATE STRENGTH OF CONNECTION M1 AND M2

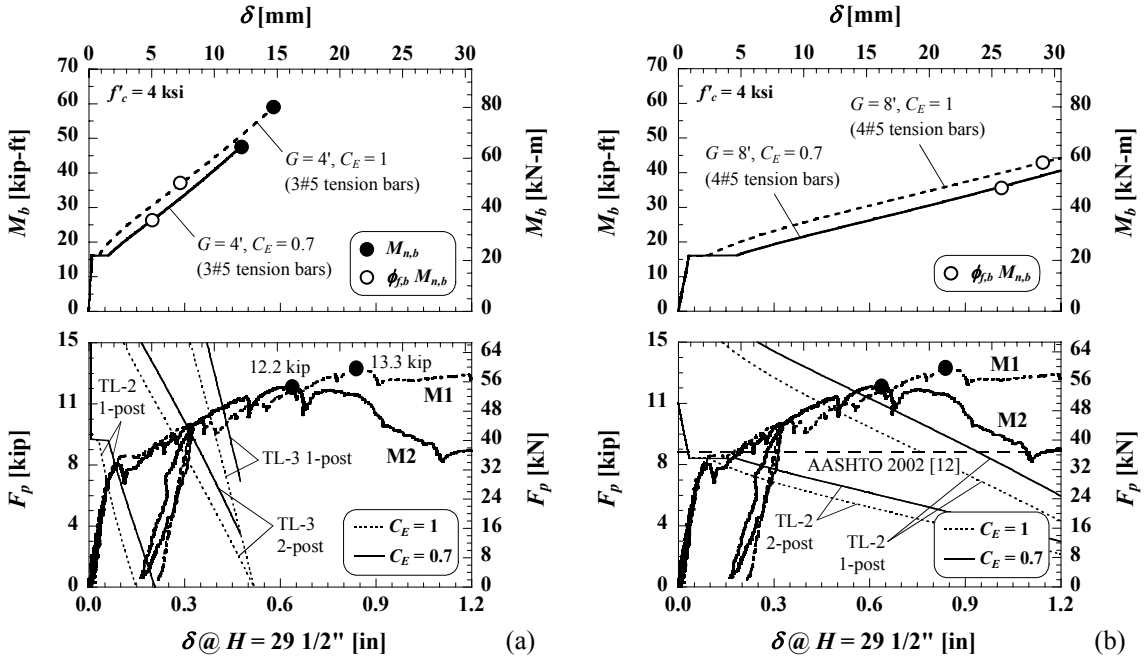

FIGURE 4
RESISTANCE FUNCTION OF GFRP RC RAIL BEAM (THEORETICAL) AND CONNECTIONS M1 AND M2 (EXPERIMENTAL) FOR G = 4' (a) AND G = 8' (b), AND CONNECTION STRENGTH DEMAND FUNCTIONS (8)

In Figure 4(a), the static response of connections M1 and M2 are compared with the strength demand function for railing configurations comprising the beam shown in Figure

3(a) and 3(b), i.e. reinforced with three #5 bars in tension, $P = G = 4'$, and assuming a conservative 1-post failure mode for TL-2 (TL-2 1-post) and TL-3 (TL-3 1-post), and a typical 2-post failure mode for TL-3 (TL-3 2-post). Solid and dashed lines indicate beam response and post strength demand assuming the environmental reduction factor for the guaranteed GFRP bar strength (typically 90-110 ksi) as $C_E = 0.7$, as recommended for design purposes, and $C_E = 1$, respectively. Solid circles mark the nominal capacity of the beam section and the strength level of the connections. Blank circles mark the design moment of the beam section. It is seen that the design appears highly redundant for TL-2 even assuming a rather conservative 1-post failure mode. TL-3 demand is not satisfied when $C_E = 0.7$ and the beam design capacity is considered instead of the nominal value, although this may not be representative of the actual crash test conditions. Additional reinforcement and/or increase in the rail beam width may be considered for upgrade. It is also noted that a TL-3 open post GFRP RC railing with similar geometry and reinforcement was recently successfully crash tested [7].

In Figure 4(b), a railing configuration with an additional #5 tension bar in the beam, $P = 4'$ and $G = 8'$, is evaluated for TL-2 demand under both 1-post and 2-post failure mode assumptions. For comparison purposes, the horizontal dashed line indicates the post strength demand according to the AASHTO Standard Specifications [12], where the required 10 kip load applied at the center of gravity of the rail beam has been scaled to the correspondent 8.96 kip applied at $H_e = 2'$. With respect to Figure 4(a), it is seen that design is controlled by the connection instead of the rail beam. The static response of the railing appears adequate for TL-2, especially if the 2-post failure mode is considered, which is consistent with the results of crash tests on other similar TL-2 or higher level steel RC open-post railings commonly used in the US.

CONCLUSIONS

A systematic approach for the design and analysis of open post GFRP RC railings has been presented. The proposed methodology is consistent with the geometrical and structural design bases set forth in the AASHTO LRFD specifications [10], with appropriate modifications to comply with the ACI 440 guidelines for concrete internally reinforced with FRP bars [3].

Resistance functions were defined by imposing force equilibrium and displacement compatibility while evaluating realistic failure scenarios. Design examples for constant rail profile and different beam reinforcement and gap opening length configurations have been presented. Preliminary results, to be corroborated by full-scale crash testing [8], indicate that performance is consistent with that of similar steel and one GFRP RC counterparts crash tested to date.

ACKNOWLEDGEMENT

The financial support of the University of Missouri-Rolla University Transportation Center on Advanced Materials and NDT Technologies is acknowledged. The assistance of industry members of the NSF I/UCRC "Repair of Bulding and Bridges with Composites" (RB^2C), Hughes Brothers, Inc. and Strongwell Corp., in supplying the FRP reinforcement for rail and deck slab, respectively, is acknowledged. Thanks are extended to the personnel of the UMR Structures Laboratory for valuable help in the test phases.

REFERENCES

[1] Bradberry, T.E., "Fiber-reinforced-plastic Bar Reinforced Concrete Bridge Decks," *Proc. 80th Annual Transportation Research Board Meeting*, Jan. 9-13, 2001, Washington, DC, CD-ROM #01-3247.

[2] Nanni, A., "North American Design Guidelines for Concrete Reinforcement and Strengthening Using FRP: Principles, Applications and Unresolved Issues," *Construction and Building Materials*, Vol. 17, No. 6-7, 2003, pp. 439-446.

[3] American Concrete Institute Committee 440, "Guide for the Design and Construction of Concrete Reinforced with FRP Bars," *ACI 440.1R-05*, in press, 2006.

[4] Federal Highway Administration, *Bridge Rail Guide 2005*, http://www.fhwa.dot.gov/bridge/bridgerail/index.cfm (accessed January 25, 2005).

[5] Matta, F., Nanni, A., Galati, N., Ringelstetter, T.E., Bank, L.C., Oliva, M.G., Russell, J.S., Orr, B.M., and Jones, S.N., "Prefabricated Modular GFRP Reinforcement for Accelerated Construction of Bridge Deck and Rail System," *Proc. FHWA Accelerated Bridge Construction Conference*, December 14-16, 2005, San Diego, CA, pp. 129-134.

[6] El-Salakawy, E., Benmokrane, B., Masmoudi, R., Brière, F. and Breaumier, E., "Concrete Bridge Barriers Reinforced with Glass Fiber-Reinforced Polymer Composite Bars," *ACI Structural Journal*, Vol. 100, No. 6, 2003, pp. 815-824.

[7] Buth, C.E., Williams, W.F., Bligh, R.P., Menges, W.L., and Haug, R.R., "Performance of the TxDOT T202 (MOD) Bridge Rail Reinforced with Fiber Reinforced Polymer Bars," *TTI Research Report 0-4138-3*, Texas Transportation Institute, 2003.

[8] Ross, H.E., Sicking, D.L., Zimmer, R.A., and Michie, J.D., "Recommended Procedures for the Safety Performance Evaluation of Highway Features," *NCHRP Report 350*, 1993.

[9] Mak, K.K., and Bligh, R.P., "Assessment of NCHRP Report 350 Test Conditions," *Transportation Research Record 1797*, 2002, pp. 38-43.

[10] American Association of State Highway and Transportation Officials, "Load and Resistance Factor Design (LRFD) Bridge Design Specifications," AASHTO, 2nd Edition, 1998.

[11] Mak, K.K., and Sicking, D.L., "Rollover Caused by Concrete Safety-Shaped Barrier," *Transportation Research Record 1258*, 1990, pp. 71-81.

[12] American Association of State Highway and Transportation Officials, "Standard Specifications for Highway Bridges," AASHTO, 17th Edition, 2002.

[13] Hirsch, T.J., "Analytical Evaluation of Texas Bridge Rails to Contain Buses and Trucks," *TTI Research Report 230-2*, Texas Transportation Institute, 1978.

Third International Conference on FRP Composites in Civil Engineering (CICE 2006)
December 13-15 2006, Miami, Florida, USA

RAPID CONSTRUCTION OF CONCRETE BRIDGE DECK USING PREFABRICATED FRP REINFORCEMENT

Fabio Matta
(Graduate Research Assistant, University of Missouri-Rolla, Rolla, MO, USA)

Antonio Nanni
(V. & M. Jones Professor, University of Missouri-Rolla, Rolla, MO, USA)

Thomas E. Ringelstetter
(Graduate Research Assistant, University of Wisconsin-Madison, Madison, WI, USA)

Lawrence C. Bank
(Professor, University of Wisconsin-Madison, Madison, WI, USA)

ABSTRACT
The development of durable structural systems for accelerated bridge construction is key to reducing the economic and social costs associated with replacement operations on a large scale. This paper reports on the field application of stay-in-place reinforcing panels, entirely made of glass fiber reinforced polymer components and specifically developed for the rapid construction of concrete bridge decks. The salient features of the system are illustrated, along with significant research and development outcomes. The five-day construction of the cast-in-place deck and open-post rail of Bridge 14802301 in Greene County, MO, is documented, and the major outcomes outlined. The project demonstrates how lightweight and noncorrosive FRP reinforcement is a practical alternative to steel, with the potential of versatile structural forms that add relevant constructibility and economic advantages.

KEYWORDS
Bridge Deck, Fiber Reinforced Polymers, Accelerated Bridge Construction.

1. INTRODUCTION

During the last four years, increasing investments have been made to support the research and development of innovative technologies for accelerated bridge construction, primarily under the sponsorship of the Federal Highway Administration (FHWA), the American Society of State Highway and Transportation Officials (AASHTO Technology Implementation Group), and the Transportation Research Board (TRB Task Force on Accelerating Innovation in the Highway Industry). Emphasis has been placed on improving safety and minimizing traffic disruption while enhancing quality and durability. The issue arises from the urgent need of upgrading and maintaining a significant portion of the bridge inventory while facing inevitable budget restrictions. Redecking operations are rather frequent, since corrosion of steel reinforcement is a major instrument of degradation in reinforced concrete (RC) decks and safety appurtenances. In the case of off-system bridges, cost-benefit analysis, contractors know-how and equipment availability typically result in the adoption of either partial or full-depth cast-in-place (CIP) technologies. The most popular solution limits the use of prefabricated elements to standardized partial-depth precast prestressed concrete panels as structural stay-in-place (SIP) forms between the girders, with CIP concrete topping, as opposed to traditional removable plywood forms. SIP steel metal deck forms, with a full-depth CIP configuration that eliminates the problem of reflective cracks, are less attractive due to three major drawbacks: a) safety concerns due to risks of accidental damage of relatively thin metal sheets, resulting in local buckling problems under wet concrete load; b) corrosion issues under aggressive environments; c) efficient inspection of the underside of the deck is complicated.

In the project presented herein, an innovative prefabricated glass Fiber Reinforced Polymer (FRP) SIP reinforcement

has been selected to construct the replacement deck of Bridge 14802301 in Greene County, MO. Corrosion resistant FRP reinforcement gratings and SIP form plates are integrated into very large-size modular panels. The structural form takes advantage of FRP composites tailorability and lightweight to provide improved constructibility, resulting in enhanced construction speed and safety.

2. PREFABRICATED STAY-IN-PLACE FRP REINFORCEMENT

2.1 Description and Detailing

The FRP SIP panels are prefabricated assemblying off-the-shelf pultruded glass/vinylester components, typically used in floor grating applications in corrosive environments, into a three-dimensional grating made of two (top and bottom) layers (Figure 1). The main load-carrying elements are 38 mm I-bars, spaced at 100 mm on-center, which run continuously in the direction perpendicular to traffic (transverse). Both shape and spacing of the I-bars have been thought to allow ease of walking over the three-dimensional assembly. Three-part cross rods, spaced at 100 mm on-center and running through pre-drilled holes in the I-bars web in the direction parallel to traffic (longitudinal), provide shrinkage and temperature reinforcement, enhance the in-plane rigidity of each reinforcing layer, and constrain the core concrete to ensure mechanical compatibility with the structural I-bars. Top and bottom reinforcing layers are integrated using two-part vertical connectors that space them at 100 mm on-center. The two components forming the connectors are shaped to be epoxy-bonded to the I-bars and then fastened together. The formwork consist of 3.2 mm thick and 1.22 m long plates that are epoxy-bonded to the I-bars in the bottom layer.

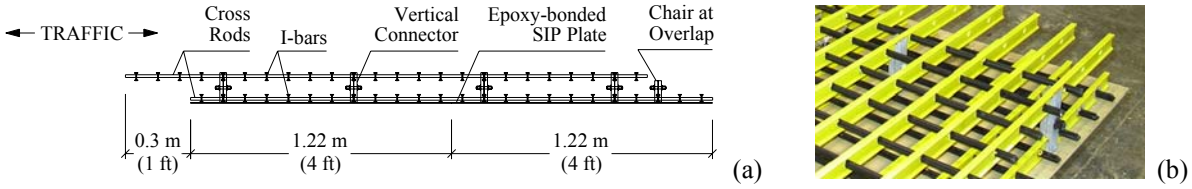

Figure 1: Prefabricated FRP SIP Reinforcement Panels: Longitudinal Section (a) and Close-up (b)

The system concept, detailing and construction procedure have been addressed to improve constructibility by introducing original solutions when needed, and constantly seeking input from practitioners. Each SIP panel has a width of 7.06 m, a typical length of 2.44 m (Figure 1(a)), and a weight of about 409 kg (23.7 kg/m^2). The width corresponds to that of the bridge deck minus 127 mm per side, to allow a traditional drip edge notch to be formed on-site. The use of large-size and lightweight panels allows easy placement of the SIP reinforcement on the bridge girders with single picks of a crane at four anchorage points. Hence, both time-consuming and labor-intensive setting/removing of plywood forms and tying of rebars are eliminated. Adjacent panels are connected in a non-mechanical fashion by means of 0.30 m overlaps, formed by offsetting the top and bottom grating layers (Figure 1(a)), thereby preserving a degree of continuity in the longitudinal direction (Figure 1(a) and Figure 2(a)). 3.2 mm thick strips are inserted to cover the SIP plate-to-plate butt joints in order to prevent concrete leaking during casting (Figure 2(b)). When using steel girders, each SIP unit is anchored to the top flanges via stainless steel threaded bolts at every 2.44 m, keeping the bottom reinforcing layer in place with 6.3 mm thick FRP washers (Figure 2(c)). Holes in the SIP plate are drilled on site. When composite action is sought between girders and deck, the panels can be supplied with pre-drilled holes with longitudinal and transverse spacing of 10 cm on-center to accommodate welded shear studs. No cambering of the panels is required to match the roadway crown, which is formed using the finishing machine. The length and layout of the end panels are designed to fit the actual bridge length and accommodate the expansion joints. Since glass FRP is easy to saw-cut, adjustments can be readily made on site (Figure 2(d)).

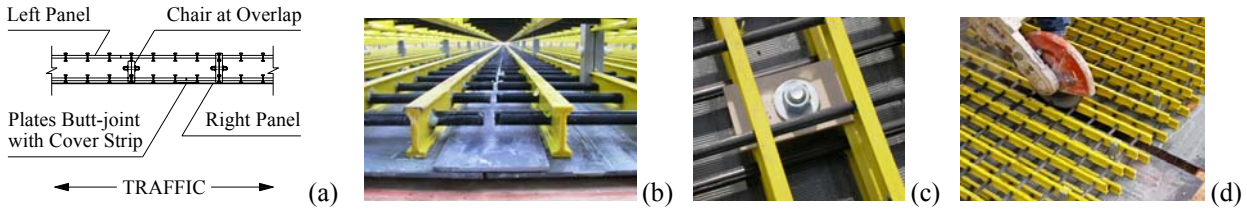

Figure 2: Panel-panel Connection (a, b); Anchoring to Girder (c); End Panels at Expansion Joint (d)

The steel-free reinforcement system is completed with the prefabricated glass FRP rebar cages of a newly designed open post Modified Kansas Corral Rail (Matta and Nanni, 2006). Cut-out pockets in the panels overhang reinforcement facilitate insertion of the post cages at the correct spacing. The continuous top rail reinforcement is made of either 2.44 m or 4.88 m long cages with 1.22 m rebar splices, thought to be rapidly mounted prior to rail forming. Again, the use of lightweight FRP cages greatly simplifies handling and mounting operations, while eliminating on-site rebar tying that is particularly labor-intensive in this case.

2.2 Research and Development

Extensive research and development work during the last 14 years has demonstrated the structural effectiveness of pultruded FRP gratings as internal reinforcement of concrete bridge decks. Two recent pioneer construction projects have been completed in Wisconsin, USA (Bank et al., 2006; Berg et al., 2006). The solution presented herein features the last-generation system, and the first with fully-integrated reinforcement and SIP forms (Ringelstetter et al., 2006). The project Special Provisions included FRP Material Specifications, in compliance with a model specification developed for the FHWA (Bank et al., 2003). Performance Specifications were also defined for the SIP panels by imposing stress and deformation limitations to test panels when simulating typical construction loads, i.e. vertical and lateral loads, in-plane racking, vertical load on overlaps, and wet concrete load (Matta et al., 2005).

The FRP RC open post rail was designed following the ACI 440 guidelines (ACI, 2006) to meet the AASHTO LRFD (AASHTO, 1998) and Standard Specifications (AASHTO, 2002). In the case of the LRFD provisions, where a yield-line approach is recommended to evaluate the equivalent transverse static strength, deformation compatibility was assumed to account for the lack of moment redistribution in FRP RC structures, along with conservative failure scenarios (Matta and Nanni, 2006). In addition, the end posts located at the expansion joints and approach deck, where rail continuity is not provided, were designed to exceed the required crash Test Level 2 strength F_T = 120 kN. The deck and rail design was validated through laboratory testing of full-scale deck slabs and rail post/deck connections, which was performed at key steps of the optimization process, and confirmed the significant safety margin of the layout selected for the field implementation (Matta et al., 2005).

3. FIVE-DAY BRIDGE REDECKING

The old Bridge 14802301 (Greene County, MO) slab-on-girder superstructure, built in 1933, was in need of replacement because of severe corrosion-induced degradation of deck and safety appurtenances, and increased load requirements. The load rating was 3.9 t (2004), versus an original design based on a 9.1 t truck load with 30% impact factor. The new superstructure has four symmetrical spans of 11.3 m (exterior) and 10.7 m (interior) length, for a total length of 43.9 m. The cross section comprises four W610×25 steel girders spaced at 1.8 m on-center and acting non-compositely with a 178 mm thick deck. The out-to-out deck and clear roadway width are 7.3 m and 6.7 m, respectively. The girders are continuous over two spans, with a closed expansion joint at the central support.

Transition from research and development to field implementation was conducted in coordination with the manufacturers of the FRP deck and rail reinforcement, and the engineer of record. The construction operations were planned with the contractor parties to minimize the amount of time and work. Construction of the RC deck and railing from the SIP panel installation to rail casting is documented in Figure 3. The job was completed in November 2005 in five days, instead of the typical 2-3 weeks needed for similar steel reinforced bridges built by the contractor. Installation of the deck panels was finalized in six hours during the first day by six workers. During the second day, the 36 rail post cages were mounted, the deck details formed (expansion joints, chamfers, drip edges), and the finishing machine was set. Deck casting and finishing was completed in the third day. The remaining two days were used to mount the open post concrete rail top continuous cages and the formwork, and finally casting.

4. CONCLUSIONS

The first application project of a innovative prefabricated FRP reinforcement for rapid bridge deck construction has been presented. The use of very large-size and lightweight modular stay-in-place panels, comprising a double-layer grating with epoxy-bonded form plates and designed for improved constructibility, eliminates the need of formwork and on-site tying of reinforcing bars. The five-day redecking resulted in over 70% reduction in deck construction time, with a similar reduction in labor cost. Shape and spacing of the reinforcing profiles, devised to facilitate

walking over the three-dimensional assembly, allowed an increase of about 50% in concrete placement productivity while improving safety and working conditions, as confirmed by the field workers.

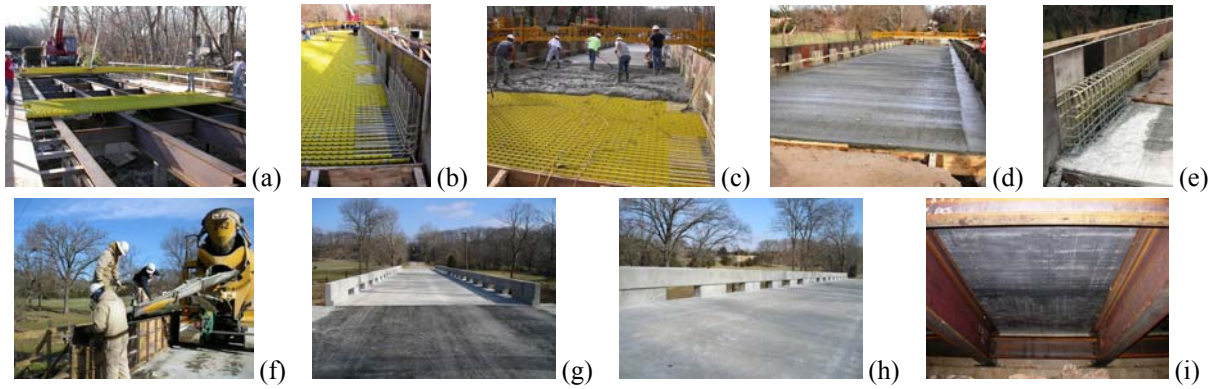

Figure 3: Bridge Redecking Operations: Panels Installation (a); Mounting of Post Cages (b); Deck Casting (c) and Finishing (d); Mounting of Top Rail Cages (e); Rail Casting (f); Finished Superstructure (g-i)

A conservative cost estimate for the deck as-built is \$409/m^2 (\$38/ft^2), of which \$280/m^2 (\$26/ft^2) from the prototype FRP panels delivered to the site. The amount increases to \$483/m^2 (\$44.9/ft^2) including the cost of the open post railing (\$271/m, \$82.6/ft). The competitive potential of the proposed system is also enhanced by the durability of FRP reinforcement, with prospective increased service life and reduced maintenance costs.

5. ACKNOWLEDGEMENTS

The financial support of the US DOT, the UMR UTC on Advanced Materials and NDT Technologies, and the Federal Highway Administration, thorugh the Innovative Bridge Research and Construction Program, is acknowledged. The assistance of Strongwell and Hughes Brothers, industry members of the UMR NSF I-U/CRC "Repair of Building and Bridges with Composites" (RB^{2}C), is also acknowledged. Thanks are due to Greene County, MoDOT, Great River Engineering, Hartman Construction, and Master Contractors LLC, for active support.

6. REFERENCES

American Association of State Highway and Transportation Officials (1998). *AASHTO LRFD Bridge Design Specifications*, 2nd edition, AASHTO, Washington, DC.

American Association of State Highway and Transportation Officials (2002). *Standard Specifications for Highway Bridges*, 17th edition, AASHTO, Washington, DC.

American Concrete Institute Committee 440 (2006). *ACI 440.1R-06 - Guide for the Design and Construction of Concrete Reinforced with FRP Bars*, ACI, Farmington Hills, MI.

Bank, L.C., Gentry, T.R., Thompson, B.P., and Russell, J.S. (2003). "A Model Specification for FRP Composites for Civil Engineering Structures". *Construction and Building Materials*, Vol. 17, No. 6-7, pp. 405-437.

Bank, L.C., Oliva, M.G., Russell, J.S., Jacobson, D.A., Conachen, M.J., Nelson, B., and McMonigal, D. (2006). "Double Layer Prefabricated FRP Grids for Rapid Bridge Deck Construction: Case Study". *Journal of Composites for Construction*, Vol. 10, No. 3, pp. 204-212.

Berg, A.C., Bank, L.C., Oliva, M.G., and Russell, J.S. (2006). "Construction and Cost Analysis of an FRP Reinforced Concrete Bridge Deck". *Construction and Building Materials*, Vol. 20, No. 8, pp. 515-526.

Matta, F., and Nanni, A. (2006). "Design of Concrete Railing Reinforced with Glass Fiber Reinforced Polymer Bars", *Proceedings of 2006 ASCE-SEI StructuresCongress*, CD-ROM, 9 pp.

Matta, F., Nanni, A., Galati, N., Ringelstetter, T.E., Bank, L.C., Oliva, M.G., Russell, J.S., Orr, B.M., and Jones, S.N. (2005). "Prefabricated Modular GFRP Reinforcement for Accelerated Construction of Bridge Deck and Rail System", *Proceedings of FHWA Accelerated Bridge Construction Conference*, pp. 129-134.

Ringelstetter, T.E., Bank, L.C., Oliva, M.G., Russell, J.S., Matta, F., Nanni, A. (2006). "Development of a Cost-Effective Structural FRP Stay-In-Place Formwork System for Accelerated and Durable Bridge Deck Construction". *Proceedings of 85th Transportation Research Board Annual Meeting*, CD-ROM #06-2218, 16 pp.

COMPOSITES 2005 Convention and Trade Show
American Composites Manufacturers Association
September 28-30, 2005
Columbus, Ohio USA

Pultruded Grid and Stay-in-Place Form Panels for the Rapid Construction of Bridge Decks

by

Fabio Matta
Nestore Galati
Antonio Nanni

CIES-University of Missouri, Rolla, MO

Thomas E. Ringelstetter
Lawrence C. Bank
Michael G. Oliva

University of Wisconsin, Madison, WI

Abstract

The impact of the economic and social costs associated with bridge deck rehabilitation and replacement presents the need to develop durable structural systems that can be rapidly installed. Extensive R&D work funded by the Federal Highway Administration (FHWA) demonstrated the feasibility of using FRP pultruded gratings for the rapid construction of steel-free bridge decks. The technology was recently implemented in pilot field applications in Wisconsin, U.S.A. This paper reports on the development and detailing of a new glass fiber reinforced polymer (GFRP) stay-in-place (SIP) formwork to be applied as reinforcement system in the superstructure replacement of a slab-on-girder bridge in Greene County, MO. The modular SIP panels, developed to meet prescriptive material and structural performance specifications, consist of a top and a bottom grid layer comprising 1-1/2" (38 mm) pultruded I-bars and cross rods in the direction perpendicular and parallel to traffic, respectively. The grid layers are connected via two-part shear connectors. The bottom I-bars are bonded onto a 1/8" (3.2 mm) plate that acts as a formwork. The system will be complemented by a concrete open-post railing reinforced with GFRP rebars. First laboratory testing confirmed that the punching shear capacity of simply supported gridform reinforced deck slabs considerably exceeds the design service load, while the presence of the form plate greatly enhances the stiffness with respect to non-SIP double-layer grating reinforced counterparts.

Introduction

Corrosion of the steel reinforcement within bridge decks and safety appurtenances is a major instrument of degradation, with effects accruing from the use of deicing salt on roads and exposure to harsh environments. The use of pultruded GFRP rebars as internal reinforcement of decks and railings ideally eliminates the issue and simplifies installation, and is emerging as a practical alternative to conventional steel reinforcement (Bradberry 2001, Buth et al. 2003, El-Salakawi et al. 2003). Due to the peculiar physical and mechanical properties of FRP materials, the design philosophy of FRP reinforced concrete structures is substantially different from that of traditional reinforced concrete, and design guidelines are fairly well established (ACI 2003, Nanni 2003).

The variety of commercially available pultruded elements enables one to devise different reinforcement strategies. In the project presented herein, large-size GFRP pultruded SIP panels comprising a double-layer grid and a formwork plate (gridform), have been selected to construct the deck of the new Bridge 14802301 in Greene County, MO. Replacement of the current slab-on-girder superstructure is needed because of its precarious conditions (Fig. 1) and increased load requirements. The new superstructure has four symmetrical spans of 37' (11.3 m) exterior and 35' (10.7 m) interior, for a total length of 144' (43.9 m). The cross section comprises four W24×84 girders spaced at 6' (1.8 m) and acting non-compositely with a 7" (178 mm) thick deck, with an out-to-out deck and clear roadway width of 24' (7.3 m) and 22' (6.7 m), respectively. The girders are piecewise continuous over two spans, with a closed expansion joint at the central support. To date, extensive research has demonstrated the effectiveness of using pultruded FRP gratings as internal reinforcement of bridge decks (Bank et al. 1992, Bank and Xi 1993, 1995). Together with durability, the key feature of the proposed solution is the rapidity of installation. This is ensured by no need of tied-in-place reinforcement, lightweight of the prefabricated gridform panels (about 4.7 lb/ft^2, 23 kg/m^2), and the use of SIP formwork. All aspects of the design, detailing and construction procedure have been addressed to improve constructibility.

The system will be complemented by a modified open-post Kansas Corral Rail internally reinforced with GFRP rebars. In reality, when using GFRP SIP gratings and formwork, a fully integrated rail reinforcement composed of similar pultruded elements would be an ideal alternative. The objective is to develop a competitive all-in-one reinforcement system to be rapidly installed prior to casting of the concrete.

GFRP SIP Form and Reinforcement Panels

Gridform Description and Construction Details

The width of each prefabricated panel is 24' (7.3

m), corresponding to the out-to-out deck width, typical length is 8' (2.4 m), and thickness 5-5/8" (143 mm), as shown in Fig. 2, for a total weight of about 900 lb (408 kg). The assembly comprises four pultruded glass/vinylester (GV) components (Fig. 3): a) 1-1/2" (38 mm) pultruded I-bars, spaced at 4" (102 mm) on-center, which run continuously along the deck width, i.e., perpendicular to traffic, and are the main load-carrying elements; b) three-part pultruded cross rods, spaced at 4" (102 mm) on-center, which run through pre-drilled holes in the I-bars web in the direction parallel to traffic, contributing to the in-plane rigidity of the structural assembly and mechanically constraining the core concrete to ensure load transfer to the I-bars; c) two-part shear connectors, which space the grid layers 2.5" (63 mm) apart and provide structural integrity to the gridform, thereby allowing large-scale panels to be lifted in a single pick of a crane and placed on the bridge girders; d) 1/8" (3.2 mm) thick pultruded plate adhesively bonded to the outer face of the bottom I-bars, which does not have structural function and acts solely as formwork.

The top and bottom grid layers of each panel are off-set such that adjacent SIP panels can be easily field spliced by means of non-mechanically connected 1' (305 mm) overlaps (Fig. 4a), thereby providing continuity in the longitudinal direction (parallel to traffic). Two 11'-11"×3"×1/8" (3.6 m×76 mm×3.2 mm) pultruded strips will be inserted to cover the butt-joint between the form plates, in order to avoid any concrete leakage during pouring. End panels were specifically designed to fit the closed expansion joints.

No bending of the panels is required in the transverse direction to match the roadway crown, which will be formed in place using the deck finishing machine, and in the longitudinal direction to accommodate the relatively small girder camber.

Upon placement directly over the steel girders, the flat panels need to be anchored to ensure stability during the construction process and in the long term. Automatic end welded threaded rods will be used to hold down the bottom layer grating, in combination with 1/4" (6.3 mm) thick GFRP washers. The anchors will be rapidly welded on-site after drilling of circular holes through the GFRP form plate.

The detail of the gridform panel edge is illustrated in Fig. 4b. The form plate extends throughout the entire deck width, whereas the I-bars are trimmed to ensure a 1" (25 mm) concrete cover. The drip edge is formed using a pultruded GFRP 1"×1"×1/8" (25 mm×25 mm×3.2 mm) L-shape epoxy bonded to the bottom plate end along the entire bridge length. The two outer cross-rods are removed from the top grating, in order to facilitate insertion and securing of the reinforcement cage for the railing post, which will be carried out in the field prior to lifting and placement of the panels. Fig. 4c shows the connection between the deck and the 4' (1.2 m) long and 10" (0.25 m) thick rail post, developed to provide the required strength while being geometrically compatible with the gridform layout.

Material and Performance Specifications

The project Special Provisions included Material Specifications for the pultruded grid elements, defined in compliance with a model specification recently developed for the FHWA (Bank et al. 2003), and Performance Specifications for the gridform assembly. This provides the manufacturers with a set of acceptance criteria to be met to develop their own double-layer formwork and reinforcement panels, given specified quantities for the total cross-sectional area of FRP in the grid layers and maximum/minimum spacing between the grating components.

Based on the ratio of glass to resin, three classes of GV materials were specified for the structural elements of the grating, i.e., GV-1, GV-2 and GV-3 for cross-rods, I-bars and shear connectors, respectively (Bank et al., 2004). The three GV materials are characterized by a minimum total fiber volume fraction of 55%, 45% and 40%, and longitudinal fiber volume fraction (relative to the total fiber volume fraction) of 90%, 75% and 50%, respectively.

The Performance Specifications were defined to ensure the ability of the selected gridform to maintain integrity throughout the entire bridge construction process. Resistance of the gridform to picking loads during lifting, handling and placing on the bridge girders, without excessive permanent deformations, is typically ensured if the panels can be lifted without damage using four simultaneous pickup points. Limitations were imposed to stresses in individual structural elements and deformations of full-scale test assemblies, subjected to forces representative of that applied during the construction phases, i.e., a) Vertical construction loading before and during casting of the concrete; b) Lateral loads applied to the top surface; c) In-plane racking; d) Vertical Load on splice overlap; and e) Wet concrete loading. Requirements from a) to d) were defined for a similar double-layer grating system, successfully used in a recent project (Bank et al. 2004).

Requirement e) was added for the present SIP form application, since the panels have to withstand the vertical load of the wet concrete, while remaining stable and exhibiting limited deformation. To ensure a satisfactory performance, a simply supported test sub-assembly of the gridform, having a span length between the supports replicate of actual the girder spacing, must resist a vertical load equivalent to that of the concrete bridge deck applied uniformly to the bottom surface using sand or a

similar material. A limiting stress of 50% of the FRP tensile strength in any FRP component was imposed. The downward deflection limit of 0.5" (13 mm) of the bottom surface, relative to the fixed support, was intended to prevent a dead load elastic deformation of the panels in excess of 1/180 of the form span length, or 0.25" (6.3 mm) when the gridform is placed over multiple supports, similar to the AASHTO design specifications for conventional deck SIP formwork (AASHTO 1998).

Testing of Gridform under Concrete Loading

A non-destructive test was performed on a 7'×8' (2.1 m×2.4 m) panel sub-assembly to assess the response under the load of wet concrete. Simple supports were aligned and spaced at 6'-4" (1.9 m) center-to-center, i.e., nearly the same girder spacing of 6' (1.8 m) proposed for the new Bridge 14802301. The panel was loaded with an increasing volume of sand until a uniform pressure of about 87.5 lb/ft^2 (427 kg/m^2) was attained (Fig. 5), which corresponds to that induced by a 7" (178 mm) thick concrete layer, with a 1.5" (38 mm) cover to the outer face of the top I-bars. Load and midspan deflection were measured at various intervals and are reported in Fig. 6. A maximum deflection of 0.42" (10.7 mm) was observed at the centerline of the simply supported panel 24 hours after placement of the sand. Therefore, the expected dead load deflection for a three-span continuous panel replicate of the bridge configuration was calculated as 0.22" (5.7 mm), thus in compliance with the Performance Specifications.

GFRP Reinforced Open-Post Concrete Rail

Rail Description and Detailing

The development of GFRP reinforced concrete railings is of primary importance to develop a truly steel-free bridge deck system. In the present case, the ideal solution is clearly to use pultruded I-bar and cross-rod grids integrated with the gridform. The concept is illustrated in Fig. 7 for a typical continuous concrete barrier configuration.

Results from crash testing of a Test Level 3 open-post rail (and deck) reinforced with pultruded GFRP bars, conducted in compliance with the performance specifications in NCHRP Report 350 (Ross et al. 1993), provided experimental evidence of the acceptable performance of the system when subjected to vehicle impact load (Buth et al. 2003). A similar solution was proposed for the the current project. A modified Kansas Corral Rail open-post concrete rail, reinforced with GFRP pultruded bars, was designed. The design objective was twofold: first, the rail should have the same or greater design strength of steel and GFRP reinforced counterparts under different possible failure modes; second, the reinforcement layout should be simpler than that of the open-post Kansas Corral Rail, as suggested by the engineer-of-record. Fig. 8 depicts a typical thru-post reinforcement layout. The railing has a cross section that replicates that of the Kansas Corral Rail, with a height increased from 27" (686 mm) to 30" (762 mm) to further reduce the risk of roll-over.

The GFRP rebars will be tied in cages using plastic ties. Lightweight cages will be preassembled in relatively large moduli, i.e., post reinforcement cages, including the rail/deck connection, and 8' (2.4 m) and 16' (4.9 m) top beam reinforcement cages. The components will be delivered to the site and the post cages rapidly tied to the gridform panels prior to installation. The beam reinforcement will be installed after pouring and finishing of the deck.

The connection between the post reinforcement and the gridform panels, shown in Fig. 4c, was designed to resist the 54 kip (240 kN) transverse load applied at a height of 24" (610 mm) from the roadway surface, as required for the correspondent rail class (AASHTO 1998).

Rail Design

The yield line method was applied for the preliminary evaluation of the resistance of the concrete rail to lateral load. Upon postulation of admissible collapse mechanisms, the ultimate load is determined via the Principle of Virtual Work, according to the general formulation shown in Fig. 9, wherein $F_{T,u}$ is the ultimate lateral load, applied at a height $H_e \geq 24$" (610 mm) from the roadway and uniformly distributed along $L_T = 4$' (1.2 m); δ is the average virtual displacement of the rail along L_T; $\phi_f M_{n,i}$ is the design moment of the GFRP reinforced section i considered in the collapse mechanism, computed as per ACI 440.1R-05 (ACI 2005); and φ is the rotation at the section i given as a function of δ, H_e, length of opening, O, and length of post, P.

The theoretical strength determined assuming the collapse mechanisms illustrated in Fig. 10 is summarized in Fig. 11. Although the 2 post/3 span failure mode is typically assumed as applicable for open-post concrete railings (Hirsch 1978), other failure modes are considered to provide a better understanding of the overall performance. In particular, the strength of the end portion of the rail, i.e., at the approach deck and at the expansion joints, is verified to exceed the required $F_T = 54$ kip (240 kN) even when considering a single post, with the connected deck section engaged as a resisting structural member, and neglecting any contributions of adjacent portions of the deck. A similar failure mechanism assumed at an intermediate post (1 post/2 span), without accounting for any contribution from posts nearby, still yields a theoretical ultimate strength of 50.5 kip (225 kN).

Punching Shear Strength of Full-Scale Gridform Reinforced Deck Panel

Test Specimen and Set-up

Full-scale testing of a simply supported 7'×8'×7" (2.1 m×2.4 m×178 mm) gridform reinforced concrete panel was conducted at the Structures and Materials Testing Laboratory (SMTL) at the University of Wisconsin, Madison, WI. The specimen was constructed indoors over 8" (203 mm) wide concrete block supports spaced at 6'-4" (1.9 m) on-center, at approximately 1'-4" (0.4 m) off of the lab floor. A Wisconsin DOT Grade D, Size 1 (3/4", 19 mm maximum aggregate size) concrete design mix, with a 28-day target compressive strength of 4,000 psi (28 MPa), was utilized. During concrete pouring, a maximum midspan deflection of 0.332" (8.4 mm) was measured, which is associated to a value of 0.175" (4.4 mm) in case of continuous three-span configuration, thus significantly below the prescribed limit.

Since the overlap between adjacent panels represent the weakest portion of the reinforcement grid, the test specimen included a lap splice positioned nearly flush with the edge of the loading plate, as sketched in Fig. 12. This set-up ensured that the diagonal punching shear failure surface would propagate through the non-mechanical grid connection. Deflections were continuously recorded using linear variable differential transformers (LVDTs) and a strain potentiometer, while the load cell provided the values of the applied load. Strain gauges were mounted on the upper concrete surface and on the bottom FRP plate. Load was applied using a 200 kip closed-loop servo-hydraulic actuator, which was mounted on a steel frame connected to the laboratory structural floor. A 10"×2'-1"×2" (0.25 m×0.64 m×51 mm) neoprene rubber bearing pad was interposed between the 8"×2'-1"×2" (0.2 m×0.64 m×51 mm) loading steel plate and the concrete surface, thereby simulating the contact area of a typical truck tire.

Prior to testing, the slab was subjected to ten 0-21-0 kips load-unload conditioning cycles, with 21 kip (93.4 kN) corresponding to the 16 kip (71.2 kN) HS20-44 truck wheel service load increased by a 30% impact factor (AASHTO 1998). The ultimate capacity of the test specimen was then determined by manually applying a monotonic load until failure was attained. Load-control mode was initially selected, and changed to displacement-control at about 25 kip (111.2 kN), thus loading the deck panel in a more controlled manner as it approached failure. The loading progression was paused at different stages to allow for the observation of cracking and general inspection.

Test Results

Ultimate capacity of the simply supported deck panel was 124.9 kip (555.6 kN), with a maximum deflection of 0.67" (17 mm). Failure occurred in a brittle fashion clearly due to punching shear, with the neoprene pad pushed into the top of the slab. A number of flexural cracks were observed at the midspan region, starting at a load level of 36.5 kip (162.4 kN). The applied load-deflection trace, labeled G1 (G = gridform), is shown in Fig. 13. The slab surface area within the edges of the bearing pad interested by failure initiation can be seen in Fig. 14, wherein the wood block between the actuator and the specimen was inserted to support the actuator.

The path followed by the shear crack slightly varied depending on whether or not the fracture surface intersected the panels overlap, as can be clearly recognized in Fig. 15. On the right hand side, where the splice was located, shear crack progressed diagonally through the thickness of the slab, in the direction of the butt-joint between the cross-rods of the bottom FRP grating, eventually separating the adjacent I-bar from the bonded form plate. This confirms that, despite the overlap region representing a relatively weaker area of the slab, the overall structural response of the panel is adequate. On the left hand side, fracture also developed diagonally, but did not progress downwards to the interface between I-bars and bonded plate. Instead, once the crack reached the level of the top flange of the bottom I-bars, it abruptly turned horizontal, progressing in the same direction until it reached the edge of the slab.

Comparison with Previous Tests

In a previous experimental program, three simply supported slab panels reinforced with a similar double-layer pultruded grid, shown in Fig. 16 , were tested to failure (Jacobson et al. 2004). The only differences with respect to the present reinforcement configuration were the absence of the bottom formwork plate, and the adoption of an 8" (203 mm) slab thickness, where the bottom grating was supported by chairs that provided a 1" (25 mm) clear concrete cover between the outer surface of the I-bars and the deck underneath surface. This was not needed with the new solution, since the bottom grating is directly bonded to the SIP form, thereby allowing to reduce the concrete thickness from 8" (203 mm) to 7" (178 mm) by assuming a conventional flexural design approach.

The load-deflection traces of the three double-layer grating reinforced specimens, labeled J1, J2 and J3 (J = Jacobson), are plotted in Figure 13 together with that of G1. Fig. 17 summarizes the values of ultimate load and deflection for all specimens. It is noted that G1 exhibited a significantly higher stiffness than J1, J2 and J3, with an ultimate deflection about three times lower. This is essentially attributed to the significant contribution of the 1/8" (3.2 mm) thick epoxy bonded form panel, which apparently acted compositely with the 7" (178 mm) deck

section, providing additional tensile reinforcement.

Theoretical Prediction of Punching Shear Capacity

Fig. 18 shows an empirical design equation recently developed at the University of Wisconsin, Madison, to predict the ultimate punching shear capacity of concrete slab panels reinforced with double-layer pultruded gratings (Jacobson 2004). The proposed approach proved to be effective both in case of flexurally restrained and simply supported specimens, even in presence of an panel-to-panel non-mechanical connection. The punching shear capacity, V_{UW}, is expressed as a function of the reinforcement ratio, ρ, given by the area of FRP reinforcement in tension, A_f, divided by bd, where b is the width of the rectangular cross section considered, d is the distance from the extreme compression fiber to the centroid of the FRP reinforcement; the 28-day concrete compressive strength, f'_c; and the critical perimeter measured at a distance of $1.5d$ from the edge of the loaded area, $u_{1.5}$. $u_{1.5}\, d$ represents the vertical surface area over which the shear strength provided by the concrete, V_c, acts.

Utilizing the as-built dimensions of G1 specimen and the average concrete cylinder compressive strength of 4,347 psi (30 MPa), the predicted punching shear capacity is calculated as 124.1 kip (552 kN), which is in excellent agreement with the experimental ultimate load of 124.9 kip (556 kN). Following the same procedure, the predicted design capacity of a 7" (178 mm) thick concrete deck reinforced with the gridform system, accounting for a concrete compressive strength f'_c = 4,000 psi (28 MPa), is V_{UW} = 109.7 kip (488 kN), which is in excess of five times greater than the HS20-44 wheel service load including the impact factor.

Conclusions

A new pultruded GFRP stay-in-place formwork and internal reinforcement for concrete bridge decks, referred to as gridform, has been introduced herein. The system will be complemented by a concrete railing reinforced with GFRP rebars. The proposed solution will be implemented for the superstructure replacement of a slab-on-girder bridge in Missouri. Along with the well known characteristics of durability ensured by the use of FRP reinforcement, the distinct advantage of the gridform system is the speed of installation. Design and detailing of the composite SIP aimed at competitively combining structural efficiency with ease of installation and constructibility. This was further ensured by compliance with material and performance specifications developed for pultruded GFRP reinforcement cages.

The experimental punching shear capacity of a 7'×8'×7" (2.1 m×2.4 m×178 mm) gridform reinforced deck panel, with simple supports spaced at 6'-4" (1.9 m) center-to-center, was measured as 124.9 kip (556 kN). The value is over five times greater than the typical HS20-44 service wheel load required by the AASHTO Bridge Design Specifications (AASHTO 1998), in agreement with previous extensive experimental work on similar specimens. It is remembered that in the actual bridge deck, additional capacity will be provided by the constraining effect due to structural continuity of the deck over three 6' (1.8 m) spans between the girder supports. The result of an empirical design formula recently proposed to compute the punching shear capacity of concrete slabs reinforced with double-layer pultruded gratings (Jacobson 2004), is in excellent agreement with the experimental value.

Acknowledgements

The authors wish to thank Greene County, MO, Great River Engineering of Springfield, MO (engineer-of-record), Strongwell Corp. and Hughes Brothers Inc., for their valuable contributions. The support of the University of Missouri-Rolla University Transportation Center on Advanced Materials and NDT Technologies, and of the Federal Highway Administration (FHWA) through the Innovative Bridge Research and Construction (IBRC) Program, is gratefully acknowledged.

References

American Association of State Highway and Transportation Officials (1998), "Load and Resistance Factor Design (LRFD) Bridge Design Specifications," AASHTO, 2nd edition.

American Concrete Institute (2005), "Guide for the Design and Construction of Concrete Reinforced with FRP Bars," ACI 440.1R-05, American Concrete Institute, Farmington Hills, MI.

Bank, L.C., Gentry, T.R., Thompson, B.P., and Russell, J.S. (2003), "A Model Specification for FRP Composites for Civil Engineering Structures," *Construction and Building Materials*, 17(6-7), 405-437.

Bank, L., Oliva, M., Russell, J., Jacobson, D., Conachen, M., Nelson, B., and McMonigal, D. (2004), "Super-Sized Double-Layer Pultruded Gratings," *COMPOSITES 2004 Convention and Trade Show*, American Composites Manufacturers Association (ACMA), Oct. 6-8, 2004, Tampa, FL, CD-ROM.

Bank, L.C., and Xi, Z. (1993), "Pultruded FRP Grating Reinforced Concrete Slabs," *Fiber-Reinforced-Plastic for Concrete Structures - International Symposium* (eds. A. Nanni and C.W. Dolan), SP-138, American Concrete Institute, Farmington Hills, MI, 561-583.

Bank, L.C., and Xi, Z. (1995), "Punching Shear Behavior of Pultruded FRP Grating Reinforced Concrete Slabs," *Non-metallic (FRP) Reinforcement for Concrete Struc-*

tures (ed. L. Taerwe), RILEM Proceedings 29, E&FN Spon, London, 360-367.

Bank, L.C., Xi, Z., and Munley, E. (1992), "Performance of Doubly-Reinforced Pultruded Grating/Concrete Slabs," *Proceedings of the 1st International Conference for Advanced Composite Materials in Bridges and Structures* (eds. K.W. Neale and P. Labossiere), October 6-9, Sherbrooke, Canada, Canadian Society for Civil Engineering, 351-360.

Bradberry, T.E. (2001), "Fiber-reinforced-plastic Bar Reinforced Concrete Bridge Decks," *Proceedings of the 80th Annual Transportation Research Board Meeting*, Jan. 9-13, 2001, Washington, DC, CD #01-3247.

Buth, C.E., Williams, W.F., Bligh, R.P., Menges, W.L., and Haug, R.R. (2003), "Performance of the TxDOT T202 (MOD) Bridge Rail Reinforced with Fiber Reinforced Polymer Bars," *TTI Research Report 0-4138-3*, Texas Transportation Institute, College Station, TX.

El-Salakawy, E., Benmokrane, B., Masmoudi, R., Brière, F. and Breaumier, E. (2003), "Concrete Bridge Barriers Reinforced with Glass Fiber-Reinforced Polymer Composite Bars," *ACI Structural Journal*, 100(6), 815-824.

Hirsch, T.J. (1978), "Analytical Evaluation of Texas Bridge Rails to Contain Buses and Trucks," *TTI Research Report 230-2*, Texas Transportation Institute, College Station, TX.

Jacobson, D.A. (2004), "Experimental and Analytical Study of Fiber Reinforced Polymer (FRP) Grid-Reinforced Concrete Bridge Decking," M.S. Thesis, University of Wisconsin, Madison, WI.

Nanni, A. (2003), "North American Design Guidelines for Concrete Reinforcement and Strengthening Using FRP: Principles, Applications and Unresolved Issues," *Construction and Building Materials*, 17(6-7), 439-446.

Ross, H.E., Sicking, D.L., Zimmer, R.A., and Michie, J.D. (1993), "Recommended Procedures for the Safety Performance Evaluation of Highway Features," *Report 350*, National Cooperative Research Program (NCHRP), Transportation Research Board, Washington, D.C.

(a)

(b)

Figure 1 – Degradation of concrete deck, steel girders (a) and safety appurtenance (b) on Bridge 14802301, Greene County, MO

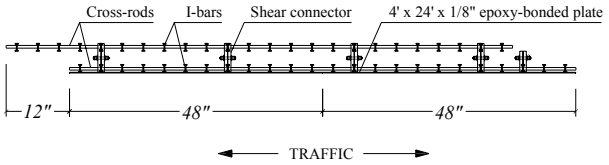

(a)

(b)

Figure 2 – Typical pultruded GFRP gridform panel: longitudinal section (a) and 24'×8' full-scale mock-up on steel girders (b) (1"=25.4 mm, 1'=0.305 m)

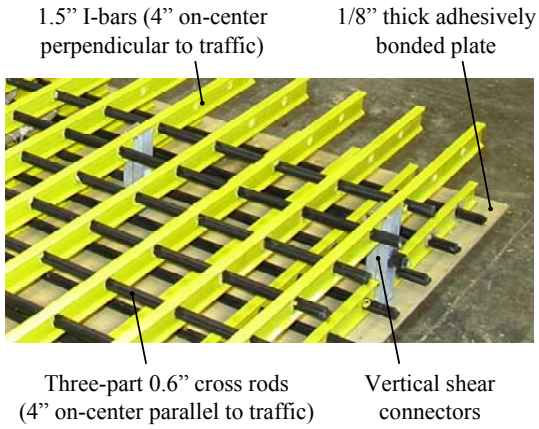

Figure 3 – Close-up of gridform (1”=25.4 mm)

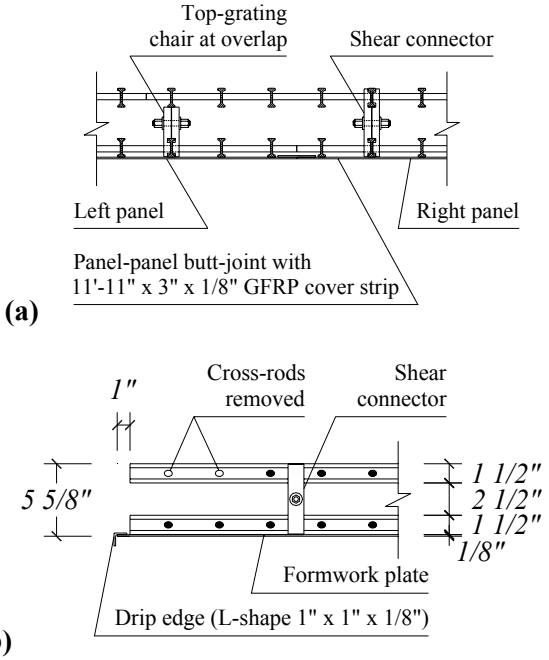

Figure 4 – Construction details: longitudinal panel-to-panel joint (a), edge of panel (b), and deck/post connection reinforcement (c) (1”=25.4 mm, 1’=0.305 m)

Figure 5 – Test set-up of gridform under uniform sand load

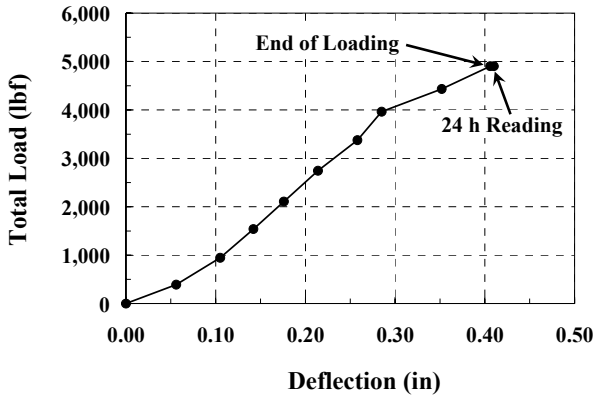

Figure 6 – Load-midspan deflection trace of gridform panel under uniform sand load (1 in=25.4 mm, 1 lbf=4.45 N)

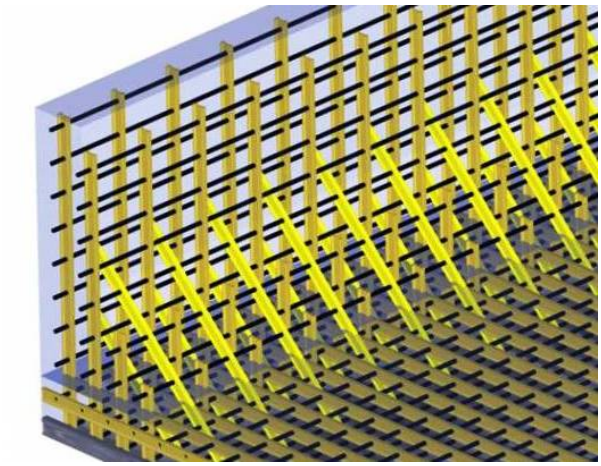

Figure 7 – Rendering of typical pultruded grid reinforced deck and railing system

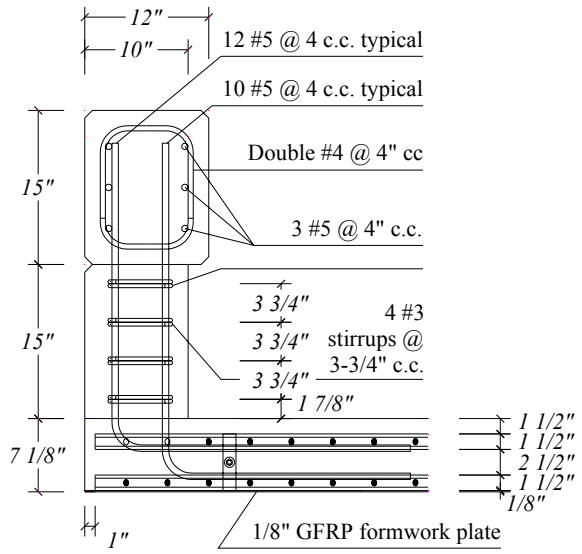

(a)

(b)

Figure 8 – Typical thru-post GFRP reinforcement layout (a) and full-scale post/overhang sample (b) (1”=25.4 mm)

$$F_{T,u}\delta = \sum_i \phi_f M_{n,i} \varphi\left(\delta, O, P, H_e\right)$$

Figure 9 – General energy balance equation to calculate rail resistance to transverse load for admissible collapse mechanisms

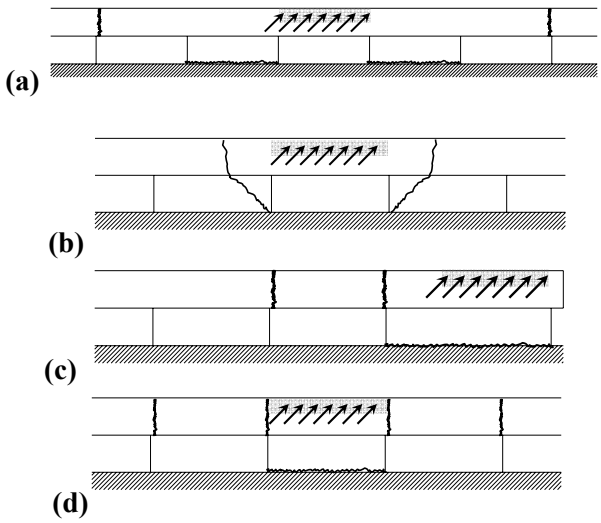

Figure 10 – Failure modes of open-post concrete rail: 2 post/3 span (a); 2 post/2 span (b); 1 end post/1 span (c); 1 post/2 span (d)

Failure mode	$F_{T,u}$* (kip)
2 post / 3 span[a]	58.7
2 post / 1 span	Not Applicable
1 end post / 1 span	55.9
1 post / 2 span	50.5

* No contribution of deck portions adjacent to post is considered in failure mechanisms. Environmental reduction factor C_E = 0.7 assumed for design strength of GFRP bars

[a] Typically accepted for design purposes (Hirsch 1978). Design lateral load F_T = 54 kip (AASHTO LRFD 1998)

Figure 11 – Lateral strength of GFRP reinforced concrete rail as per yield line analysis (1 kip=4.45 kN)

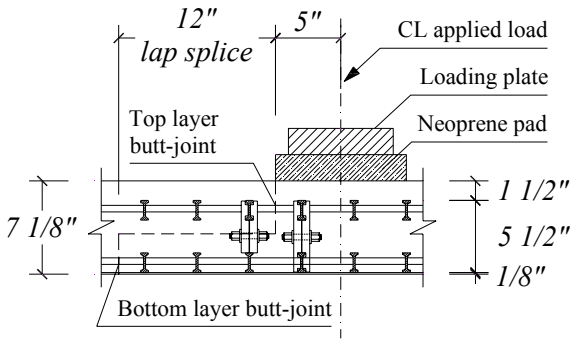

Figure 12 – Detail of gridform lap-splice (1"=25.4 mm)

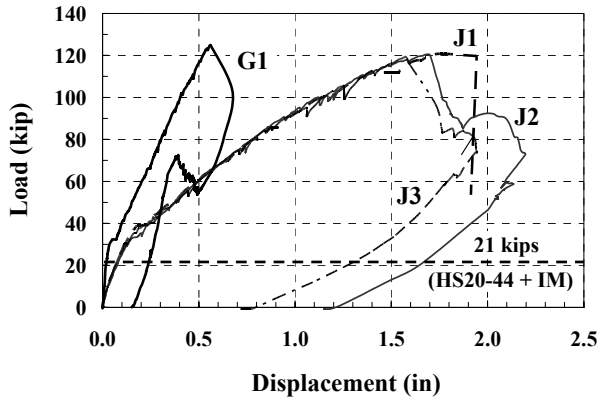

Figure 13 – Load-displacement traces for simply supported deck panels reinforced with gridform, G1 (present), and double-layer pultruded grating, J1, J2 and J3 (Jacobson 2004) (1 in=25.4 mm, 1 kip=4.45 kN)

Figure 14 – Imprint of punching shear failure initiation on specimen G1

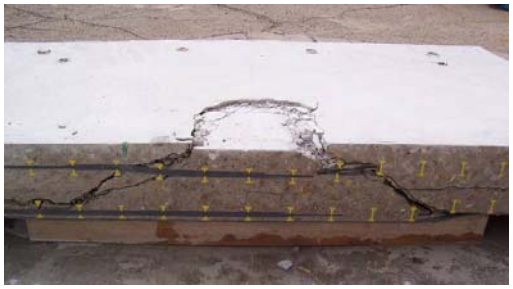

Figure 15 – Section through punching failure surface of specimen G1

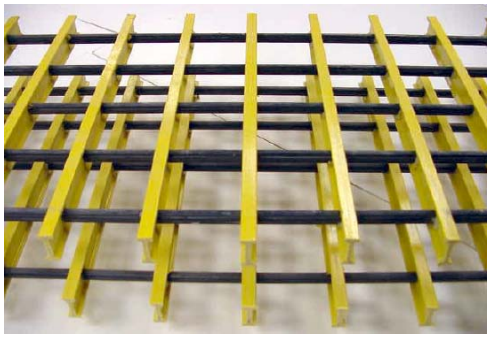

Figure 16 – Double-layer pultruded grating used in specimens J1, J2 and J3 (Jacobson 2004)

Specimen	Failure Load (kip)	Deflection (in)
J1	119.7	1.94
J2	120.2	1.70
J3	119.3	1.56
G1	125.0	0.56

Figure 17 – Experimental ultimate capacity of simply-supported gridform (G1) and double-layer grating (J1, J2, J3) reinforced deck panels (1 in=25.4 mm, 1 kip=4.45 kN)

$$V_{UW} = 4.5\frac{\sqrt[3]{\rho f_c'}}{\sqrt[4]{d}}u_{1.5}d$$

(d and $u_{1.5}$ in mm, f_c' in MPa)

Figure 18 – Empirical equation to predict punching shear capacity of flexurally restrained and simply supported deck slabs reinforced with double-layer pultruded grids (Jacobson 2004)

Proceedings

2005 FHWA Accelerated Bridge Construction Conference - Path to Future

San Diego, California, Dec, 14-16, 2005

Edited By
Atorod Azizinamini, Ph.D., P.E.

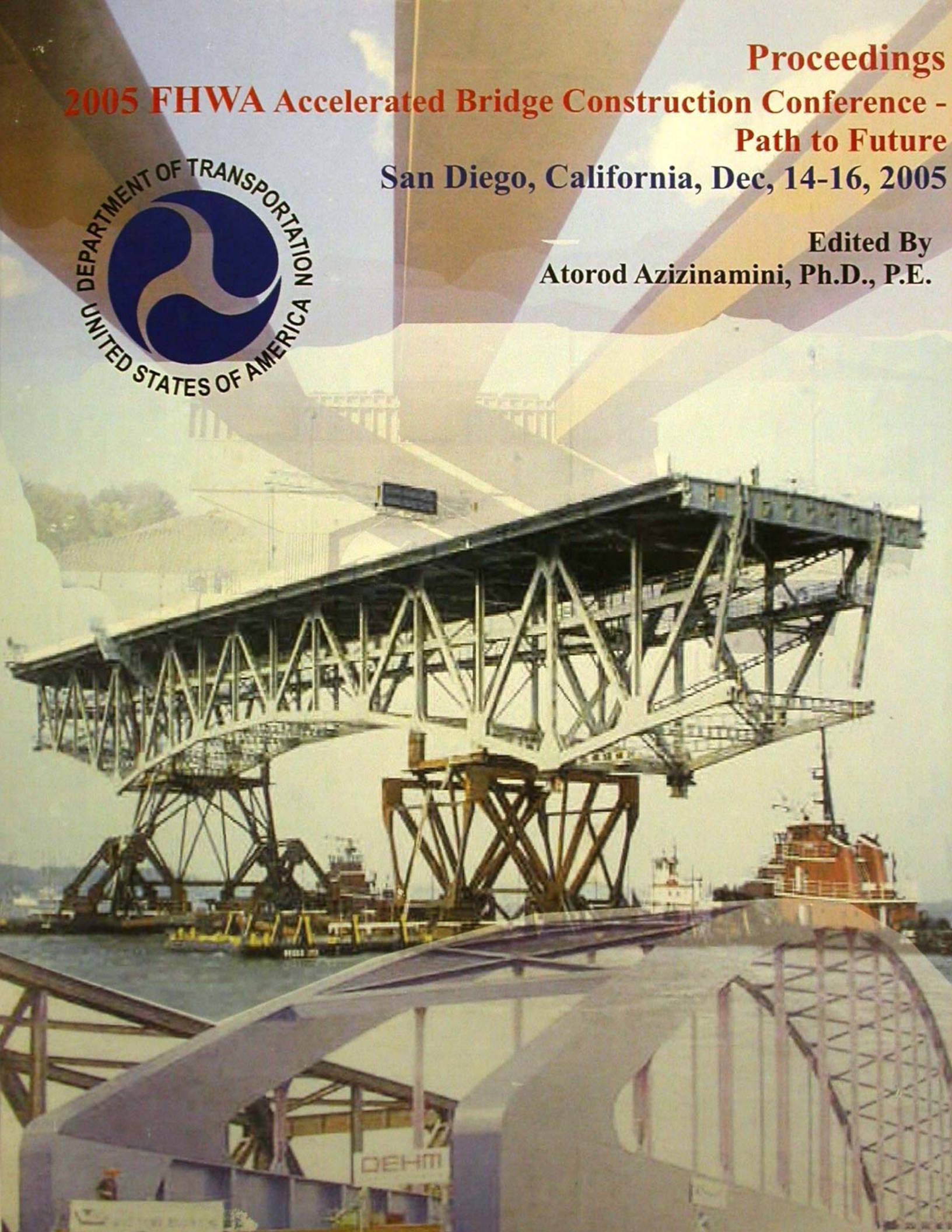

Matta, F., Nanni, A., Galati, N., Ringelstetter, T.E., Bank, L.C., Oliva, M.G., Russell, J.S., Orr, B.M., and Jones, S.N. (2005), "Prefabricated Modular GFRP Reinforcement for Accelerated Construction of Bridge Deck and Rail System," *Proc. FHWA Accelerated Bridge Construction Conference – Path to Future*, San Diego, CA, December 14-16, 2005, ed. A. Azizinamini, Federal Highway Administration, 129-134.

PREFABRICATED MODULAR GFRP REINFORCEMENT FOR ACCELERATED CONSTRUCTION OF BRIDGE DECK AND RAIL SYSTEM

Fabio Matta, Antonio Nanni, Nestore Galati
Center for Infrastructure Engineering Studies, University of Missouri-Rolla, 1870 Miner Circle Dr., Rolla, MO 65409

Thomas E. Ringelstetter, Lawrence C. Bank, Michael G. Oliva, Jeffrey S. Russell
Department of Civil and Environmental Engineering, University of Wisconsin-Madison, 1415 Engineering Dr., Madison, WI 53706

Brian M. Orr, and Spencer N. Jones
Great River Engineering of Springfield, Inc., 2826 S. Ingram Mill, Springfield, MO 65804

ABSTRACT

There is an increasing interest by Departments of Transportation in the development and implementation of durable structural systems for accelerated bridge construction. The main objective is to minimize construction costs, and the impact of the economic and social costs associated with rehabilitation or replacement of a significant portion of the US bridge inventory. This paper reports on the development of an innovative glass fiber reinforced polymer (GFRP) reinforcement for the rapid construction of concrete bridge deck and parapet systems. The deck reinforcement comprises prefabricated modular stay-in-place (SIP) panels (gridforms), consisting of two-layer, three-dimensional grating made of off-the-shelf pultruded shapes, with an epoxy-bonded bottom formwork plate. Pre-assembled GFRP rebar cages are utilized as reinforcement for the open-post concrete parapet. Detailing and construction procedures have been addressed to improve safety and constructibility. Laboratory testing demonstrated the structural adequacy of gridform reinforced slabs under design service loads, and of a first post/deck connection configuration. The system will be implemented in the construction of the new Bridge 14802301 in Greene County, MO, scheduled for completion in November 2005.

INTRODUCTION

Over one quarter of the US bridges are classified as either structurally deficient or functionally obsolete (1). 23% of them, *i.e.*, about 37,000 bridges, are concentrated in the states of Texas, Pennsylvania, Oklahoma, and Missouri. A major instrument of degradation is the corrosion of metallic structural members and steel reinforcement within concrete decks and connections with safety appurtenances, accruing from the routine use of deicing salts on roads and exposure to harsh environments. Increased load requirements further emphasize the need for substantial structural upgrades. The impact of the economic and social costs of such operations calls for the development of competitive and durable structural systems that can be rapidly installed.

The effectiveness of prefabricated pultruded FRP gratings as internal reinforcement of concrete bridge decks has been demonstrated in a number of laboratory tests (2, 3, 4) and pioneer field implementations (5, 6). In addition to the corrosion-resistance typical of advanced composites,

the key features of the solution are ease and speed of installation. Time consuming tying of reinforcing bars is eliminated, while the lightweight of FRP grating dramatically facilitates handling operations of large-scale panels. Furthermore, the use of a SIP configuration, not always practical when adopting conventional metallic forms due to corrosion related issues, would eliminate the need for extensive falsework.

In the project presented herein, large-size GFRP SIP grating panels comprising a double-layer three-dimensional grating and a formwork plate, denoted as gridform, and pre-assembled GFRP rebar cages for both post and rail beam, have been developed and integrated to construct the concrete deck and a newly designed Modified Kansas Corral Rail (MKCR) of the new Bridge 14802301 in Greene County, MO. The structure is scheduled for completion in November 2005. Replacement of the current slab-on-girder superstructure is needed because of its precarious conditions and increased load requirements. The current load rating is 4.3 ton from an original estimate of 11.7 ton, due to extensive degradation of the concrete deck, with through thickness holes up to 1.5' diameter, and diffuse thickness loss of the top flange up to 30%. The deterioration of the connections between deck and safety appurtenances also poses safety concerns. The new superstructure has four spans of 37' exterior and 35' interior, for a total length of 144'. A closed expansion joint at the center support separates the two-span continuous steel girders. The cross section comprises four W24×84 girders spaced at 6' on-center, and acting non-compositely with a 7" thick deck (clear cover of 1.5"). The out-to-out deck and clear roadway width are 24' and 22', respectively. Design, detailing and construction procedures have been addressed to ensure structural adequacy and improve safety and constructibility during installation, in a joint effort between the Center of Infrastructure Engineering Studies at the University of Missouri-Rolla, the University of Wisconsin-Madison, the Greene County Highway Department, Great River Engineering of Springfield (engineer-of-record), Hartman & Co. (contractor), Strongwell (manufacturer of the gridform deck panels) and Hughes Brothers (manufacturer of the GFRP rebars for rail reinforcement).

GFRP STRUCTURAL REINFORCEMENT SYSTEM

Gridform Panels Description and Installation Procedure

Each prefabricated panel has a width of 23'-2", *i.e.*, the out-to-out deck width minus 5" per side, which will be formed on-site. Typical length is 8', and thickness 5-5/8", for a total weight of about 900 lb. The length of the end panels is designed to fit the actual bridge length, and accommodate the expansion joints. The gridforms are made of four pultruded off-the-shelf glass/vinylester components (Figure 1(a)): a) 1-1/2" (38 mm) pultruded I-bars, spaced at 4" on-center and running continuously in the direction perpendicular to traffic (transversal), which are the main load-carrying elements; b) three-part pultruded cross rods, spaced at 4" on-center and running through pre-drilled holes in the I-bars web in the direction parallel to traffic (longitudinal), which enhance the in-plane rigidity of the assembly, mechanically constrain the core concrete to allow load transfer to the I-bars, and provide shrinkage and temperature reinforcement; c) two-part shear connectors, shaped to be epoxy-bonded to the I-bars and fastened with a 3/8" GFRP bolt and nut, which provide structural integrity to the three-dimensional gridform by spacing the grating layers 2.5" apart; and d) 1/8" plates epoxy-bonded to the outer face of the bottom layer I-bars, which act as a formwork.

Cut-out pockets within the overhang reinforcement facilitate insertion of the GFRP rebar post cages at the correct spacing. The detail at a typical thru-section post is illustrated in Figure 1(b), where the I-bars are cut 9" shorter than the form plate at both edges. Upon tying of the post cages, the lightweight gridforms can be lifted with a single pick of a crane (6) at four anchorage points, and placed over the steel girders. The top and bottom grating layers are off-set by 1', thereby allowing the easy field splicing of adjacent panels by means of non-mechanical overlaps (Figure 1(a)), and providing some continuity in the longitudinal direction. Vertical anchoring is ensured by means of 1" diameter steel threaded rods spaced at 8' along each girder, used in combination with washer and nut to hold down the bottom layer grating, in order

to stabilize the structure during construction and service life. The rods can be installed either in pre-drilled holes through the top flange thickness, or via automatic end welding if the equipment is available, while drilling of the circular holes through the form plates is done on-site. Deck casting is carried out after forming the 5" concrete drip edge. This solution is preferred since more practical than using pultruded L- or T-shape drip edges connected to the bottom plate, as initially envisaged (7). Concrete leaking between the panels due to girders camber is prevented by inserting 11'-7"×3"×1/8" pultruded strips to cover each butt-joint between the gridform plates. It is also noted that no bending of the panels is required to match the roadway crown, which is formed in place using the deck finishing machine. The rebar cages for the continuous rail beam, pre-assembled with a length up to 16', are then mounted prior to forming and pouring of the concrete parapet. 4' long GFRP splice rebars are used to connect adjoining cages.

The project Special Provisions included Material Specifications for the pultruded gridform components, defined in compliance with a model specification recently developed for the FHWA (8), and Performance Specifications for the gridform. Limit stresses and deformations were imposed to individual structural elements, and full-scale test panels, respectively, to be subjected to forces representative of that applied during the construction phases: a) vertical construction loading prior and during concrete pouring; b) lateral loads applied to the top surface; c) in-plane racking; d) vertical load on splice overlaps; and e) wet concrete loading (7).

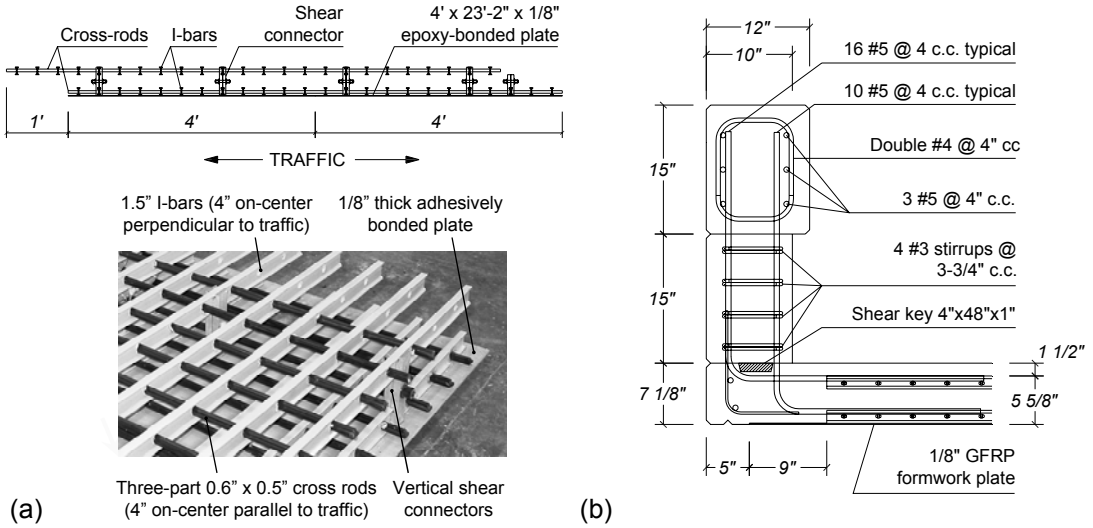

Figure 1 – Typical gridform panels configuration (a), and thru-post reinforcement layout (b).

The cost of the prototype gridform panels for this project is \$26/ft^2, which is significantly lower than that of earlier SIP generation. The approach proposed may become competitive in case of larger-scale production, and valuing the intrinsic savings due to durability properties, and decisive reduction of time-consuming operations with consequent minimized traffic disruption.

Open-Post Rail GFRP Reinforcement Design and Layout

A MKCR internally reinforced with GFRP rebars was designed to complement the deck reinforcement, and develop a truly steel-free bridge deck/rail system. Previous research demonstrated the feasibility of the solution (9, 10). The design objectives were: a) exceed the minimum resistance of Test Level 2 (TL-2) (11), *i.e.*, the category of the open-post rail replaced (12). An equivalent lateral static strength F_T = 27 kip is required to resist the impact of a 4,500 lb pickup truck at 45 mph, with crash angle of 25°. Measures to upgrade the system to the TL-3 category were also evaluated; and b) devise a simple reinforcement configuration geometrically compatible with the gridform layout, allowing rapid pre-assembling of separate post/connection and longitudinal rail beam cages by trained personnel, and easy installation on-site. 4' long

posts and openings were used, instead of the original 3' and 7', respectively. The cross section replicates that of the MKCR, with a height increased from 27" to 30" to reduce the risk of roll-over. The reinforcement layout is illustrated in Figure 1(b).

The rail system was designed in compliance with ACI 440.1R-05 (13). It is emphasized that the linear elastic behavior of FRP rebars does not allow for moment redistribution following yielding at a section where the full capacity is attained, as in the case of steel reinforced sections. Therefore, the assumption of a given failure mode is admissible as long as both equilibrium and deformation compatibility are verified. For the same reason, in the present case, a failure mode involving a single post and two adjacent 4' rail beam spans, assumed fixed at the beam/post joint section, is initially postulated in lieu of a generally accepted and less conservative failure mode where two post/deck connections reach their ultimate capacity (14). The main unknown is the moment-rotation response of the connection system, which is affected (not necessarily concurrently) by the developable tensile stress of the bent rebars within the deck, the behavior of the construction joint, the effectiveness of the anchorage of the post tension rebars, and the contribution of adjacent deck portions.

The cost of the pre-assembled GFRP rail reinforcement is $59/lin.ft, which in perspective should not dramatically exceed the total cost of $90/lin.ft of a conventional Federal Lands MKCR (12).

EXPERIMENTAL CHARACTERIZATION

Gridform Reinforced Deck Panel

A 7'×8'×7" gridform reinforced slab, simply supported at 6'-4" on-center, was subjected to static testing. A concrete design mix with 3/4" maximum aggregate size, and 28-day compressive strength of 4,000 psi, was utilized. A maximum midspan deflection of 0.332" was measured during concrete pouring, corresponding to 0.175" in case of continuous three-span configuration. The value is significantly below the prescribed limit of 0.25" for conventional SIP formwork (11). The specimen included a lap splice positioned flush with the edge of the neoprene loading pad (Figure 2(a)), to assess the response at the weakest area of the reinforcement. The punching shear capacity was 124.9 kip, *i.e.*, nearly six times the 21 kip load corresponding to the 16 kip HS20-44 truck wheel service load increased by a 30% impact factor, as shown in the load-deflection plot in Figure 2(b).

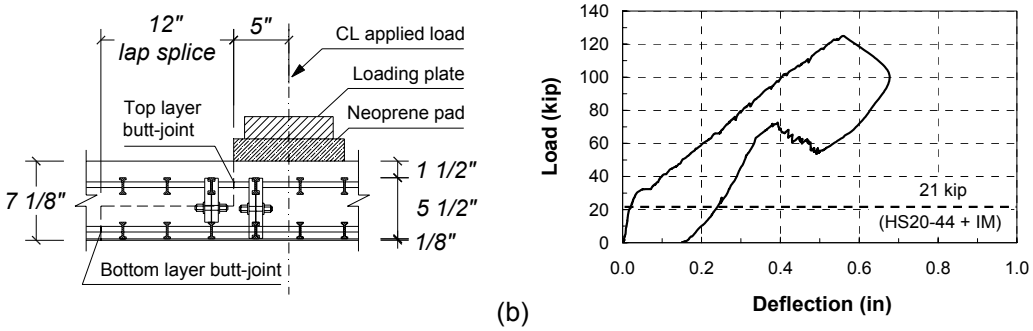

Figure 2 – Detail of gridform lap-splice in test specimen (a), and load-deflection trace (b).

It is noted that the theoretical capacity of 124.1 kip, calculated according to the design equation proposed by Jacobson (15), is in excellent agreement with the experimental value (7).

Rail Post/Deck Connection

Full-scale proof test of a post/deck overhang subassembly was performed to assess the connection resistance and actual rotational stiffness. Figure 3(a) and Figure 3(b),(c) show the

connection configuration tested, and the test setup, respectively. The post was cast on a 8' (twice the post length)×9' gridform reinforced slab, supported over two floor steel beams spaced 3' on-center, and tied to the strong floor using six dywidag steel bars. The overhang length was 3' from the center of the exterior support. Preliminary linear elastic finite element analysis was performed to select test boundary conditions which allowed a deflection profile linearly proportional to that of a real MKCR under the same load conditions. The assembly was instrumented with several strain gauges and displacement transducers.

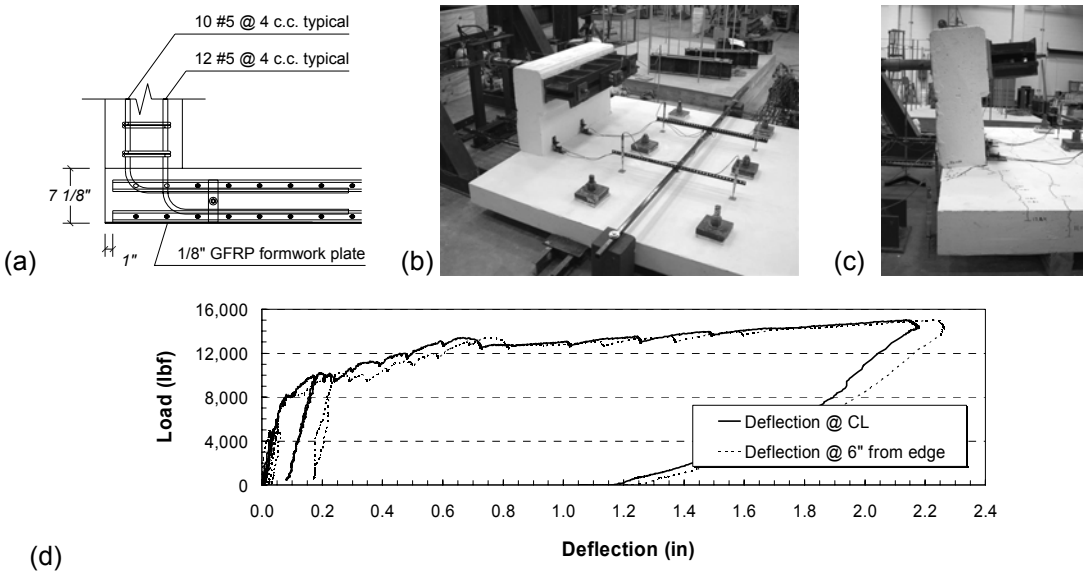

Figure 3 – Schematic of post/deck connection tested (a), test setup (b),(c), and load-deflection profile (d).

Quasi-static load was uniformly applied at 2' from the slab surface by means of a 4' long restraint beam, using a hydraulic jack tied to a reaction frame. An ultimate load of 15.1 kip was attained, corresponding to 45% of the nominal bending capacity of a 4' long slab section, accounting for the contribution of the GFRP rebars only. First cracking initiated at a load of 7.6 kip due to post shear-off at the post/deck interface, where no shear key was included, in order to simulate a construction joint often encountered in practice. Fracture developed within the deck along the concrete/top grating I-bars interface up to a load of 13 kip, followed by an essentially post-mortem diagonal crack started in proximity of the I-bar ends and progressed within the deck. Figure 3(d) shows the load-deflection profile as recorded using two string transducers on top of the rail post (2'-5 3/4" from the slab surface) at the midsection and at 6" from the edge, respectively. The moment-rotation response of the connection would allow a theoretical transverse rail resistance of 47.8 kip (34.9 kip considering the nominal concrete compression strength), assuming a one post-two beam failure scenario. The beam design flexural strength, $(\varphi M_n)_b$, would be reached at an horizontal deflection of 0.36" (0.26"), and bending moment at the connection of 11.2 kip-ft (10 kip-ft), *i.e.*, 74% (66%) of the ultimate capacity. Even though the lateral strength of the configuration largely exceeds the TL-2 requirement, the improved version in Figure 1(b) aims at improving the post/deck continuity by including a shear key, reducing the congestion of FRP underneath the post by introducing cut-out pockets, and increasing strength and stiffness by optimizing the reinforcement layout.

CONCLUSIONS

A novel prefabricated modular GFRP reinforcement for concrete bridge deck and rail systems has been presented. Together with the durability characteristics typical of FRP reinforcement, the distinct advantage of the proposed solution is the speed of installation. Full-scale proof testing of deck panel and post/deck overhang specimens provided experimental evidence of

the structural adequacy of the system, which will be implemented in the upcoming superstructure replacement of a slab-on-girder bridge in Greene County, MO.

ACKNOWLEDGMENTS

The authors wish to thank Greene County, MO, Strongwell Corp., and Hughes Brothers, Inc., for valuable contributions. The support of the University of Missouri-Rolla University Transportation Center on Advanced Materials and NDT Technologies, and of the Federal Highway Administration through the Innovative Bridge Research and Construction Program, is acknowledged.

REFERENCES

1. Federal Highway Administration Bridge Programs NBI Data (2005), Deficient Bridges by State and Highway System, *http://www.fhwa.dot.gov/bridge/defbr04.xls*.
2. Bank, L.C., Xi, Z., and Munley, E. (1992), "Performance of Doubly-Reinforced Pultruded Grating/Concrete Slabs," *Proc. 1st Int. Conf. for Advanced Composite Materials in Bridges and Structures* (eds. K.W. Neale and P. Labossiere), 351-360.
3. Bank, L.C., and Xi, Z. (1993), "Pultruded FRP Grating Reinforced Concrete Slabs," *Fiber-Reinforced-Plastic for Concrete Structures - International Symposium* (eds. A. Nanni and C.W. Dolan), SP-138, American Concrete Institute, Farmington Hills, MI, 561-583.
4. Dieter, D.A., Dietsche, J.S., Bank, L.C., Oliva, M.G., and Russell, J.S. (2002), "Concrete Bridge Decks Constructed with FRP Stay-in-Place Forms and FRP Grid Reinforcing," Transp. Res. Rec. No.1814, *Journal of the Transportation Research Board*, 219-226.
5. Bank, L.C., Oliva, M.G., Russell, J.S., Dieter, D.A., Dietsche, J.S., Hill, R.A., Gallagher, B., Carter, J.W., Woods, S., and Anderson, G.H. (2003), "Details and Specifications for a Bridge Deck with FRP Formwork, Grid and Rebar," Proc*. Fibre-reinforced Polymer Reinforcement for Concrete Structures / FRPRCS-6* (ed. K.H. Tan), 1301-1310.
6. Bank, L.C., Oliva, M.G., Russell, J.S., Jacobson, D.A., Conachen, M.J., Nelson, B., and McMonigal, D. (2004), "Super-Sized Double-Layer Pultruded Gratings," *Proc. Composites 2004 Convention and Trade Show*, American Composites Manufacturers Association (ACMA), CD-ROM.
7. Matta, F., Galati, N., Nanni, A., Ringelstetter, T.E., Bank, L.C, and Oliva, M.G. (2005), "Pultruded Grid and Stay-in-Place Form Panels for the Rapid Construction of Bridge Decks," *Proc. Composites 2005 Convention and Trade Show*, ACMA, CD-ROM.
8. Bank, L.C., Gentry, T.R., Thompson, B.P., and Russell, J.S. (2003), "A Model Specification for FRP Composites for Civil Engineering Structures," *Construction and Building Materials*, 17(6-7), 405-437.
9. Buth, C.E., Williams, W.F., Bligh, R.P., Menges, W.L., and Haug, R.R. (2003), "Performance of the TxDOT T202 (MOD) Bridge Rail Reinforced with Fiber Reinforced Polymer Bars," *TTI Research Report 0-4138-3*, Texas Transp. Inst., College Station, TX.
10. El-Salakawy, E., Benmokrane, B., Masmoudi, R., Brière, F. and Breaumier, E. (2003), "Concrete Bridge Barriers Reinforced with Glass Fiber-Reinforced Polymer Composite Bars," *ACI Structural Journal*, 100(6), 815-824.
11. American Association of State Highway and Transportation Officials (1998), "Load and Resistance Factor Design (LRFD) Bridge Design Specifications," AASHTO, 2nd edition.
12. Federal Highway Administration, and California Department of Transportation (2005), Bridge Rail Guide 2005, *http://www.fhwa.dot.gov/bridge/bridgerail/bridgerail.pdf*.
13. American Concrete Institute (2005), "Guide for the Design and Construction of Concrete Reinforced with FRP Bars," *ACI 440.1R-05*, ACI, Farmington Hills, MI (to be released).
14. Hirsch, T.J. (1978), "Analytical Evaluation of Texas Bridge Rails to Contain Buses and Trucks," *TTI Research Report 230-2*, Texas Transp. Inst., College Station, TX.
15. Jacobson, D.A. (2004), "Experimental and Analytical Study of Fiber Reinforced Polymer (FRP) Grid-Reinforced Concrete Bridge Decking," M.S. Thesis, University of Wisconsin, Madison, WI.